A Screen for novel factors involved in Pluripotency and X-Chromosome Reactivation

Serena Francesca Generoso

TESI DOCTORAL UPF / 2018

THESIS SUPERVISOR

Dr. Bernhard Payer

Gene Regulation, Stem Cells and Cancer Programme,
Center for Genomic Regulation
DEPARTMENT OF EXPERIMENTAL AND HEALTH SCIENCE

"One may not reach the dawn
save by the path of the night"
Kahlil Gibran

Acknowledgements

First of all, I would like to thank my parents.
Siete sempre stati l'esempio da seguire. Mi avete insegnato a lavorare con impegno, onestà e a non lasciarmi abbattere dalle difficoltà ma a trarne un insegnamento per il futuro. Mi avete aiutato a credere in me stessa e a rimanere me stessa nonostante tutto. Negli ultimi quattro anni mi avete dato tutto il vostro sostegno. Senza la vostra fiducia nelle mie scelte non sarei stata in grado di affrontare questo capitolo della mia vita con la stessa attitudine.
Ringrazio la mia famiglia tutta, soprattutto mia cugina Carla. Grazie per supportarmi e "sopportarmi" da sempre.
Ringrazio la mia amica Adriana, anche se a distanza, abbiamo condiviso l'esperienza del dottorato, sostenendoci nei momenti belli e in quelli brutti.

I would like to thank my supervisor, Bernhard, for giving me the possibility to carry out my PhD Thesis in his laboratory.
You gave me the opportunity to grow professionally and personally during my PhD. I could learn a lot and expand my scientific knowledge. Especially, I want to thank you for the trust you have shown me during these four years.

I want to express my special thanks to the Payer Lab: Antonio, Anna, Pauline, Jackie, Moritz, Shafqat and Mercedes. Thanks Lab, for sharing this time with me, with valuable advices and conversations, not only work related.

Antonio, we were the first members of the Payer Lab. We lived this adventure together sharing the desk and good and bad times. And above all, we joined our forces and we faced together the biggest challenge of our PhD: RNA FISH! I wish you all the best.

Pauline, your coffee addiction has been a blessing. Thanks for all the coffee breaks we shared together. But most of all, thanks for your support, your optimism and for all the chats, science related and not. And thanks for sharing your interest in art with me.

Anna, gracias por tu ayuda y tu paciencia. Sin ti el lab no funcionaría. Gracias por ser siempre disponible y por haberme animado en los momentos más complicados.

Un grazie speciale alla parte italiana (presente e passata) del gruppo: Jackie ed Emanuela. Abbiamo condiviso questo percorso insieme, anche se in momenti diversi. La vostra presenza e il vostro supporto è stato molto importante per me, soprattutto la possibilità di potermi esprimere con voi nella mia lingua mi ha fatto sentire a casa.

A special thanks to Maria. We started in the lab together with Antonio and Bernhard. I appreciated the help that you gave me at the beginning to feel comfortable in the lab besides my shyness.

During these four years I could supervise three students: Vanessa, Raffaele and Marta. I would like to thank them for their patience and the enthusiasm that they showed, especially Raffaele. It has been a great opportunity for me. It pushed me to improve myself,

professionally and personally. It also helped me to communicate and give back a bit of what I have been learning.

Thanks to Julia for being a friend and a great support during my all PhD. I really appreciated your help and advices.

To develop a part of the project I received precious help and competence from Vicky. You introduced me to the STORM world and together we faced up and down in our experiment but eventually we managed. So, I would like to thank you for your help and kindness.

I would like to thank Lucas Carey and his student Marta. We shared a collaboration project together and this gave me the opportunity to work on something different, know new interesting people and learn a bit more about the yeast world.

I would like to thank all the people of the GRSC program, the staff of the core facilities, especially Erika, Eva, Alex and Oscar from the FACS unit. During these four years we spent a lot of time together, having conversations and jokes. They have been extremely helpful in carrying out my crazy experiments, giving me their technical support and advices.
Thanks also to Imma and Gemma for always being very helpful and professional.

Table of contents

ABSTRACT

A classic example of epigenetic gene regulation is X-Chromosome Inactivation (XCI) in female mammals, where one of the two X chromosomes is inactivated for dosage compensation between the sexes. However, XCI is reversed during mammalian development by reactivation of the inactive X chromosome (XCR) in the epiblast cell lineage in the inner cell mass of the late blastocyst and in germ cells, thereby coupling X-reactivation with pluripotency.

To study XCR we used induced pluripotent stem cell (iPSC) reprogramming, which recapitulates the reactivation of the inactive X *in vitro*. We performed a screen during iPSC reprogramming by knocking down the expression of candidate genes picked from a single cell microarray expression screen in blastocysts.

We thereby identified candidates, whose knockdown had an effect on both acquisition of pluripotency and X-Reactivation. However, we also identified factors, with a specific role in XCR, without affecting reprogramming to iPSCs. This suggests that XCR is not an absolute requirement for iPSC reprogramming and that the two processes can be uncoupled. Among these factors, there was the cohesin complex member Smc1a. In experiments based on Super resolution microscopy (STORM), we observed a preferential enrichment of Smc1a on the active compared to inactive X, suggesting a role in shaping the Xa structure. Therefore, we conclude that cohesin-mediated changes in X-chromosome structure are a key step during the XCR process.

RESUMEN

Un ejemplo clásico de la regulación epigenética del genoma es la Inactivación del Cromosoma X (XCI) en los mamíferos femeninos, donde uno de los dos cromosomas X está inactivado para la compensación de dosis entre los sexos. Sin embargo, la XCI se revierte durante el desarrollo de los mamíferos mediante la reactivación del cromosoma X inactivo (XCR) en el linaje de las células epiblásticas en la masa celular interna del blastocisto tardío y en las células germinales, acoplando así la XCR con la pluripotencia. Para estudiar la XCR se utilizó la reprogramación de células madre pluripotentes inducidas (iPSC), que recapitula la XCR in vitro. Se realizó un cribaje reduciendo la expresión de genes candidatos, seleccionados a partir de un microarray de expresión en blastocitos. Este ensayo permitió identificar factores cuya expresión reducida tiene un efecto tanto en la adquisición de la pluripotencia como en la XCR. Sin embargo, también se identificaron factores con un rol específico en la XCR. Esto sugiere que la XCR no es un requisito absoluto para la reprogramación de las iPSC, y que los dos procesos se pueden desacoplar. Se identificó el miembro Smc1a del complejo de cohesina. Mediante microscopía de súper resolución (STORM) se observó un enriquecimiento preferencial de Smc1a en el cromosoma X activo en comparación con el X inactivo, lo que sugiere un papel en la configuración de la estructura del X activo. Por lo tanto, concluimos que los cambios mediados por cohesina en la estructura del cromosoma X son un paso clave durante el proceso de reactivación del X.

Introduction

Chapter 1. X dosage compensation

In numerous organisms there is a major difference in terms of chromosomes between sexes. Males and females differ in their dose of X chromosomes. In each species, an essential process called dosage compensation ensures that somatic cells of either sex express equal levels of X-linked genes. The strategies for dosage compensation are different but, in all cases, the X chromosome of one sex is targeted to modulate gene expression. In *C.elegans* XX worms are hermaphrodites and XO worms are male (Madl and Herman 1979). Hermaphrodite worms keep both X chromosomes active, but reduce transcript levels from each X chromosome by half (Meyer and Casson 1986). In *Drosophila* male flies double the transcription activity of their single X chromosome (Belote and Lucchesi 1980). In mammals, females (XX) silence the transcription of one X chromosome, therefore, both males and females have only one active X chromosome **(Fig. I1)**. The first evidence of a mechanism of dosage compensation emerged in 1949 when Barr and Bertram described the presence of a structure in the nuclei of only female cells of various mammalian species (Barr and Bertram 1949). In 1957 Ohno and colleagues showed that this structure is derived from one of two female X chromosomes (Ohno 1967). Shortly later, in 1961, Mary Lyon described experiments on X-linked coat color genes expression in female mice. In order to explain the heterogeneous pattern observed in mosaic mice, she hypothesized that in each female cell one of two X chromosomes is stably inactivated (Lyon 1961). Further experiments demonstrated the heritability of the inactive state from one cell generation to the next (Davidson et al. 1963) and confirmed the occurrence of X inactivation in human females (Beutler et al. 1962). Studies in human females with

multiple copies of X showed that all chromosomes in excess of one are inactivated. This has been generalized as "*n*-1 rule", based on the fact that if an individual has *n* X chromosomes, then *n*-1 is inactivated (Ohno 1967).

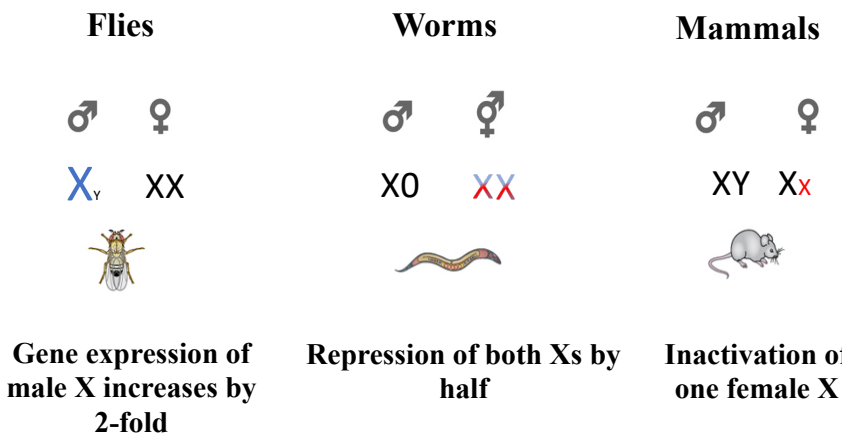

Figure I1 Different mechanisms of dosage compensation. Organisms use different strategies to equalize X-linked gene expression between males (XY or XO) and females (or hermaphrodites; XX). Female mammals randomly inactivate one X chromosome. Male fruit flies double the transcription rate of their single X chromosome. Hermaphrodite worms half the expression of both X chromosomes.

1.1 X Chromosome Inactivation: Initiation

X chromosome Inactivation (XCI) is one of the most remarkable examples of epigenetic gene regulation in mammals. One of the two X chromosomes of female cells is inactivated. XCI requires *Xist* (X-inactive-specific transcript), a long non-coding RNA (lncRNA) that

binds *in cis* and accumulates along the entire chromosome from which is transcribed (Carolyn J. Brown et al. 1991; C J Brown et al. 1992). Coating of the chromosome with Xist RNA triggers the silencing of the X-Chromosome (Penny et al. 1996; Lee et al. 1996).

Xist expression is regulated by genetic loci within its chromosomal locus known as the X inactivation center (*Xic*), which contains several regulatory elements. Within the 3' region are the promoter and regulatory elements for expression of the *Tsix* non-coding RNA gene. It is originating 15 kb downstream of *Xist* and is transcribed in antisense orientation of *Xist* and acts as its repressor (J T Lee and Lu 1999; J T Lee, Davidow, and Warshawsky 1999). Tsix is expressed in ESCs and becomes up-regulated during differentiation on the active X-Chromosome (Xa) and downregulated on the inactive X-Chromosome (Xi), where Xist is expressed. Studies in *Tsix*-mutant female cells show that X-inactivation takes place on the X where it is absent, leading to Xist upregulation and suggesting a role in Xa choice (J T Lee and Lu 1999). However, recent studies show that *Tsix*-mutant cells sometimes express Xist from both alleles so, those cells are removed and only the ones with *Xist* monoallelic expression remain (Gayen et al. 2015). Therefore, *Tsix* was suggested to not be required for the choice of which chromosome is active or inactive, but to be important to prevent *Xist* ectopic expression on the Xa only after X-inactivation has initiated. This supports a stochastic model in which each X chromosome in a nucleus initiates XCI independently (Monkhorst et al. 2008). *Tsix* is activated by its enhancers *DXPas34* and *Xite,* non-coding transcripts (Cohen et al. 2007; Ogawa and Lee 2003). Two other non-coding RNA genes *Tsx* and *Linx*, have been implicated in *Tsix* regulation. *Tsx* seems to be an activator of *Tsix* (Anguera et al. 2011) while *Linx* has been described as an activator (Nora et al. 2012a), however, a more recent paper indicates that Tsix and Linx show an opposite transcriptional activity (Giorgetti et al. 2014). *Tsix* facilitates binding of the pluripotency factor PRDM14 to *Xist intron 1*, which might

allow the repression of *Xist* in pluripotent stem cells (Payer et al. 2013). Another factor recruited by *Tsix* is CCCTC binding factor (CTCF) (Kung et al. 2015). This architecture protein binds directly Tsix and Xite RNAs and seems to be involved in the pairing of the two X-chromosome at the time of random inactivation (N. Xu et al. 2007). It has been proposed that the X-chromosome pairing is involved in symmetry breaking leading to the choice of which chromosome has to be active and which the inactive. However, a recent study shows that random XCI can take place in absence of pairing (Barakat et al. 2014).

Upstream of *Xist*, at the 5' region, there is a non-coding RNA gene, *Jpx*, known as *Xist* activator during XCI (Tian, Sun, and Lee 2010). It repels CTCF, which is involved in the regulation of *Xist* by binding to the *Xist* promoter region. In fact, CTCF blocks the upregulation of *Xist* on the Xa while on the Xi it gets repelled by Jpx, allowing Xist upregulation (Sun et al. 2013). Similarly, another non-coding RNA encoded by *Ftx* locus, upstream of *Jpx*, is implicated in *Xist* activation (Chureau et al. 2011). A recent study shows that its function as *Xist* activator depends on *Ftx* transcription and not on the RNA products (Furlan et al. 2018b). Therefore, the hypothesis is that transcription across the 5' is required for the recruitment of the machinery to the *Xist* promoter while Ftx RNA is not involved in XCI (J T Lee, Davidow, and Warshawsky 1999; Luikenhuis, Wutz, and Jaenisch 2001; Takashi Sado, Hoki, and Sasaki 2005; Furlan et al. 2018a).

Located upstream of *Ftx*, there is *Rnf12/Rlim*, another activator of *Xist* (Barakat et al. 2011; Jonkers et al. 2009). RNF12 functions as E3 ligase for ubiquitin-mediated degradation of the pluripotency factor REX1, that acts at the promoter regions of both *Xist* and *Tsix* gene loci. Therefore, REX1 degradation mediated by RNF12 might up-regulate *Xist* and down-regulate *Tsix* at the same time (Pablo Navarro et al. 2010). The loci that participate in *Xist* repression and *Xist* activation are summarized in **Fig I2**.

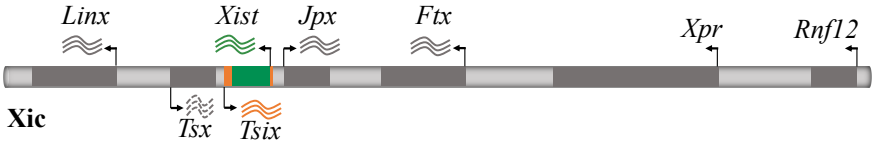

Figure I2 The X-Inactivation Center (*Xic*). The key region on the mouse X chromosome includes known elements involved in *Xist* gene regulation as noncoding RNA (lncRNA) genes and protein-coding genes (Adapted from Brockdorff and Turner 2015).

Another important region along the *Xic* is *Xist intron 1*, a binding hub for pluripotency factors such as OCT4, NANOG, SOX2, PRDM14. It is involved in direct repression of *Xist* by pluripotency factors in ESCs (Ma et al. 2011; Donohoe et al. 2009; P. Navarro et al. 2008; Nesterova et al. 2011). The depletion of OCT4, NANOG and PRDM14 leads to *Xist* upregulation but also to differentiation (Ma et al. 2011; P. Navarro et al. 2008). However, ESCs lacking *intron 1* do not dysregulate *Xist* expression in the undifferentiated state nor show perturbed XCI *in vivo* (Minkovsky et al. 2013; Barakat et al. 2011).

Like for *Xist*, also *Tsix* control elements are bound by pluripotency factors such as OCT4, REX1, SOX2, KLF4 and c-MYC. However, in this case they act as activators of *Tsix* (Donohoe et al. 2009; Pablo Navarro et al. 2010). The 5' region of *Rnf12* is also bound by NANOG, OCT4, SOX2 and PRDM14 (Pablo Navarro et al. 2011; Payer et al. 2013) and their depletion leads to upregulation of *Rnf12* in ESCs.

Particularly, PRDM14 represses *Rnf12* by recruitment of PRC2 (Polycomb repressive complex) and the deposition of H3K27me3 mark upstream of *Rnf12* (Chan et al. 2013; Yamaji et al. 2008; Payer et al. 2013)**(Fig. I3)**.

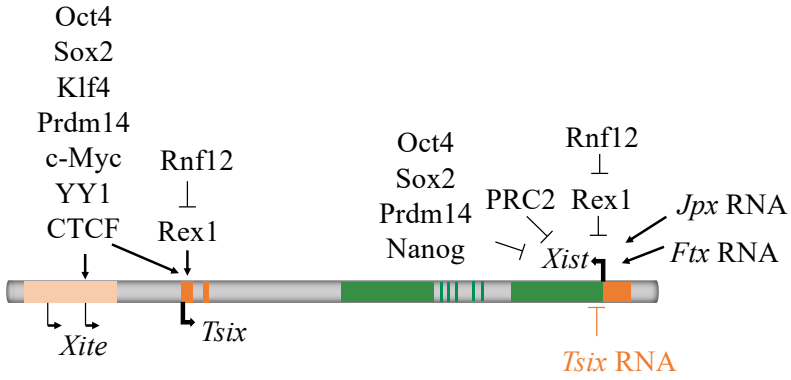

Figure I3 *Xist* and *Tsix* gene loci. The network of protein factors and lncRNAs implicated in *Xist* gene regulation is shown with arrows and bars indicating repressor and activator function, respectively. RNF12 mediates degradation of REX1, which functions both as a *Xist* repressor and a *Tsix* activator.(Adapted from Brockdorff and Turner 2015).

1.2 X Chromosome Inactivation: Xist Spreading

All the findings suggest that Xist is necessary and sufficient to trigger heterochromatin formation and transcriptional silencing on the X

Chromosome. There are different regions on Xist RNA that are responsible for gene silencing and spreading along the X. Experiments in ESCs with an inducible Xist expression system showed that the silencing can be ascribed to a conserved repeat sequence, Repeat-A, located at the 5' of the molecule. Other sequences of the molecule are mediating the coating of the X (Wutz, Rasmussen, and Jaenisch 2002a). Particularly critical for the anchoring is the sequence Repeat-C (Beletskii et al.2001; Sarma et al. 2010). This region is bound by the protein YY1 (Yin Yang 1), which traps Xist RNA at its nucleation center, formed by a trio of YY1-binding sites within the *exon 1 Repeat F* region of the *Xist* gene (Jeon and Lee 2011). RNAi experiments against YY1 or mutations in its binding sites abolish the loading of Xist RNA and chromosome coating. Moreover, YY1 has binding specificity for Xi and not for the same region on the Xa. This is explained by the fact that in YY1-binding sites located within *Xist* promoter, CpG islands are unmethylated on the Xi and methylated on the Xa (Hendrich, Brown, and Willard 1993; Norris et al. 1994). Indeed, it has been shown that YY1 is bound only to the unmethylated *Xist* allele (Joomyeong Kim et al. 2003).

Xist RNA is tightly linked with the nuclear matrix and one of the proteins critical for the anchoring is hnRNP U/SAF-A. It interacts directly with Xist and is required for the recruitment of repressive marks (Pullirsch et al. 2010; Yamada et al. 2015). hnRNP U loss of function results in diffusion of Xist RNA throughout the nucleoplasm and away from the X chromosome. This suggests that hnRNP U is involved in tethering of Xist to the Xi (Hasegawa et al. 2010; Chu et al. 2015; McHugh et al. 2015; Minajigi et al. 2015). Once Xist RNA localizes at its nucleation site, it has to spread across the X in order to achieve gene silencing **(Fig.I4)**.

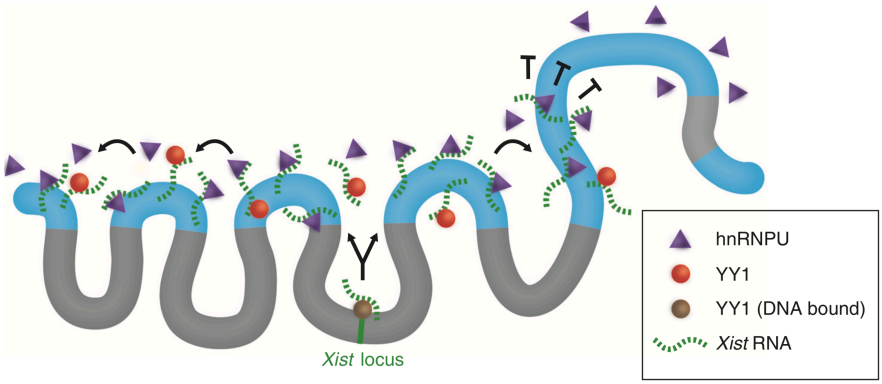

Figure I4 Xist spreading. Factors involved in Xist spreading. YY1 tethers Xist RNA at the nucleation center formed by a trio of YY1 binding sites. YY1 is also interacting with Xist RNA to facilitate the spreading. Another critical protein is hnRNP U/SAF-A, which interacts with Xist RNA and is important for its localization (Adapted from Brockdorff and Turner 2015).

1.3 X Chromosome Inactivation: Epigenetic regulation

The epigenetic regulation of X Chromosome inactivation requires the involvement of chromatin-associated proteins that are members of the Polycomb group families PRC1 and PRC2. It has been observed that components of those complexes and their repressive marks are enriched on the Xi. Specifically, H2AK119u1 and H3K27me3 are deposited on Xi by the Polycomb repressive complexes PRC1 and PRC2, respectively (de Napoles et al. 2004; Jose Silva et al. 2003). The recruitment of those factors to the Xi has been discussed for long time, and they seem dependent on Xist RNA at initiation and maintenance phase of the silencing. PRC2 seems to be recruited by Xist RNA but in order to be active and deposit the H3K27me3 mark it needs the binding of the cofactor JARID2 (Cifuentes-Rojas et al. 2014; da Rocha et al. 2014) which can bind PRC1 mark H2AK119u1 (Cooper et al. 2016). Recently, it has been proposed that noncanonical PRC1 complexes are required for the

recruitment of PRC1 and PRC2 to the Xi (Almeida et al. 2017). In fact, current evidences suggest that noncanonical PRC1 is recruited by Xist RNA through hnRNP K (Pintacuda et al. 2017) while canonical PRC1 recruitment may occur only when PRC2 is present (Almeida et al. 2017; Schoeftner et al. 2006). Both complexes seem to be dispensable for gene silencing initiation, in fact, in absence of Repeat A, they are recruited to the X but there is no transcriptional repression (Chaumeil et al. 2006; Kohlmaier et al. 2004). The Polycomb group proteins are a layer of XCI epigenetic regulation not essential for initiation of gene silencing mediated by Xist but important to propagate it (Leeb and Wutz 2007; Schoeftner et al. 2006) **(Fig.I5)**.

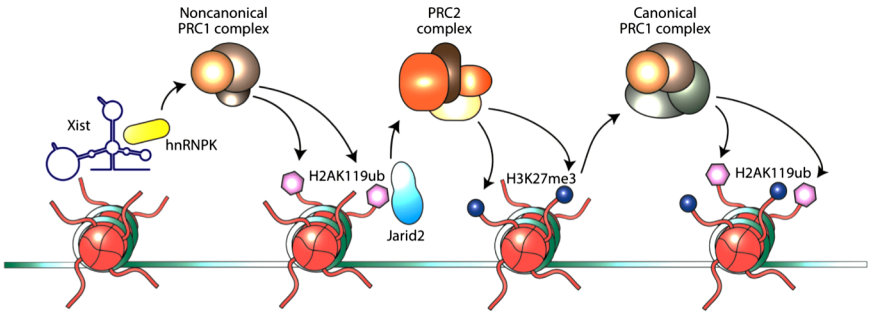

Figure I5 Epigenetic regulation. Recruitment of both PRC1 and PRC2 is dependent on Xist. Recent evidence suggests that non-canonical PRC1 is recruited through hnRNP K by Xist RNA. PRC2 recruitment depends on JARID2, which is able to interact with PRC1 mark, H2AK119ub. Canonical PRC1 recruitment occurs downstream of the PRC2 complex (Adapted from Galupa and Heard 2018).

Another important epigenetic mark is H4K20me1, a histone modification enriched on Xi catalyzed by PRSET7 (Kohlmaier et al. 2004). Its function is still unclear, but it seems related to Xi structure. In fact, there is an evidence suggesting that its lack leads to global chromosomal decondensation (Oda et al. 2009a) and it also affects chromosome

compaction in C. elegans (Lau and Csankovszki 2015). Additional modifications occur on the Xi, H3K9me3 and H3K9me2, catalyzed by specific KTM enzymes: SUV39H1and G9a respectively. Those two methyl marks could be required together for the maintenance of the inactive state (Rougeulle et al. 2004; Chadwick and Willard 2004).

1.4 X Chromosome Inactivation: Xist-Interactome

XCI involves the recruitment of many proteins to the X chromosome. Early evidence suggest that Xist might interact with those proteins because of discrete regions of the RNA sequence: Repeat A for transcriptional silencing (Wutz, Rasmussen, and Jaenisch 2002b), Repeat B-F for PRC2 recruitment (da Rocha et al. 2014), Repeat C for DNA localization (Beletskii et al. 2001). Recently, several groups have focused the research on the Xist-interactome and the factors involved in silencing. Many proteins have been identified as required for Xist spreading and/or the transcriptional silencing of the X chromosome. There are five different studies which identify a common factor: SPEN/SHARP, (Minajigi et al. 2015; Monfort et al. 2015; McHugh et al. 2015; Moindrot et al. 2015; Chu et al. 2015). According to their model, Xist recruits SPEN, which then recruits and/or activates HDAC3, a histone deacetylase. The deacetylation of histones leads to subsequent recruitment of PRC2 and H3K27me3 deposition. Depletion or deletion of SPEN do not affect Xist recruitment but transcriptional silencing. Two other proteins, which have been reported as Xist interactors are RBM15, another component of SPEN family and, WTAP, a subunit of m^6a RNA methyltransferase complex (Chu et al. 2015; McHugh et al. 2015; Minajigi et al. 2015). Knockdown of those proteins does not affect Xist localization but transcriptional repression (Moindrot et al. 2015; Monfort et al. 2015). Besides hnRNP U

as a common factor identified by those studies, an additional component of that family, hnRNP K, has been found as Xist interactor (Hasegawa et al. 2010; Chu et al. 2015; McHugh et al. 2015; Minajigi et al. 2015). Like SPEN, it is required for gene silencing and for the deposition of repressive marks. Besides hnRNP U there is another nuclear matrix protein, CIZ1, that has been identified among Xist RNA interactors (Chu et al. 2015) and contributes to *cis*-localization of Xist (Sunwoo et al. 2017; Ridings-Figueroa et al. 2017). CIZ1 is specifically enriched on the Xi and its recruitment depends on a specific domain of Xist RNA, Repeat E (Ridings-Figueroa et al. 2017; Sunwoo et al. 2017). CIZ1 knockout leads to a dispersed Xist cloud in somatic cells with no effect on Xist expression levels. CIZ1 and hnRNP U interact with Xist RNA independently from each other and both are necessary for Xist localization to the Xi (Sunwoo et al. 2017) **(Fig I6)**.

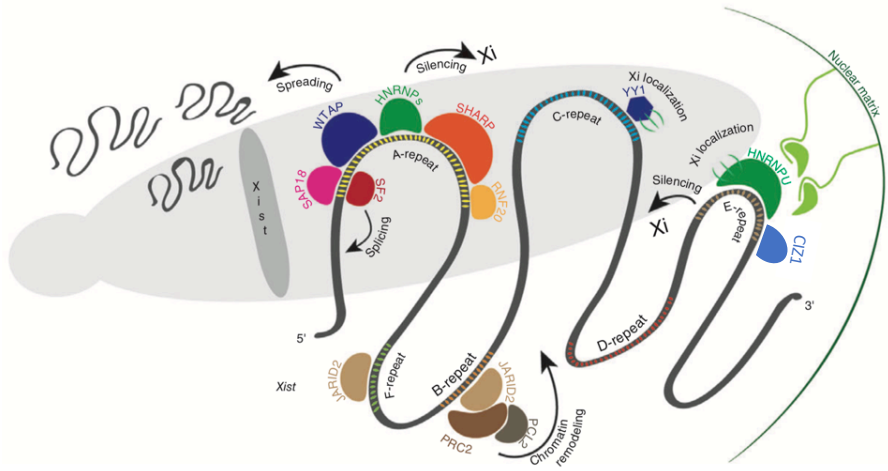

Figure I6 The Xist Interactome. Functions and interactors of Xist RNA repeat elements. The Repeat A is required for silencing and recruits many interactors as WTAP and SPEN/SHARP. The Repeat B interacts with JARID2 for chromatin remodeling. The Repeat C is important for tethering Xist to the Xi via interaction with YY1. The Repeat E tethers Xist to the Xi interacting with hnRNP U and CIZ1. Repeat F is also critical for JARID2 recruitment (Adapted from Furlan and Rougeulle 2016).

1.5 X Chromosome Inactivation: Maintenance

A late event that occurs in XCI is DNA methylation of CpG islands on the Xi that requires the de novo methyltransferase DNMT3B whereas DNMT3A and DNMT3L are dispensable (Gendrel et al. 2012). DNA methylation is required to play a dual role during XCI. First of all, it is not essential for gene silencing but to maintain X-linked genes transcriptionally inactive (Panning and Jaenisch 1996; Takashi Sado et al. 2004). And second of all, it ensures the repression of Xist on the Xa.

An atypical member of the SMC proteins (structural maintenance of chromosomes hinge domain containing 1), SMCHD1, is required for DNA methylation at many Xi CpG islands (Blewitt et al. 2008; Gendrel et al. 2012). It is enriched on the Xi and has been identified as a Xist-interacting protein (Minajigi et al. 2015). It ensures the maintenance of the inactivate state by facilitating the incorporation of H3K27me3 and other epigenetic modifications at gene loci that have been silenced (Sakakibara et al. 2018). A recent study shows how SMCHD1 can play a role in Xi architecture to facilitate Xist spreading along the chromosome (Jansz et al. 2018; Wang et al. 2018; Gdula et al. 2018).

Another late event is the incorporation of the histone variant macroH2A on the Xi (Costanzi and Pehrson 1998; Mermoud et al. 1999). Xist RNA is required to retain macroH2A on the inactive X in the latest stages of differentiation (Csankovszki et al. 1999) but, it is not sufficient for the recruitment at early stages (Mermoud et al. 1999; Wutz, Rasmussen, and Jaenisch 2002a). MacroH2A is not essential for XCI because its loss after Xist depletion does not lead to reactivation of X-linked genes (Csankovszki et al. 1999). However, its main function is to safeguard the maintenance of XCI (Hadjantonakis et al. 2001) **(Fig.I7)**.

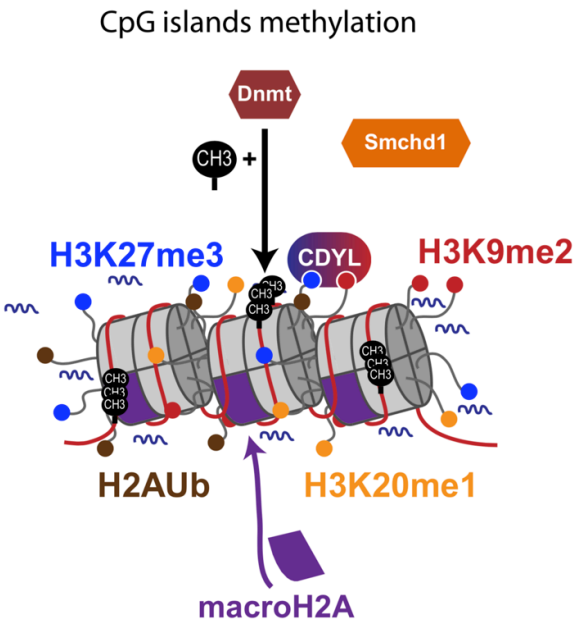

Figure I7 DNA silencing maintenance. At the latest stages of XCI, PRC1 and PRC2 complexes are no longer enriched on the Xi, and macroH2A becomes associated with the X chromosome. The latest mark is DNA methylation, deposited on the promoters of X-linked genes thanks to DNMTs proteins. SMCHD1 may play a role in deposition or maintenance of DNA methylation (Adapted from Chalignè and Heard 2014).

1.6 Some genes escape XCI

X-Chromosome Inactivation affects most of the X chromosome, however, there are some genes that escape the silencing (Berletch et al. 2011). Escapee genes show little or no silencing during early propagation of XCI. These genes include the ones located on the pseudo autosomal region on the X chromosome that pairs with the Y chromosome during male meiosis. Escapees do not require dosage compensation, because two copies are present on both male and female chromosomes. It has been

shown that only 3% of X-linked mouse genes escape X inactivation and they are located in regions of silenced chromatin compared to humans where the percentage of escapee genes is around 15% (Carrel and Willard 2005; F. Yang et al. 2010; Tsuchiya et al. 2004). The main difference could be the position of the centromeric heterochromatin that in mouse is at one end of the X which might facilitate Xist spreading. Examples of escapee genes are *Kdm5c* and *Kdm6a* that appear to be devoid of Xist RNA coating (Murakami et al. 2009).

1.7 XCI regulation during early mouse development

During mouse development, two modes of X Chromosome Inactivation ensure the silencing of one of the two female Xs in a stage-specific manner. Imprinted X-Inactivation silences preferentially the paternal X (Xp) in early embryos and the placenta. In random X-Inactivation either the Xp or the maternal X Chromosome (Xm) can be inactivated at the post-implantation stage and it persists through life. In metatherian mammals (such as marsupials) only imprinted XCI is observed, where the Xp is exclusively chosen for inactivation (Grant et al. 2012). In other eutherians than mouse, like humans or rabbits, only random X-Inactivation appears to take place (Ikuhiro Okamoto et al. 2011). In case of heterozygous X-linked mutations, random X-Inactivation results in having half of the cells with the mutation on the inactive X and with the wild-type copy on the active one, allowing a healthy phenotype. This is a big advantage compared to other species where always the same X is active as a consequence of imprinted X-Inactivation **(Fig.I8)**

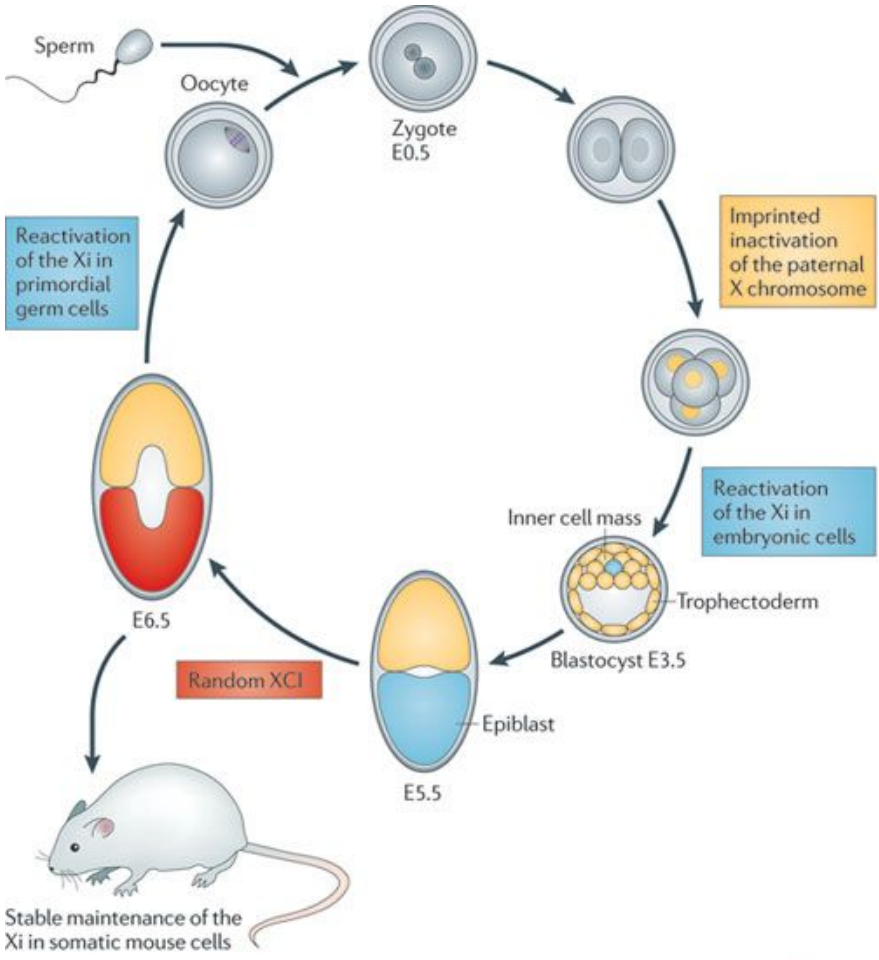

Figure I8 XCI and XCR during mouse development. Imprinted inactivation of the paternal X (yellow shading) occurs at the cleavage stage embryos. It is maintained in developing extra-embryonic tissues. The reactivation of the paternal X occurs in the inner cell mass of blastocyst (blue shading). Both X chromosomes are active in the developing epiblast between E3.5 and E5.5 (blue shading). Random XCI (red shading) of either paternal or maternal X starts around E5.5 and it is stably maintained in the somatic cells. Another wave of XCR occurs in the developing germ line (Adapted from Wutz 2011).

1.7.1 Imprinted and Random X-Inactivation

Paternally imprinted X Inactivation has been observed for the first time in marsupials (Sharman 1971). Later, it has been described in trophectoderm (TE) and primitive endoderm (PE) in mouse embryo (Nobuo Takagi and Sasaki 1975). In this case always the paternal X gets inactivated regardless of how many chromosomes are present. In male the single X chromosome is derived from the mother, therefore, it does not undergo imprinted inactivation.

Until the morula stage in mouse embryo there is a repressive imprint on the Xm preventing its inactivation. This imprint prevents Xist expression, keeping the X chromosome active. Nuclear transfer experiments have shown that this repressive Xist imprint is established during oocyte maturation (T. Tada et al. 2000). It has been thought that Tsix was required to repress Xist and prevent X-inactivation (Takashi Sado, Hoki, and Sasaki 2005; Pablo Navarro et al. 2005). It has been shown that Tsix is required to prevent Xist expression during imprinted XCI in the extraembryonic tissues (J T Lee 2000; T Sado et al. 2001). However, a recent study has shown that Tsix is dispensable for inhibiting Xist and XCI in the early embryo (Maclary et al. 2014).

After embryo implantation, imprinted X inactivation is kept in extraembryonic tissues and is critical for survival. In fact, embryo lethality occurs at post-implantation stage in *Xist*- and *Eed* mutants with defective imprinted inactivation (Marahrens et al. 1997; J. Wang et al. 2001).

Imprinted X inactivation is less stringent compared to the random one. In fact, it lacks some repressive marks as DNA methylation important for the maintenance of silencing, therefore, especially in trophoblast giant cells and trophoblast stem cells, X-linked genes might be occasionally reactivated (Corbel et al. 2013; Dubois et al. 2014; Hadjantonakis et al. 2001; T Sado et al. 2000).

Random X-Inactivation starts at the early post-implantation stage. The cells use the n-1 rule described earlier and based on that, all X chromosomes except one are inactivated per diploid set. This process is often defined as a counting while the selection of active and inactive chromosomes is random, and it is referred as a choice. The two processes are tightly linked. As mentioned before, random X-Inactivation is stringently maintained compared to the imprinted form. Therefore, it is maintained in somatic cells and their progeny throughout life. In that way adult mice result in a mosaic of cells expressing either maternally or paternally derived alleles of X-linked genes (LYON 1962; H. Wu et al. 2014).

Chapter 2. X-Chromosome Reactivation

In order to switch from imprinted XCI to random XCI, the paternal X has to be reactivated (Huynh and Lee 2003a). It takes place during blastocyst maturation between embryonic day (E) 3.5 and 4.5, specifically in the epiblast (EPI) lineage while the two extraembryonic tissues TE and PE maintain imprinted XCI. This process happens quickly, within a day and without cell division (Mak et al. 2004; I. Okamoto et al. 2004; L. H. Williams et al. 2011). As expected, it occurs by reversing the main hallmarks of XCI like Xist downregulation, removal of repressive marks and reactivation of X-linked genes.

So far, few factors are known to play a role in XCR in blastocysts. One of them is PRDM14, a pluripotency factor, which is expressed in the inner cell mass (ICM) during XCR.

XCR *in vivo* in *Prdm14-/-* mutant embryos has been shown to occur with a decrease in efficiency as a consequent failure of H3K27me3 removal from the Xp (Payer et al. 2013). In *Prdm14* mutants, XCR occurs in half

of the epiblast cells compared to an efficiency of 90% in wild-type embryos.

Like *Prdm14* also *Tsix* is involved in XCR in blastocysts. It becomes biallelically expressed in the ICM when X-Reactivation occurs, and forcing Tsix expression on the paternal X, it induces Xist downregulation (Ohhata et al. 2011). Tsix-/- mutants show as well a defective and delayed XCR in epiblast cells (Payer et al. 2013). It is possible that *Tsix* and *Prdm14* act through the same pathway as PRDM14 recruitment to Xist intron 1 is dependent on Tsix expression. Therefore, Tsix seems to ensure the recruitment of pluripotency factors for correct XCR but is not essential for the process as other mechanisms of compensation occur later on (Payer et al. 2013; Maclary et al. 2014). *Nanog* also switches from monoallelic to biallelic expression in blastocysts (Miyanari and Torres-Padilla 2012) and could help overcoming the defect in XCR in late *Tsix*-/- blastocysts (Payer et al. 2013) **(Fig. I9)**.

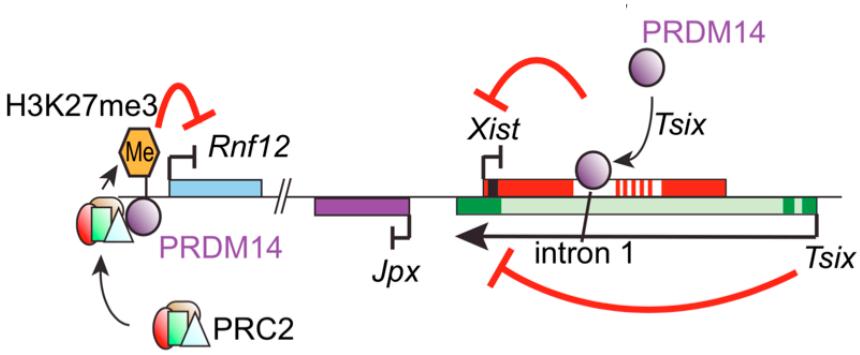

Figure I9 PRDM14 promotes XCR by repressing Xist. During XCR in embryogenesis and in pluripotent stem cells, PRDM14 binds upstream of *Rnf12* whose repression is mediated by the methylation of H3K27 through PRC2. At the same time Tsix is expressed and facilitates the binding of PRDM14 to *Xist* intron 1. All those events lead to Xist repression as key step of XCR (Adapted from Payer et al., 2013).

A recent study, based on single cell RNA-Seq of mouse blastocysts, shows that there are different genes that are reactivated at different stages and that the ones that are reactivated slowly are more enriched for H3K27me3 (Borensztein et al. 2017). It also shows that in absence of UTX, a H3K27 demethylase, the erasure of the repressive mark H3K27me3 (Hong et al. 2007; Lan et al. 2007; Agger et al. 2007) is delayed, interfering with the reactivation of the late genes. However, there are some ICM cells whose H3K27me3 erasure is complete in UTX knockout embryos. This is explained as a compensation mediated by other demethylases or a passive loss of the repressive mark. This study suggests that UTX might play a role in facilitating the reactivation of the paternal X at the blastocyst stage (Borensztein et al. 2017).

Another wave of XCR occurs after random X Inactivation in primordial germ cells (PGCs) (Monk and McLaren 1981). At this stage, it is necessary to reactivate the X chromosome in order to avoid the inheritance of an inactive Xm to the offspring. As in male embryos the Xm is the only X chromosome and in female the Xp is inactivated, the consequence of XCR failure in the germ line would be a functional nullisomy for X-linked genes.
The XCR process in germ cells might be different from the one in the epiblast. In fact, XCR in germ cells is a slower process that takes several days with multiple cell divisions (Chuva de Sousa Lopes et al. 2008; Sugimoto and Abe 2007), while it occurs within a day in the epiblast in the absence of cell division. The difference might due to the fact that random XCI is more stringently maintained and that also DNA methylation needs to be erased in germ cells during XCR.

2.1 X-Reactivation and Pluripotency

Besides its natural occurring context *in vivo*, *XCR* has been studied by using a number of experimental systems: nuclear transfer, cell fusion, induced pluripotent stem (iPS) cells and *in vitro* germ cell derivation.

In the first case, a somatic nucleus is transferred into enucleated oocytes to recapitulate a fertilized egg. Cloned mice show random XCI, mirroring the normal XCR/XCI cycle during development. However, in the placenta of cloned mice the inactive state is maintained of the somatic donor cell, as extraembryonic tissues do not go through XCR (Eggan et al. 2000). The kinetics of XCR and XCI in cloned embryos is therefore consistent with the one that occurs during normal embryogenesis. However, in cloned embryos derived from ES cells as donor cells, with two active X chromosomes, random XCI also occurs in extra embryonic tissues, substituting for imprinted XCI.

Experiments of cell fusion to study XCR have been performed with embryonic carcinoma (EC) cells, derived from teratocarcinoma that show some pluripotency and are able to differentiate into three germ layers. Fusion experiments between female somatic cells and ECs can induce the reactivation of the Xi of the somatic cells (N Takagi et al. 1983; Forejt et al. 1999). Similar fusion experiments have been realized with mouse ES cells showing the capability of promoting Xi reactivation in somatic cells (M. Tada et al. 2001a; José Silva et al. 2006; Evans and Kaufman 1981). In addition, another type of cell fusion is the one with embryonic germ (EG) cells that can be derived from PGCs and maintained in culture showing the same characteristics as ES cells. The fusion between somatic cells and EGCs induces Xi reactivation and is also accompanied by the

erasure of genomic imprints consistent with PGC development (M. Tada et al. 1997). Furthermore, the recent generation of PGC-like cells (PGCLCs) from ES cells is very important in that regard as it also allows to study XCR in the germ cell lineage *in vitro* (Hayashi et al. 2012; Ohta et al. 2017) **(Fig. I10)**.

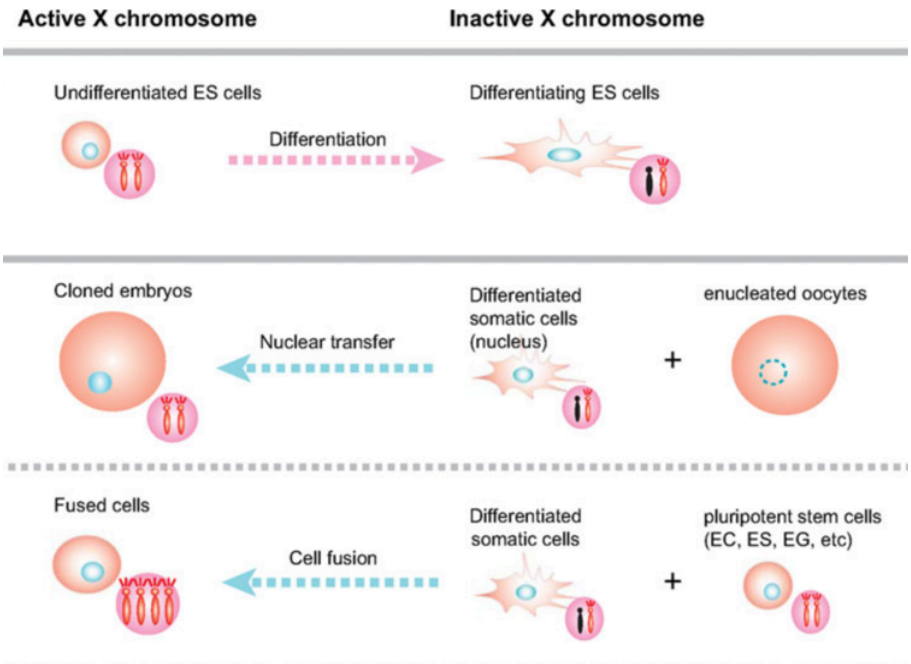

Figure I10 Experimental systems to study XCR. a) Upon differentiation of mouse female ES cells in somatic cells random XCI occurs. b) Experiments of somatic cell nuclear transfer into oocytes or cell fusion with mouse ES or EG cells can be used to study the reactivation of the X chromosome (Adapted from Ohhata and Wutz 2013).

2.2 X-Reactivation and Reprogramming of iPSCs.

An alternative system to study XCR is the reprogramming of mouse somatic cells into induced pluripotent stem cells (iPSCs) by overexpressing four transcription factors OCT4, SOX2, KLF4 and c-MYC (Takahashi and Yamanaka 2006b). Female mouse iPSCs have two active X chromosomes and upon differentiation they can undergo random XCI (Maherali et al. 2007) **(Fig.I11)**.

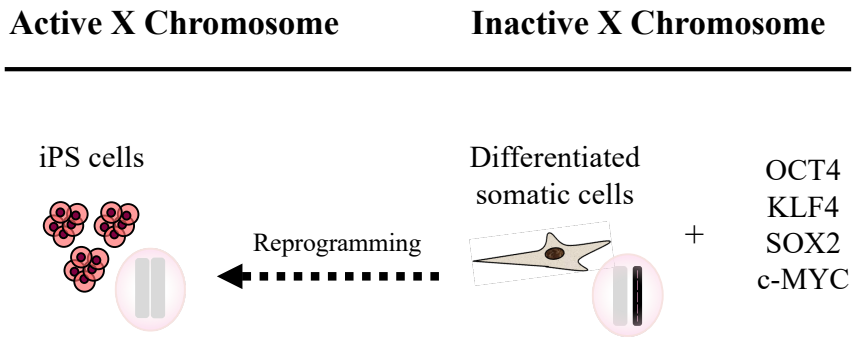

Figure I11 iPS cell reprogramming. Expression of four factors Oct4, Sox2, Klf4 and c-Myc can reprogram somatic cells into pluripotent cells and recapitulate the reactivation of the Xi (Adapted from Ohhata and Wutz 2013).

The big advantage of this system is that it allows to follow the sequence of events that lead to X chromosome reactivation (Pasque et al. 2014). It has been shown that XCR occurs as a late event in the reprogramming stage. The expression of reprogramming factors is not sufficient for the repression of Xist but, similar to XCR in the blastocyst, it happens after the reactivation of NANOG and PRDM14, which repress *Rnf12* (Payer et al. 2013; Pablo Navarro et al. 2011). However, the reactivation of X-linked genes occurs later, when other pluripotency factors such as DPPA4 and PECAM1 become expressed (Pasque et al. 2014). Therefore, XCR

seems to be linked to pluripotency induction during reprogramming to iPSCs.

As *Tsix* is important to prevent *Xist* ectopic expression on the Xa (J T Lee, Davidow, and Warshawsky 1999; Luikenhuis, Wutz, and Jaenisch 2001; Takashi Sado, Hoki, and Sasaki 2005; Pablo Navarro et al. 2005) lead to the hypothesis that it might be also required for *Xist* repression and XCR during reprogramming. However, in iPS cells XCR takes place, even in the absence of Tsix (Pasque et al. 2014; Payer et al. 2013).

In addition, it has been shown that the sequence of Tsix expression is reversed during reprogramming. In fact, it is reactivated first on the Xa and then on the Xi before reactivation of X-linked genes.

In this regard, different is the expression pattern of macroH2A that is enriched on the Xi only late in differentiation (Pasque et al. 2011; Mermoud et al. 1999) and it is retained on the Xi until late stages of reprogramming (Pasque et al. 2014).

Similar to macroH2A, the DNA demethylation on the Xi occurs late during reprogramming, only after Nanog reactivation. On major question is, if demethylation is due to passive and/or active mechanisms, for example involving TET proteins. It has been shown that TET1 and TET2 are dispensable for XCR and Xi-demethylation that probably proceeds through a passive mechanism (Pasque et al. 2014). However, further studies will be needed to unequivocally reveal the mechanism of DNA-demethylation during XCR.

Together, those studies show that XCR is tightly linked to the activation of the pluripotency program **(Fig.I12)**.

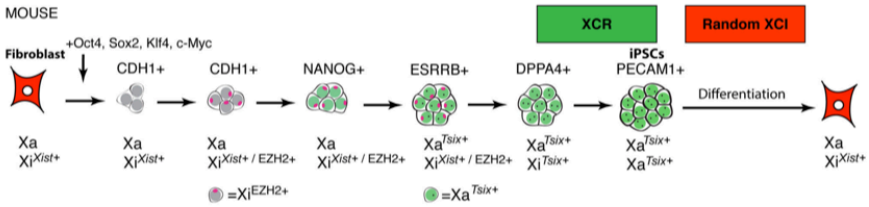

Figure I12 Stages of X-Reactivation in mouse iPSC. Shown the sequential induction of CDH1, NANOG, ERRB, DPPA4 and PECAM1. Establishment of EZH2 is represented as a pink dot whereas Tsix is shown by a black dot (Adapted from Pasque and Plath 2015).

2.3 Epigenetic modifications in iPS cell reprogramming

Reprogramming of somatic cells into induced pluripotent stem (iPS) cells involves major epigenetic changes regarding genome-wide modifications of histones and DNA methylation. The first iPSCs were generated in the lab of Yamanaka in 2006 by ectopic expression of four transcription factors: OCT4, SOX2, KLF4 and c-MYC (Takahashi and Yamanaka 2006a; Takahashi et al. 2007). Since then, the efficiency and the completeness of the system have been improved with the development of alternative approaches (Di Stefano et al. 2014; Vidal et al. 2014; Bar-Nur et al. 2014; Rais et al. 2013).

Cells undergo massive changes when reprogramming occurs. In particular many epigenetic modifiers are recruited to help the cells to go through this process. First of all, one of the earlier barriers to reprogramming is the histone modification H3K9me3 that marks heterochromatin in somatic cells. It has been shown that depletion of H3K9 methyltransferases such as SETDB1 increases the efficiency of iPSCs formation (Sridharan et al. 2013). Another study showed that along the reprogramming process many

regions of the somatic cells genome are mostly characterized by the H3K9me3 chromatin mark that makes them resistant to the OKSM binding (Soufi, Donahue, and Zaret 2012). The removal of this mark leads to full iPSC reprogramming.

In contrast, active chromatin marks such as H3K4me2 are distinctive of some enhancers involved in pluripotency at the early stages of the reprogramming (Koche et al. 2011). Other histone modifying enzymes are the H3K4me3 reader WDR5, which helps the interaction with OCT4 (Ang et al. 2011) or the H3K27 demethylase UTX that facilitates somatic cell reprogramming (Mansour et al. 2012). Other demethylases involved are KDM2A/2B that act on H3K36 and the histone remodeling complex BAF that increases the reprogramming efficiency by facilitating the interaction of OCT4 with its targets (Liang, He, and Zhang 2012; Singhal et al. 2010).

Then there is the histone variant macroH2A, known for its role as a repressive mark in gene silencing and XCI. Experiment of nuclear transfer showed that MacroH2A acts as barrier for somatic cell reprogramming (Pasque et al. 2011). Therefore, its removal increases iPSC formation up to 25-fold (Pasque et al. 2012).

Another important role in reprogramming is played by histone chaperones. The histone H3/H4 tetramer chaperon, APLF, can accelerate the reprogramming by enhancing the expression of E-cadherin and helping the mesenchymal-epithelial transition (MET) (Syed et al. 2016). In a recent study, by performing two RNAi screens to identify players in iPSCs formation, two subunits of CAF-1 complex have been identified as the most important hits (Cheloufi et al. 2015). CAF-1 is a histone chaperone responsible for the incorporation of old and new histones into chromosomes (Smith and Stillman 1989). That study shows that the suppression of those two subunits makes the chromatin more accessible at enhancer elements at the early reprogramming stage (Cheloufi et al.

2015). The main histone variants and modifiers in reprogramming are summarized in **Fig. I13**.

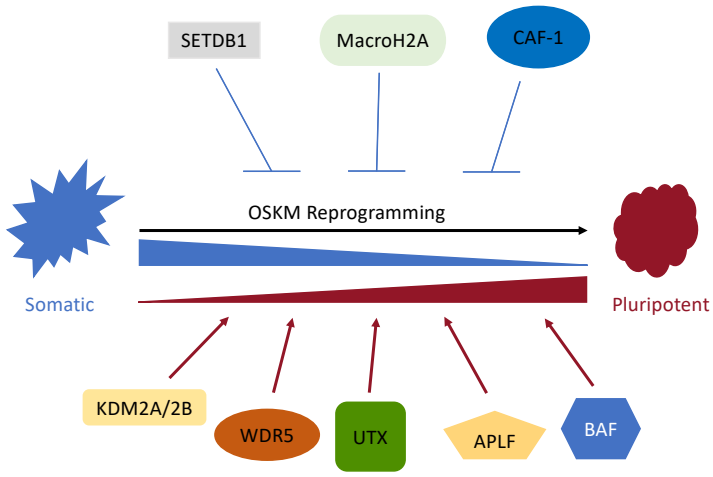

Figure I13 Epigenetic modifiers in iPS cell reprogramming. The modifiers above can inhibit the reprogramming such as SETDB1, etc. whereas the ones at the below including UTX, BAF, etc. can act as reprogramming enhancers (Adapted from Wang et al., 2017).

One of the distinctive marks of transcriptional silencing and heterochromatin formation is the methylation of CpG dinucleotides. Their methylation is catalyzed by DNA methyltransferases (DNMTs). There are three canonical DNMTs: DNMT3A/B are responsible for the *de novo* methylation while DNMT1 is required for methylation maintenance. It has been shown that DNA methylation acts as a barrier for somatic reprogramming. Therefore, the inhibition of DNMTs by addition of the inhibitor 5-aza-cytidine (5-AZA) increases the iPSC formation efficiency more than 30-fold (Mikkelsen et al. 2008).

On the other hand, DNA demethylation can occur through two mechanisms: passive or active DNA demethylation. The passive

mechanism is dependent on downregulation of DNMT expression and involves passive dilution of methylation during DNA replication. The active DNA demethylation is induced by catalyzing enzymes of the TET dioxygenases (TET1/TET2/TET3) family, which can convert 5-methylcytosine (5mC) to 5-hydroxymethylcytosine (5hmC) (Tahiliani et al. 2009). The 5hmC can be further converted to 5-formylcytosine (5fC) and 5-carboxylcytosine (5caC) by TET proteins, which can be recognized by thymine DNA glycosylase (TDG) and converted into unmodified cytosine to achieve active DNA demethylation (He et al. 2011).

TET1 and TET2 are up-regulated during reprogramming and they both interact with NANOG (Minor et al. 2013; Costa et al. 2013). TET2 overexpression can increase the reprogramming efficiency and moreover, a recent study shows that ablation of TET2 almost completely abolishes reprogramming to iPSCs (Sardina et al. 2018).

TET1, on the contrary, can promote or suppress reprogramming depending on the absence or presence of vitamin C (Esteban et al. 2010). TET1 deficiency increases the reprogramming and its overexpression affects it in the presence of vitamin C by modulating the MET. In the absence of vitamin C, TET1 enhances reprogramming independently of MET (J. Chen et al. 2013). However, another study shows that depletion of TET1 or TDG impairs somatic cell reprogramming by inhibiting MET (Hu et al. 2014), suggesting that TET1 might enhance the reprogramming at the late stage. Besides the epigenetic chromatin modifications, a recent study identified N^6-methyladenosine (m^6A), a modification of eukaryotic mRNA mediated by METTL3, as a promoter of the reprogramming. However, how this modification plays a role in reprogramming in combination with DNA methylation is still unknown (T. Chen et al. 2015).

Chapter 3. X Chromosome Architecture

Differences between Xi and Xa territories have been described since long time. Ohno was the first one to hypothesize that the inactive X-chromosome in Barr Body's structure was more compact than its homologue. However, it was not clear if the difference was due to a reduced volume or a difference in terms of their relative shapes or surface areas (Ohno and Haushka 1960). Studies on female cells from amniotic fluid showed that, in terms of volume, the Xa was not significantly larger than the Xi, approximatively 1.2x. In contrast, a difference in their shapes was evident in fact, the surface area of the Xa was greater than that of the Xi around 1.9x (Bischoff et al. 1993). Further studies on the same cell type confirmed the Xi territory has a spherical shape and smooth surface while the Xa's has a flattened shape and more irregular surface (Eils et al. 1996; Dietzel et al. 1998). Experiments of quantitative 3D multicolor fluorescence in situ hybridization (FISH) provided an additional evidence that the Xi has spherical shape in contrast to an ellipsoidal Xa and the Xi compaction is 1.2-fold higher than the one observed for the Xa (Giorgetti et al. 2014; Teller et al. 2011a; Naughton et al. 2010a).

The development of Chromosome Conformation Capture technique opened the possibility of investigating the 3D conformation of the chromosomes in the nucleus (Nagano et al. 2013; Lieberman-Aiden et al. 2009a; Dekker et al. 2002). Specifically, though he 4C-seq method that allows to generate interaction profiles between one locus of interest and all other loci in the genome, it has been shown that silenced genes on the Xi make fewer long-range interactions than do genes on the Xa, where active genes interact with other active regions. Escapee genes on the Xi, however, make contacts with other escapee genes (Splinter et al. 2011).

Chromosome conformation carbon capture (5C) allows to obtain contact maps showing interactions between all loci within a region of interest. This technique has been used to investigate the 3D structure of the mouse X Chromosome.

Particularly, it determined that the region around *Xist* locus is formed by discrete regions within which sequences preferentially contact each other and are called Topologically Associated Domains (TADs). Contacts across regions outside are much less frequent (Nora et al. 2012b). The Hi-C protocol extends the 5C and allows to determine all DNA-DNA interactions (Lieberman-Aiden et al. 2009b). The use of this technique showed that TADs were not specific to the region around *Xist*, but were observed to occur along all chromosomes, both in mouse and human (Dixon et al. 2012). The development of in situ Hi-C performed on intact nuclei and the following sequencing permits to define contact maps for both the maternal and the paternal chromosomes in human cells. Those maps revealed differences between the Xa and the Xi. The map of the Xa shows features seen in all autosomes with TADs presence whereas the Xi is devoid of those features and is partitioned in two mega-domains separated by a hinge region containing the macrosatellite repeat DXZ4, which encodes a lncRNA and it is conserved across the mammals (Rao et al. 2014). Further experiments, performed in mouse cells, confirmed the same conformational differences between active and inactive X chromosomes (Deng et al. 2015; Minajigi et al. 2015). In mouse as well, the macrosatellite DXZ4 was found at the hinge domain of the inactive X but also the minisatellite Ds-TR, not found in human (Horakova, Calabrese, et al. 2012; Darrow et al. 2014). Overall the bipartite structure is conserved across the mammals however the hinge domain in mouse is located centrally while in human it is on the long arm of the chromosome (Deng et al. 2015) **(Fig. I14)**.

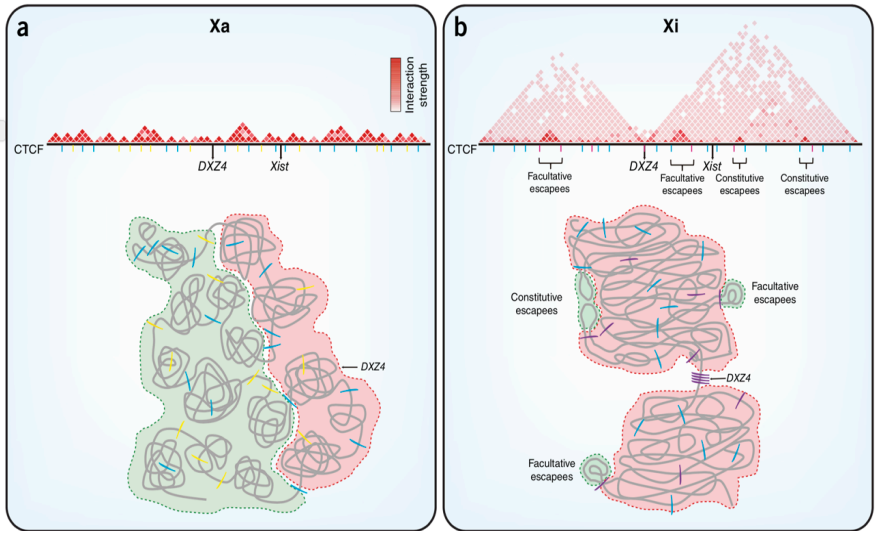

Figure I14 X-Chromosome topology. a) shown on the Xa the typical TAD organization of the active and repressive compartment. b) The Xi is organized into two repressive super domains separated by *DXZ4* locus. A few TAD-like structures are visible and are associated with facultative and constitutive escapees (Adapted from da Rocha and Heard 2017).

Besides TADs formation, another type of long-range intra-chromosomal interactions are the "loops". They are defined as enhanced contacts between distant loci which interact via CTCF. They can exist within and between TADs. High-resolution Hi-C data showed that the human Xi, but not the Xa, has a series of superloops, defined as extremely long range loops (Rao et al. 2014).

Superloops formation occurs between Xist, DXZ4 and FIRRE, another lncRNA on the Xi (Hacisuleyman et al. 2014, 2016) which binds CTCF only on the Xi (Rao et al. 2014; Horakova, Moseley, et al. 2012). In mouse those superloops were not detected by two studies (Deng et al. 2015; Giorgetti et al. 2016) but confirmed by a third one and, this might

reflect the difference in terms of cell type or methods (Darrow et al. 2016).

To investigate the role of the hinge in the Xi structure, a CRISPR/Cas9 approach has been used to remove 200kb region including *Dxz4* locus from the Xi. It revealed that the Xi bipartite structure was disrupted however, the XCI establishment was not affected (Giorgetti et al. 2016). The same experiment was performed in human deleting a large 300kb region. It resulted in the loss of the two megadomains and the Xi-specific DXZ4-FIRRE "superloop". The same deletion on the Xa does not have effect (Darrow et al. 2016). The deletion of Xist leads to a restoration of TADs on the inactive X towards an Xa-like state, with a possible recovery of most Xa-specific CTCF sites (Splinter et al. 2011; Minajigi et al. 2015). This result demonstrates that Xist has a major role in defining the structure of the inactive X **(Fig.I15)**.

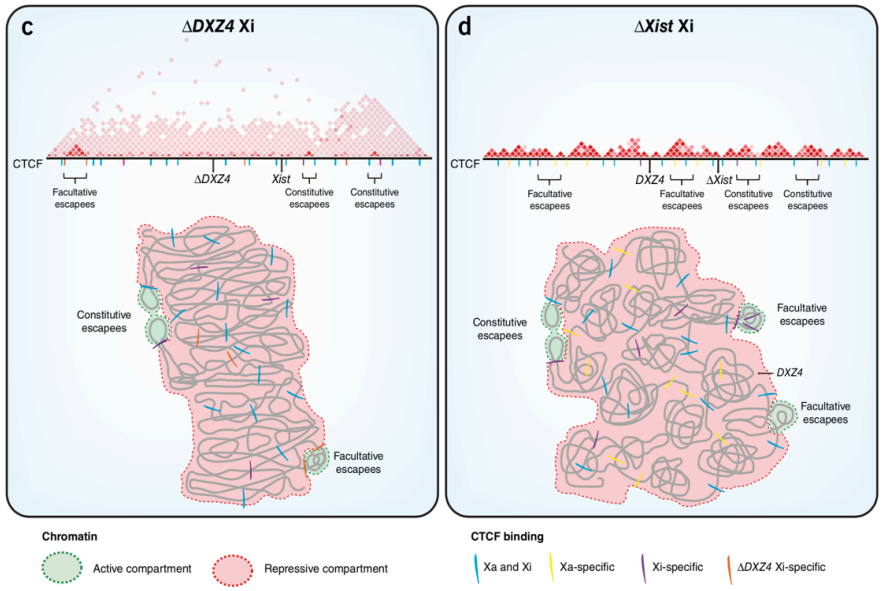

Figure I15 X-Chromosome topology (2). c) *DXZ4* deletion leads to a loss of the bipartite structute of the Xi and merging of the two repressive domains d) *Xist* deletion leads to the restoration of TADs to an Xa-like state (Adapted from da Rocha and Heard 2017).

This observation found a further confirmation in a recent study showing that the high order structures, megadomains and "superloops", are not necessary for XCI biology (Froberg et al. 2018). In fact, as already shown in other studies, the deletion of DXZ4 disrupts the megadomains on the Xi but it has no effect on gene silencing (Giorgetti et al. 2016; Darrow et al. 2016; Bonora et al. 2018; Froberg et al. 2018). In the same manner, the ablation of FIRRE on the Xi causes the deletion of "superloops", however, without any impact on the XCI. Indeed, those structures are not necessary for Xist spreading or chromosome wide silencing. They might occur in concomitance or as consequence thereof (Froberg et al. 2018).

3.1 Structure of the Inactivation Center (Xic) and Xist spreading in 3D

The *Xist* gene locus is part of a multi-megabase region of the X-Chromosome known as X Inactivation Center (*Xic*), which contains negative and positive regulators of the XCI. It has been shown that the X Inactivation Center is divided in two neighboring TADs with its boundary located between *Xist* and *Tsix* promoters. The *Xist* TAD contains the *Xist* promoter, its 5′ sequence and its positive regulators, including *Jpx*, *Ftx*, *Xpr* and *Rnf12* loci. The *Tsix* TAD contains the *Tsix* promoter, the 5′ sequence of *Tsix* and its activators, *Xite*, *Tsx* (Nora et al. 2012a). Within the Xist TAD, *Jpx*, *Ftx*, *Xist* show physical interactions (Nora et al. 2012a). In the same manner, it has been proposed that before XCI Tsix and Xite physically interact to promote Tsix expression and prevent Xist activation (Tsai et al. 2008). By contrast, on the future Xi, the interaction between Tsix and Xite is lost. Therefore, Tsix is repressed and the interaction between Xist and Jpx is activated (Nora et al. 2012a). The two TADs are separated by a region called RS14, located at 3' end of Xist. This region can bind CTCF and forms the boundary between *Xist* and *Tsix* TADs (Nora et al. 2012a; Tsai et al. 2008; Spencer et al. 2011) **(Fig.I16)**.

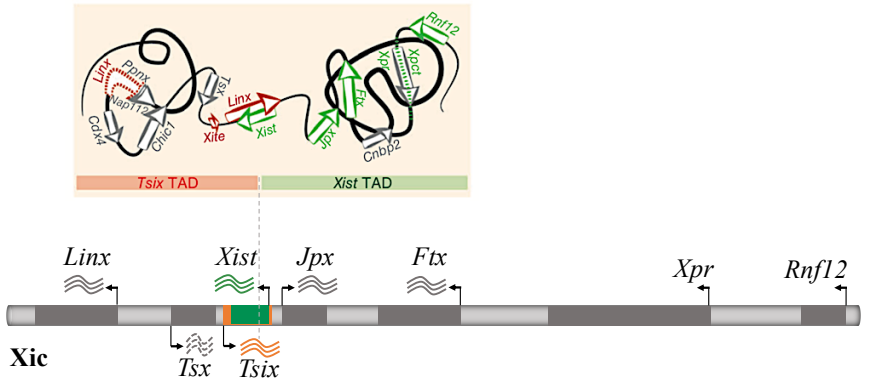

Figure I16 *Xist* and *Tsix* TADs. Schematic representation of the X-Inactivation Center (Xic) partitioned in two topologically associated domains (TADs). The *Tsix* TAD includes repressors of XCI (in red), while the *Xist* TAD encompasses XCI activators (in green) (Adapted from Furlan and Rougeulle 2016).

Once Xist is upregulated, it is still unclear how it can spread silencing on a 150Mb scale. However, recently, two high resolution RNA-DNA interaction detection methods, RAP (RNA Antisense Purification) and CHART-seq (Capture Hybridization Analysis of RNA Targets with deep sequencing), described the process (Engreitz et al. 2013; Simon et al. 2013). Those two techniques show that Xist follows a two-step mechanism, initially it accumulates at the targeting gene-rich islands through the Repeat A and then, it spreads to silence neighboring gene-poor domains. Moreover, it has shown that Xist does not spread linearly but it uses a proximity-mediated mechanism in a way that regions close to the locus in a 3D space are the first one coated, even if those sites are many megabases away when measured linearly on the chromosome (Engreitz et al. 2013). This result has been confirmed by ectopically expressing Xist from site away from its locus (Tang et al. 2010). In fact,

in the same way it shows that Xist spreading depends on the existing 3D conformation of the X-chromosome.

Once XCI takes place, the two chromosomes can move to different subnuclear positions. The Xa does not have a specific position in the nucleus whereas Xi has two preferential locations: the nuclear periphery and next to the nucleolus (perinucleolar). By microscopy it has been shown that the Xi is at the nuclear envelope in 75-80% of interphase cells. During cell differentiation, some TADs on the Xi become lamina associate domains (LADs). A new study has shown that the Xi is recruited to the nuclear lamina via lamin B receptor (LBR), a protein binding to Xist-lncRNA (C.-K. Chen et al. 2016; McHugh et al. 2015; Minajigi et al. 2015) It is required to complete Xist coating across the chromosome. During S phase 80-90% of the Xi migrates to the perinucleolar site. The Xi seems to form a ring around the nucleolus which is enriched of SNF2 H, required for heterochromatin replication (Zhang, Huynh, and Lee 2007). The deletion of *Xist* causes a loss in association of the Xi to the nucleolus and as well *Xist* insertion on an autosome induces its association to the nucleolus. In addition to Xist, DXZ4 and FIRRE might help anchoring the Xi to the nucleolus. Both lncRNAs DXZ4 and FIRRE are bound by nucleophosmin, a protein located at the periphery of the nucleolus (Fan Yang et al. 2015). In addition, both DXZ4 and FIRRE on the Xi appear adjacent to the edge of the nucleolus and might tether it there. However, it is still not clear which is the mechanism behind it. A recent study shows that FIRRE is expressed from the Xi and its loss causes a decrease in association with the nucleolus and a loss of the repressive mark H3K27me3 on the Xi, but it does not cause reactivation of X-linked genes (Fan Yang et al. 2015). Both lncRNAs are also bound by CTCF and knocking down *Ctcf* expression causes a reduction in the association of FIRRE and DXZ4 with the perinucleolar region. CTCF also interacts with nucleophosmin and plays a role in tethering Xist and the

other lncRNAs to the nucleolus. Those data suggest that the association of the Xi to the nucleolus has a role in gene silencing and X-inactivation-maintenance **(Fig.I17)**.

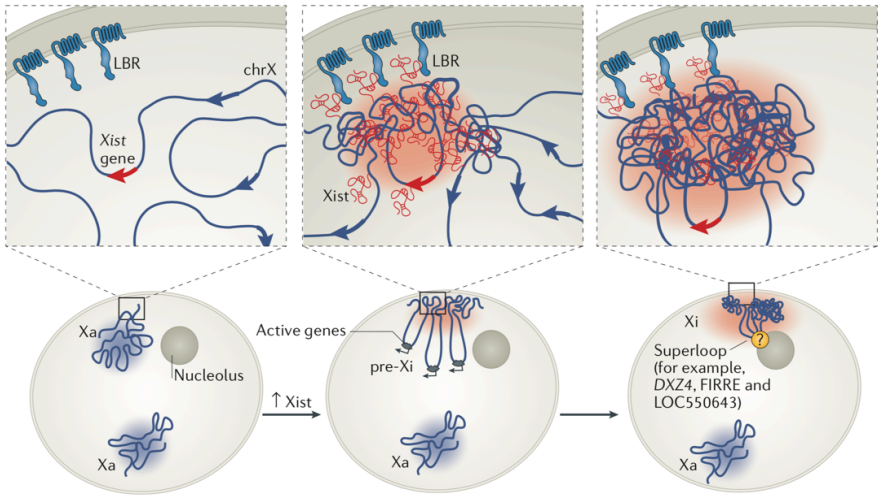

Figure I17 The final journey through the space. Before XCI, both X chromosomes are active and not strongly associated with nuclear lamina (left). Once Xist has been expressed, it starts spreading across the future inactive chromosome and interacts with the lamin B receptor (LBR) inducing the localization of the X chromosome to the nuclear lamina (middle). Finally, active genes are sequestered into the Xist compartment (red area) and silenced (right). During this process, two mega-domains appear on the inactive X, separated by a hinge at the *Dxz4* locus. DXZ4 is associated with the nucleolus and forms super-loops with specific loci including the ones encoding FIRRE (Adapted from da Rocha and Heard 2017).

3.2 Cohesin and CTCF code for 3D genome topology

As explained earlier, the chromosome architecture is characterized by long range intra-chromosomal interactions: TADs and "loops" (Rao et al. 2014). Another structural level is represented by "compartments", formed by interactions between chromatin of similar epigenetic states. A-compartments is characterized by regions enriched for active genes (euchromatin) whereas B-compartments harbor regions enriched for repressed genes (heterochromatin) (Rao et al. 2014, 2017; Schwarzer et al. 2017; Lieberman-Aiden et al. 2009a; Nora et al. 2017; Rowley et al. 2017). The boundaries of TADs and loops are enriched for the zinc finger protein, CTCF (Dixon et al. 2012). CTCF is a protein with insulator activity (Bell, West, and Felsenfeld 1999) and one of the first factors described as being involved in chromatin looping (Splinter et al. 2006; Handoko et al. 2011). It is associated and positions cohesins on chromatin, which are key chromatin components (Wendt et al. 2008) and together they lie at the anchor of the loops (Rao et al. 2014; Splinter et al. 2006) and TADs (Dixon et al. 2012; Rao et al. 2014; Nora et al. 2012a; Lieberman-Aiden et al. 2009b) to help regulating the genome folding.

3.2.1 Cohesin structure and function

As shown in **Fig. I18**, the multi subunit complex cohesin, is composed by two structural maintenance of chromosomes (SMC) subunits SMC1 and SMC3 which associate to form a tripartite ring including α-kleisin subunit, MCD1/SCC1/RAD21. SMC1 and SMC3 fold back to themselves to form antiparallel coiled-coils with a hinge domain to dimerize at one end. At the other end there is a globular ATP head to connect to the α-kleisin subunit in order to complete the cohesin ring structure and encircle

the DNA strands (Haering et al. 2002). The α-kleisin subunit interacts with additional proteins as SCC3/STROMALIN (SA), PDS5, and WAPL. The PSD5/WAPL complex releases cohesins from the chromosome by opening the interface SMC3/RAD12, while other proteins as the dimer SCC2/MAU2, load cohesin onto the DNA (Kueng et al. 2006b).

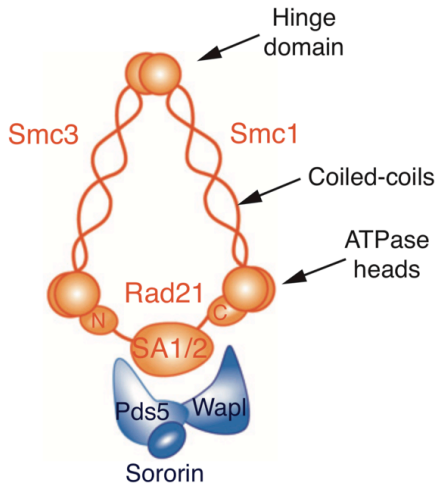

Figure I18 Structure of the cohesin complex. Cohesin is composed of four subunits (orange). SMC1 and SMC3 fold back to themselves to form antiparallel coiled-coils with a hinge domain to dimerize at one end. At the other end there is a globular ATP head to connect to the α-kleisin SCC1/RAD21 subunit in order to complete the cohesin ring structure. The α-kleisin subunit interacts with additional proteins as SCC3/STROMALIN (either SA1 or SA2 in vertebrate somatic cells), PDS5, and WAPL (blue) (Adapted from Remeseiro and Losada 2013).

The cohesin complex has multiple roles in cell division, DNA damage repair, gene transcription and chromosome architecture. The best role characterized for cohesin is sister chromatid cohesion during cell cycle (Guacci, Koshland, and Strunnikov 1997; Michaelis, Ciosk, and Nasmyth

1997). In fact, cohesin holds sister chromatids together in S phase until cell division in anaphase. The complex SCC2/MAU2 loads them onto chromatin in early G1 to mediate cohesion during cell replication and then in prophase cohesin is released by the complex PSD5/WAPL (Panizza et al. n.d.; Kueng et al. 2006a). Complete loss of cohesin subunits is lethal, breaking the cohesion between sister chromatids and precocious separation in metaphase (Michaelis, Ciosk, and Nasmyth 1997).
Cohesins have another important role in DNA double strand break repair. They accumulate near double strand breaks where they stabilize cohesion and contribute to DNA damage/repair (H. Xu et al. 2010).

3.2.2 Cohesins and Chromosome architecture.

In the last years one of the most explored function of cohesin is the role in gene regulation and chromosome architecture. Cohesins mediate gene regulation by long-range interaction loops between their binding sites and between enhancers and promoters. Their direct role in chromatin looping has been shown at several loci, where they interact with specific transcription factors (Kagey et al. 2010). In fact, after knocking down cohesin expression, the long-range interactions among regulatory regions are reduced. As described earlier, cohesins mediate chromatin loop formation in combination with CTCF. The current popular model to explain how cohesins organize chromosomes is the loop extrusion model (Alipour and Marko 2012; Goloborodko, Marko, and Mirny 2016). According to this model, the extrusion complex is formed by two cohesins rings and two CTCF proteins that act as DNA-binding subunits. When this complex is loaded onto the DNA, a tiny loop forms. The two subunits engage the DNA in an asymmetrical way, sliding in opposite directions and initiating loops formation. Loop extrusion stops either when cohesins dissociate from the DNA or when CTCF proteins detect a target motif and arrest the process, specifying the base of the loop (Rao et al. 2014; Vietri

Rudan et al. 2015; Davidson et al. 2016). Loop extrusion has been proposed to determine TADs formation. The loops are lost when cohesins are degraded but they reform when cohesins are restored (Fudenberg et al. 2016). Interestingly, compartments are not lost upon cohesin depletion, suggesting the role of additional proteins in maintaining this level of chromosome organization (Zuin et al. 2014; Sofueva et al. 2013; Seitan et al. 2013). The loop extrusion model is an attractive model that suggests how cohesin proteins could organize domains of chromatin into loops that are topologically distinct from each other **(Fig.I19)**.

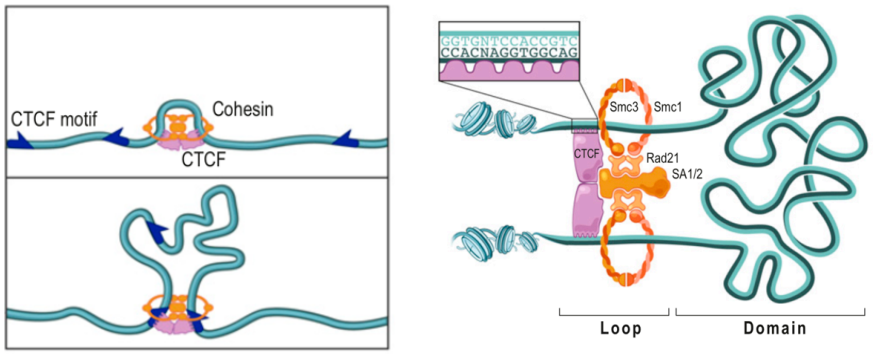

Figure I19 Loop extrusion model. The complex includes two DNA-binding subunits each has a cohesin ring (orange) and a CTCF protein (pink). A tiny loop begins to form when DNA is extruded from the complex. The two subunits involve the chromatin fiber in an antisymmetric manner, with their CTCF proteins facing the outside of the loop, scanning opposite DNA strands. The loop expands without knotting while the subunits move in opposite directions. When the CTCF proteins find a target motif on the proper strand, they can bind and arrest the progress of the subunit. Eventually the extrusion complex can dissociate (Adapted from Sanborn et al., 2015).

3.2.3 Xist RNA repels cohesins from the Xi.

By forcing or disrupting Xist expression, it has been shown that it also contributes to shape X-Chromosome conformation. In fact, forced expression of Xist RNA in ESCs induces the appearance of insulation at the mega-domain boundary region (Giorgetti et al. 2016). Therefore, Xist seems to be involved in the formation of the mega-domain boundaries. Conditional ablation of Xist (Xi*ΔXist*) from the Xi in mouse fibroblasts induces its reorganization into a similar structure as the Xa. TADs are restored on the mutant Xi and there is also an increase of cohesin binding at the same sites bound on the Xa. There are evidences that show how the binding of cohesins on the Xa is different from the Xi. Cohesins bind the X-Chromosome in a specific manner that favors the Xa conformation. In fact, there are 500-600 Xa cohesin specific sites and only 20 are specific for the Xi. The rest of ~200 sites are shared between the Xi and the Xa. Proteomic studies show that Xist directly interacts with both CTCF and cohesins (Minajigi et al. 2015). So, the hypothesis is that Xist interferes with the binding of cohesins to the Xi. It seems to act by repelling the binding in *cis* of a set of cohesins, preventing the establishment of Xa-like binding pattern (Minajigi et al. 2015). Therefore, as mentioned earlier, deletion of Xist causes the restoration of TADs and also the re-establishment of Xi-cohesins binding, proving how Xist is necessary for the maintenance of the 3D organization of the Xi (Splinter et al. 2011) **(Fig.I20)**.

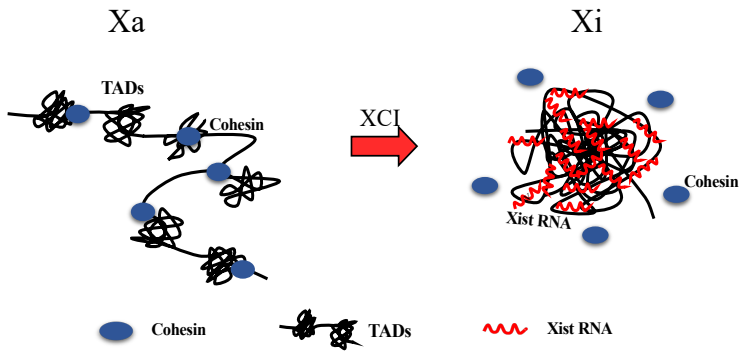

Figure I20 Xist RNA repels cohesin from the Xi. The Xa is divided in TADs and cohesin play a role in organizing this structure (left). On the Xi, *Xist* RNA displaces cohesins from critical sites leading to the loss of TADs and a more disorganized chromosome structure (right) (Adapted from Payer 2017).

An atypical member of the SMC proteins, SMCHD1 (structural maintenance of chromosomes hinge domain containing 1), is required for DNA methylation at many Xi CpG islands (Blewitt et al. 2008; Gendrel et al. 2012). This protein has been previously implicated in the compaction of human Xi (Nozawa et al. 2013). However, recent studies suggest that it is required for promoting the loss or attenuation of TADs on the Xi. Depletion of SMCHD1 induces an increase of short-range interactions at the level of TADs (Gdula et al. 2018; C.-Y. Wang et al. 2018; Jansz et al. 2018). Changes in 3D architecture of the Xi upon Smchd1 are not dependent on transcriptional changes (Gdula et al. 2018; Jansz et al. 2018). Therefore, it might play different roles at the structural and transcriptional levels.

Objectives

Although X-Chromosome Inactivation (XCI) has been well studied, multiple open questions remain to elucidate the inverse process of X-Chromosome Reactivation (XCR). To better understand it, a single cell microarray screen at the blastocyst stage of embryo development has been performed previously by my supervisor Bernhard Payer (unpublished), which is the starting point of my thesis. The screen aimed at identifying regulators of XCR, whose expression profile is anti-correlated with *Xist* during XCR in the epiblast of mouse blastocysts. My Thesis work has focused on a secondary functional screen during the reprogramming in iPSCs, testing the role of the candidates picked from the expression profiling in blastocysts. Differentiated somatic cells can be reprogrammed into induced pluripotent stem (iPS) cells by overexpressing the four transcription factors OCT4, SOX2, KLF4 and c-MYC. During this process female iPS cells reactivate the inactive X-chromosome when they start to express endogenous pluripotency factors. Thus, the hypothesis was raised that among the candidates, some of them could play a role in Pluripotency and/or X-Reactivation.

Therefore, the objectives of the Thesis work were the following:

I. To investigate if candidate factors play a role in pluripotency establishment;
II. To investigate their potential function in X-Reactivation;
II. To investigate the mechanistic role of one of the top candidates. the cohesin complex member Smc1a, during X-Reactivation.

Results

1. Work leading up to the project

1.1 Single-cell expression screen for differentially expressed genes correlated with XCR in mouse blastocysts.

Transcriptional reactivation of the Xp occurs in the mouse blastocyst during pre- to peri-implantation development. In the trophectoderm (TE) and the primitive endoderm (PE), which contribute to the placenta and yolk sac, respectively, imprinted silencing of the Xp is maintained. In contrast, in the epiblast (EPI) cells within the inner cell mass (ICM) of the blastocyst, the Xp is reactivated (Huynh and Lee 2003a). In order to identify novel factors involved in XCR, single cell microarray expression profiling has been performed by my supervisor Bernhard Payer (unpublished) looking at the blastocyst at different stages: early (E3.5), intermediate (E4.25) and late (E4.5). The main purpose was to cover the entire process before, during and after XCR.

Blastocyst embryos have been dissociated and single cells were picked from PE and EPI tissues to perform amplification and single cell microarrays (Kazuki Kurimoto et al. 2007; K. Kurimoto et al. 2006) **(Fig.R1a)**.

After generating expression profiles, 228 candidate genes with a potential role in XCR have been identified, which were selected according to the following criteria. First of all, they are lowly expressed in PE and in EPI before reactivation at E3.5. They become upregulated in female epiblast during XCR (E4.25-E4.5) and therefore are anti-correlated to *Xist*-expression, which is downregulated during XCR. The candidate factors may be also upregulated in male epiblast, which only have one X chromosome, as male pluripotent stem cells have XCR activity in fusion

experiments with female somatic cells (M. Tada et al. 2001b).

Anticorrelation with *Xist* expression in female epiblast of the first five top candidates is shown in **Fig.R1b**. In epiblast they are upregulated while in primitive endoderm, where there is no X-Chromosome Reactivation, their expression is low. In a similar way in male epiblast their expression is rising whereas *Xist* expression remains low. Among the candidates that came out there is the lncRNA Tsix, confirming its role in XCR described before (Payer et al. 2013). Based on expression change and expected likelihood of involvement in XCR according to gene ontology, 57 candidates were picked for further validation with 3 internal controls **(Fig.R1c)**.

In general, it is possible to classify those candidates in different categories according to their function: transcriptional regulation, cell cycle regulation, chromatin-related factors and other/unknow function category **(Fig.R1d)**. A complete list with the 57 candidates and controls (*) it is provided in **Table MM4** in Material and Methods.

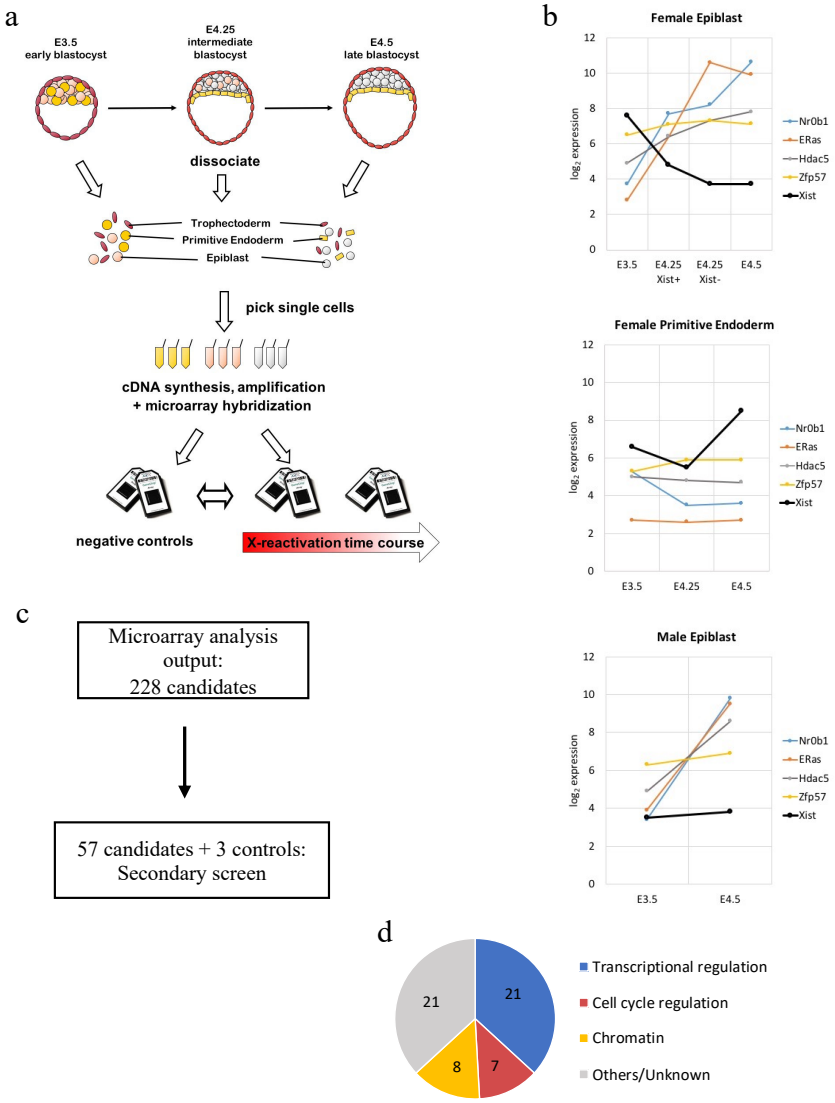

Figure R1 Single cell microarray in blastocyst. a) Microarray experiment workflow (B.Payer). b) Expression profile of the first five top candidates of the microarray in female EPI, female PE and male EPI. c) Schematic representation of the screen work-flow. d) Pie chart of candidates-related pathways.

2. Secondary functional shRNA-knockdown screen during iPSC-reprogramming.

2.1. *In vitro* iPSCs reprogramming system

As *Xist*-anticorrelation is indicative but does not guarantee a role in XCR, a secondary functional screen has been devised to validate real XCR regulators. Therefore, we used the *in vitro* iPSCs reprogramming system in which differentiated somatic cells can be reprogrammed into induced pluripotent stem (iPS) cells.

Along this process female iPS cells reactivate the inactive X-Chromosome and when re-differentiated in culture, they undergo again random X-inactivation, indicating the erasure of epigenetic memory of the previously inactive X-Chromosome during their generation (Maherali et al. 2007). This system gives us the big advantage to follow the XCR dynamics *in vitro*. We have used mouse embryonic fibroblasts (MEFs) derived from "reprogrammable" mice which are converted into iPSCs using a doxycycline (Dox)-inducible *Oct4, Klf4, Sox2* and *c-Myc* (OKSM) cassette (Stadtfeld et al. 2010). Moreover, we took advantage of boosting the reprogramming efficiency with ascorbic acid (Vitamin C) (Esteban et al. 2010).

In order to follow the XCR process along the reprogramming, the cells carry a *GFP*-transgene on the inactive X (Hadjantonakis et al. 2001) **(Fig. R2)**. It is based on the use of an X-linked GFP marker gene (*XGFP*) and MEFs that bear the *XGFP* transgene on the Xi (*XGFP*-negative cells) were sorted by FACS (fluorescence-activated cell sorting).

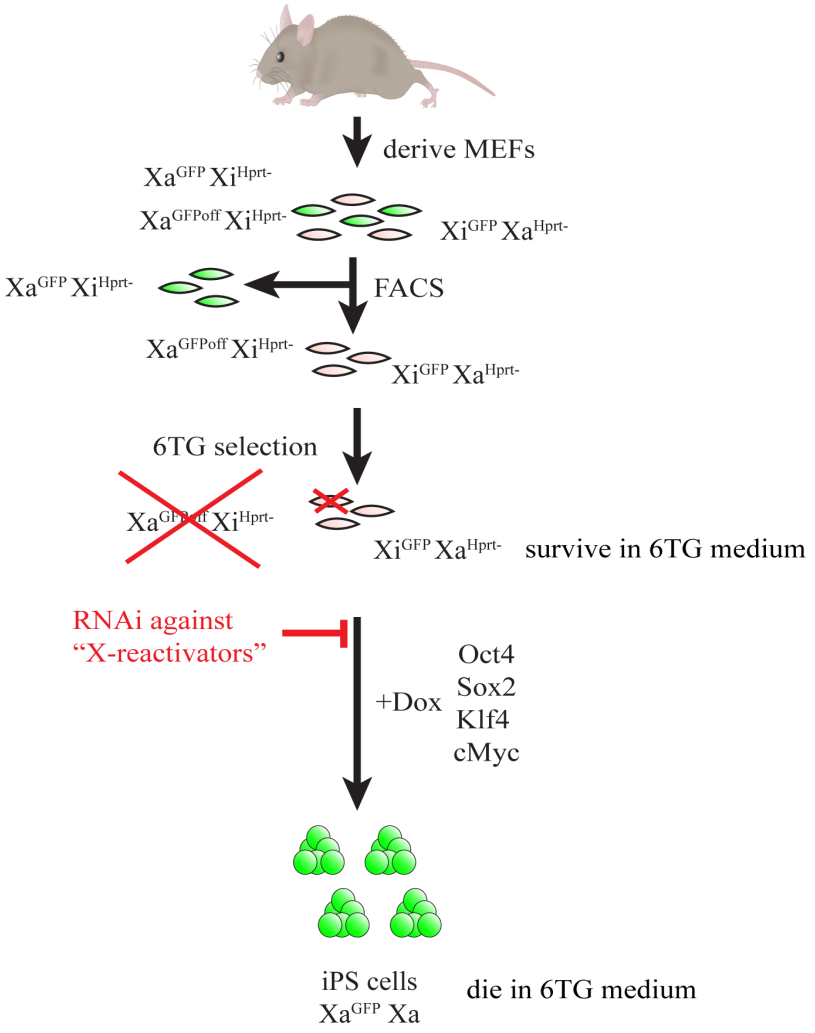

Figure R2 RNAi screen. Experimental design of the RNAi screen work- flow (B. Payer).

However, previous experiments have shown that about 0-20% (cell line-specific variation) of Xa^{GFP} seems to be silent in primary fibroblasts indicating occasional X-inactivation-unrelated silencing of the *XGFP*

transgene (Eggan et al. 2000). In order to obtain populations of cells with a clear-cut XCI state, it is necessary to get rid of those dark cells that have GFP on the active X-chromosome. We applied a drug selection scheme based on the endogenous X-linked *HPRT* gene for that purpose. In fact, our cell line besides carrying an *XGFP* transgene also has a mutation in one of the two *HPRT* alleles on the counter X-Chromosome. So, after FACS-sorting the cells to be $Xi^{GFP}/Xa^{Hprt–}$, we grow them in 6-thio-guanine (6-TG) medium, where only cells with a mutated *HPRT* gene can survive, killing those cells with a wildtype *HPRT* allele on the active X-Chromosome (Eggan et al. 2000). The sorted and 6-TG-selected XGFP-cells are reprogrammed and used to determine XCR efficiency by scoring for *XGFP* reactivation.

2.2. System characterization

Fig. R3a shows a schematic representation of the kinetics of iPSC reprogramming with our cell line. The first step was to score the reprogramming efficiency as a percent of primary colonies formed per input MEFs after Dox induction **(Fig. R3b)**. The efficiency of our system was more than 2%, improved in comparison to what has been published about the same inducible system (around 1.4% efficiency) (Stadtfeld et al. 2010). This is confirmed by one of the most common assays to assess the pluripotency state: the formation of alkaline phosphatase (AP)-positive colonies **(Fig. R3b)**.

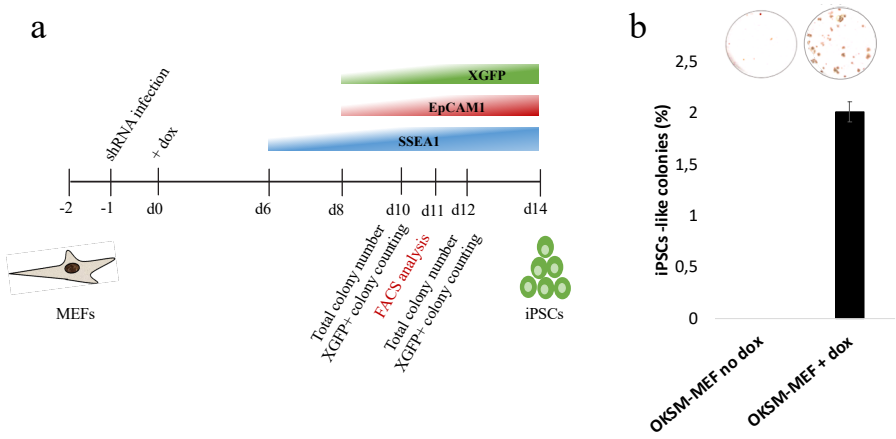

Figure R3 In vitro iPSC system (I). a) Schematic representation of the reprogramming experiment. b) Reprogramming efficiency graph: OKSM-MEF no dox control versus OKSM-MEF +dox. Reprogramming efficiency was scored as the percent of primary colonies formed per input MEFs after 14 days of dox induction. Each graph depicts data from one experiment performed in triplicate (error bars = SEM). On top is shown the alkaline phosphatase (AP) staining of d14 iPSC colonies.

Few days after dox addition, cells started to change morphology and form aggregates. The first colonies emerged after 4-5 days of OKSM expression leading to proper iPSCs around day 10. As expected, X-Chromosome Reactivation occurred as well. The first evidence of *XGFP* reactivation was visible around day 8, where few cells within the colonies started to become green. The percentage increased along the reprogramming up to reach full XCR at the endpoint of the reprogramming **(Fig. R4a)** To further refine the kinetics of iPSC reprogramming, we examined cell surface markers of pluripotency (Polo

et al. Cell 2012), which identified early (SSEA1) and late (EpCAM1) iPSC stages by FACS. At the beginning in absence of dox, non-reprogrammed MEFs and feeders were completely negative for any pluripotency marker **(Fig. R4b)**. At day 6, after emerging of the first colonies, the early marker SSEA1 showed up. At day 8, it became possible to visualize a nascent population of cells that were double-positive for SSEA1 and the late marker EpCAM1. That population became clearer at day 10. At the last stages of reprogramming the majority of cell, about 80%, was SSEA1/EpCAM1 double-positive.

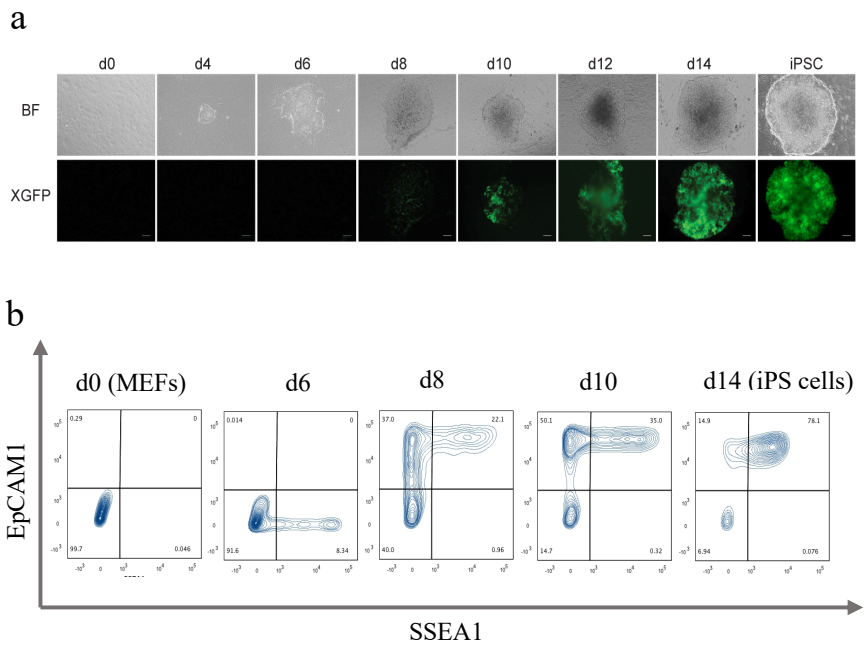

Figure R4 In vitro iPSC system (II). a) Imaging of reprogramming time points (d0-d14) showing in brightfield (BF) the colony formation and in green the XGFP reactivation. b) FACS analysis of different reprogramming time points staining the cells by two surface markers EpCAM1(y-axis) and SSEA1.

An important feature of iPS cells is the expression of endogenous pluripotency genes and independent self-renewal without exogenous OKSM expression (Polo et al. 2012; Stadtfeld et al. 2008). To ensure that the iPSCs analyzed at the end of our time-course were fully reprogrammed, we therefore withdrew dox at day 12 of reprogramming.

We further characterized reprogramming by analyzing transcriptional levels of pluripotency genes such as *Oct3/4* and *Nanog* at different time points: d6, d8, d10, d12, d14 and no dox control **(Fig. R5)**. It is important to specify that we were looking at the bulk population, meaning that it was a mixed population of reprogrammed cells, feeders and non-reprogrammed cells. We observed an upregulation of both genes starting from d6 and the levels were kept stable in the latest days when proper iPSCs were formed. We also followed the kinetics of *XGFP* reactivation at the transcriptional level. In agreement with what we saw by microscopy, XCR occurred from d8 of reprogramming onwards. Related to X-Chromosome dynamics, we also checked expression of *Xist*, the master regulator of XCI and its counterpart, *Tsix*. Around day 8 *Xist* started to be downregulated and at the same time *Tsix* started to be expressed.

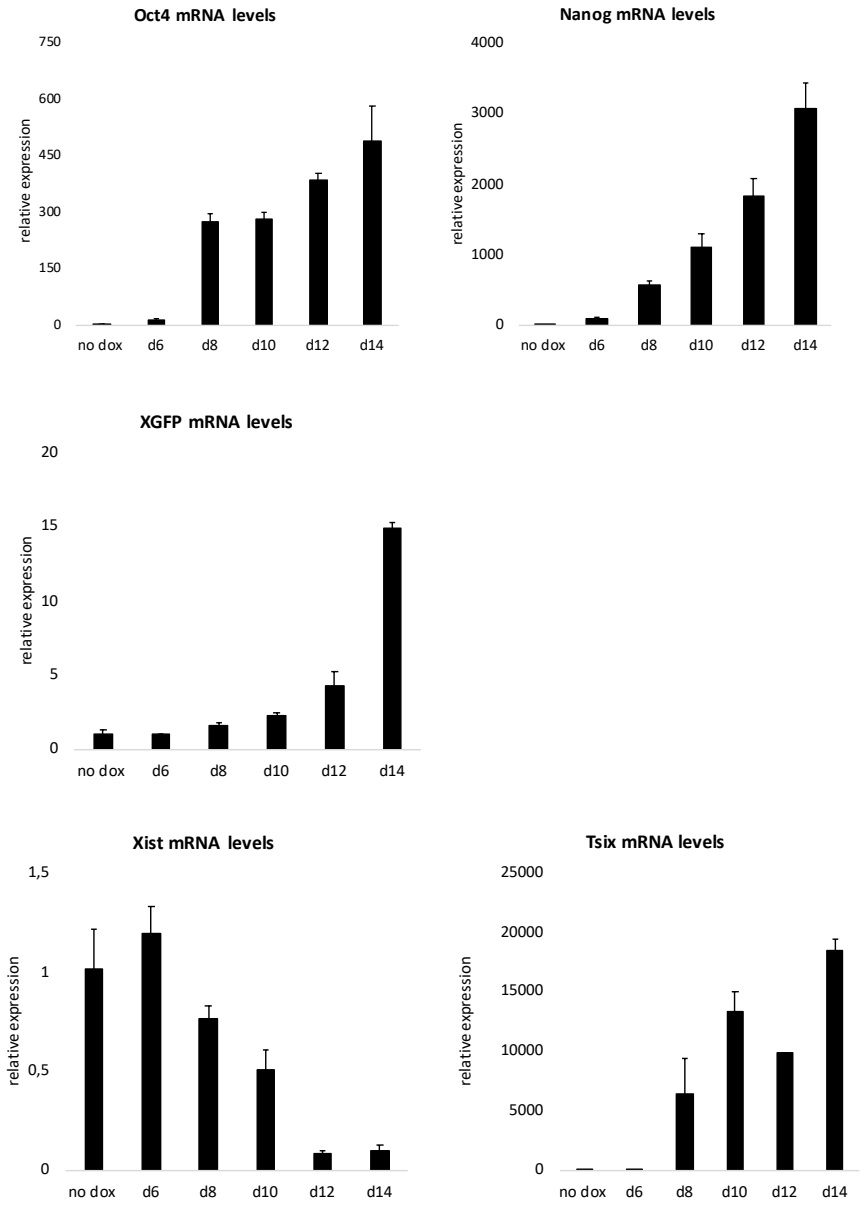

Figure R5 Transcriptional changes during iPSC reprogramming. Assessment by Real time PCR of mRNA expression levels at different reprogramming time points of key genes such as *Oct4, Nanog, Tsix, Xist* and *XGFP*-transgene reactivation**.** Expression levels are normalized by *GAPDH* relative to no dox control (set to 1) (Error bars=SEM).

3. RNAi screen in iPSCs

To investigate the putative involvement of the 57 candidates we selected from the single cell microarray screen in XCR and reprogramming, we performed a secondary RNAi screen.
We infected OKSM-MEFs with lentiviruses (Stadtfeld et al. 2010; Moffat et al. 2006) expressing either an shRNA with a not mammalian-target sequence (shLacZ) as a negative control or using 3 different shRNAs against each candidate in order to knockdown their expression **(Fig. R6a)**. We grouped the 60 candidates into two batches of 30 candidates and we performed the RNAi screen three times for each batch having two technical replicates. 24h after infecting the fibroblasts, we seeded them onto feeders and induced reprogramming by adding dox. As expected, the first colonies appeared around day 4-5. At day 8, we started seeing *XGFP* reactivation and at day 10 we counted total colony and XGFP+ colony numbers for each condition. The day after, we performed a FACS analysis looking at the pluripotent cells by staining them with two surface markers, SSEA1 and EpCAM1. Moreover, within the double positive population (SSEA1+EpCAM1+) we looked at the percentage of GFP positive cells. We used day 12 as second time point to count again the total number of colonies and the number of XGFP+ ones.

Once we started the screen, we faced the difficulty to check the knockdown efficiency for each shRNA in each screening run. Therefore, we decided to get an overall idea of knockdown efficiency by assessing the expression level of internal controls for both reprogramming and XCR process and whose virus titer was in the same range as the majority of the lentiviruses used. Specifically, we looked at *Oct3/4* and *GFP* shRNA knockdown by Real Time PCR (RT-PCR) and in both cases, on average,

for all three shRNAs the efficiency was around 80% as shown in a representative graph in **Fig. R6b**.

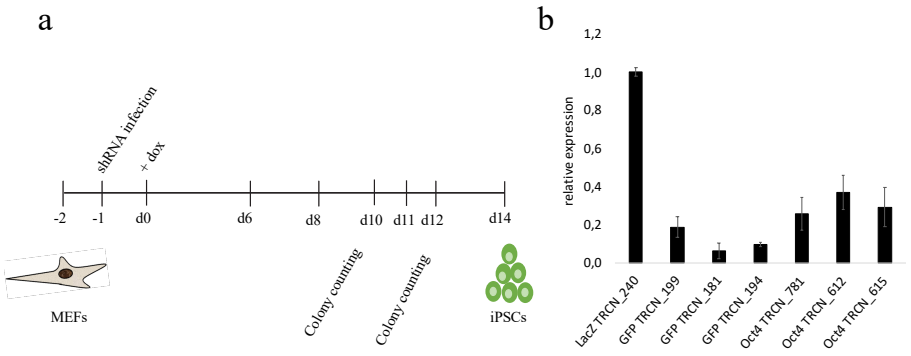

Figure R6 RNAi screen during iPSC reprogramming. a) Schematic representation of the lentiviral infection and reprogramming time course. b) Assessment of mRNA levels of Oct4 and GFP by Real time PCR 72h post infection and 48h after inducing the reprogramming by dox addition. LacZ shRNA as a control. Expression levels are normalized by *GAPDH* relative to LacZ shRNA (set to 1) (Error bars=SEM).

3.1 Factors involved in pluripotency

The first aspect we looked at was reprogramming efficiency, by assessing how the knockdown of the candidate factors was affecting iPSC colony formation. As all the picked candidates are upregulated in the epiblast lineage, which is the precursor to ESCs and all embryonic cell types, we expected many candidates to have a general role for pluripotency and stem cell reprogramming. Indeed, we observed that the knockdown of the majority of the candidates had an effect on pluripotency **(Fig. R7a-b)**.

We analyzed the absolute colony number and then calculated the reprogramming efficiency, normalizing by LacZ shRNA as negative control and compared two replicates. In order to classify our candidates into different categories, either enhancers or repressors of reprogramming, we used some positive controls whose role in pluripotency has been extensively described. First of all, known reprogramming enhancers such as OCT4 and NANOG, showed as expected low reprogramming efficiency when their expression was reduced (Jose Silva et al. 2009; Takahashi and Yamanaka 2006b). On the other hand, TCF3 and DNMT1, known repressors of reprogramming, showed an increase in terms of reprogramming efficiency when their expression was knocked down (Lluis et al. 2011; Mikkelsen et al. 2008).

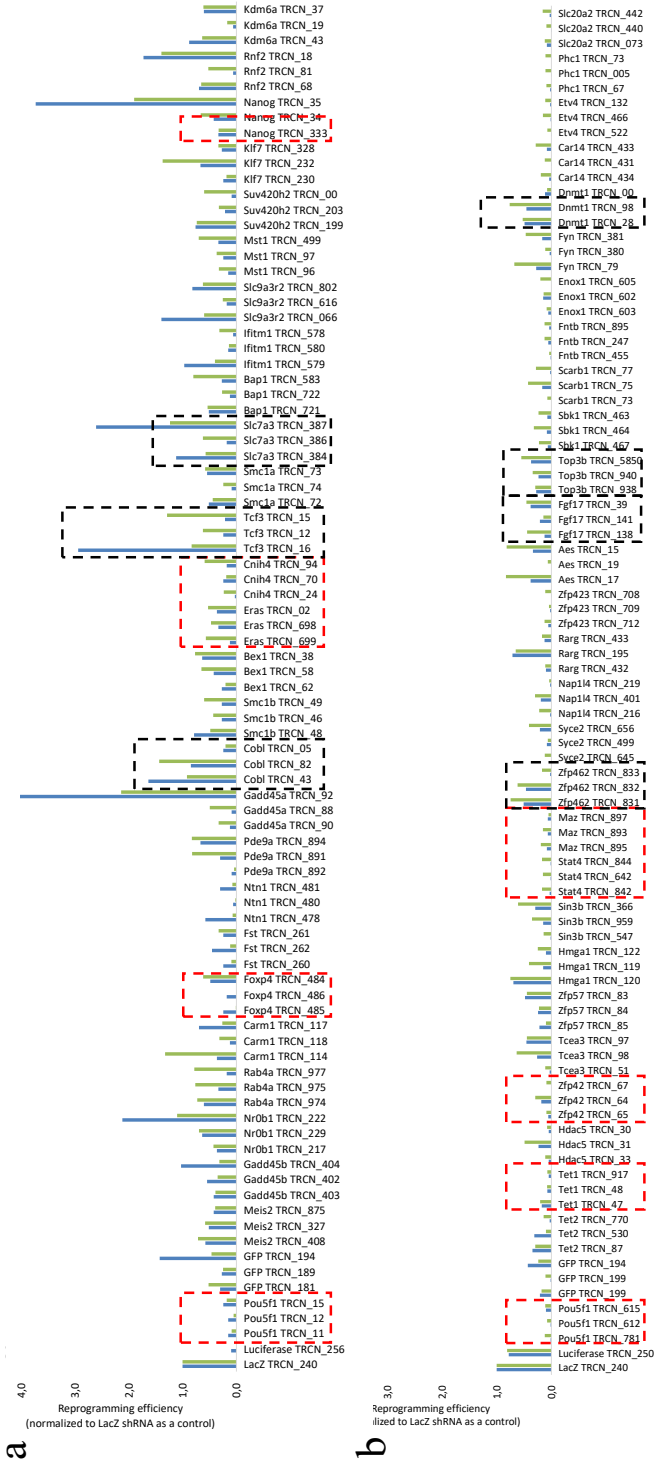

Figure R7 Reprogramming efficiency assessment. a-b) Upon knockdown of the 60 candidates and induction of iPSC formation, the reprogramming efficiency has been scored by normalizing the data to LacZ shRNA as a control (set as 1) (a: Batch1; b: Batch2). Red boxes highlight factors showing low reprogramming efficiency whereas black boxes highlight factors with higher reprogramming efficiency according to OCT4 and TCF3/DNMT1 respectively.

We identified some factors that might play a role in iPSC reprogramming as potential enhancers or repressors. Enhancers of reprogramming included factors for which at least two shRNAs showed a similar effect in different screen runs in reducing reprogramming efficiency comparable to *Oct4* or *Nanog* knockdown. Indeed, we set a cutoff according to OCT4 efficiency value and we considered 20 out 57 candidate list potential enhancers of the reprogramming. In the second group we had two factors that showed a similar effect on the reprogramming as TCF3 that we set as cutoff efficiency.

We pointed our attention on ERas, a factor that has been already described in the literature as a player in pluripotency (Takahashi, Mitsui, and Yamanaka 2003; Yu et al. 2014). We saw from the microarrays how in blastocyst its expression is up-regulated between E3.5 and E4.5 in the epiblast where *Nanog* is expressed **(Fig. R8a)**. When looking at iPSC colony formation, ERas knockdown showed a similar effect in colony reduction as Nanog shRNA **(Fig.R8b)**.

Among the other screened candidates, we also identified a novel factor, FOXP4, whose potential role in reprogramming has never been reported in literature so far (Jonghwan Kim et al. 2008; S. Li, Weidenfeld, and Morrisey 2004). It is a transcription regulator and in our screen its knockdown has a drastic effect on colony number with two shRNAs and, the third one showed as well as a decrease in iPSCs formation. In blastocyst, *Foxp4* expression increases in the epiblast and is low in primitive endoderm. In terms of colony number, *Foxp4* knockdown drastically reduces the reprogramming efficiency. **(Fig. R8a-b)**.

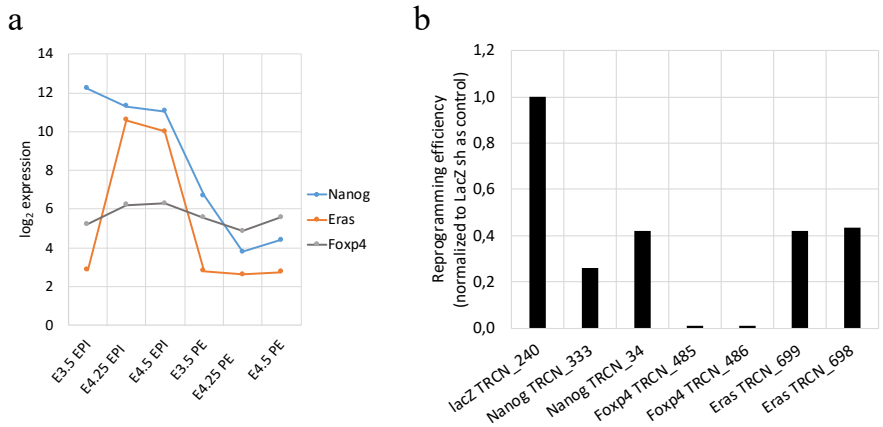

Figure R8 Selected candidates with a role in iPSC reprogramming.
a) Expression profile of *ERas*, *Foxp4* and *Nanog* in Epiblast (EPI) and primitive endoderm (PE) of E3.5 and E4.5 blastocysts. b) The graph shows the reprogramming efficiency scored upon knockdown of *ERas*, *Foxp4* and *Nanog* with 2 different shRNAs compared to LacZ control shRNA set to 1.

3.2 Factors involved in XCR

Our second and main focus was related to XCR. We scored the number of XGFP-positive colonies at two different time points: day 10 and day 12 of the reprogramming and calculated the XCR efficiency as the ratio of XGFP-positive colonies divided by the total colony number **(Fig. R9)**.

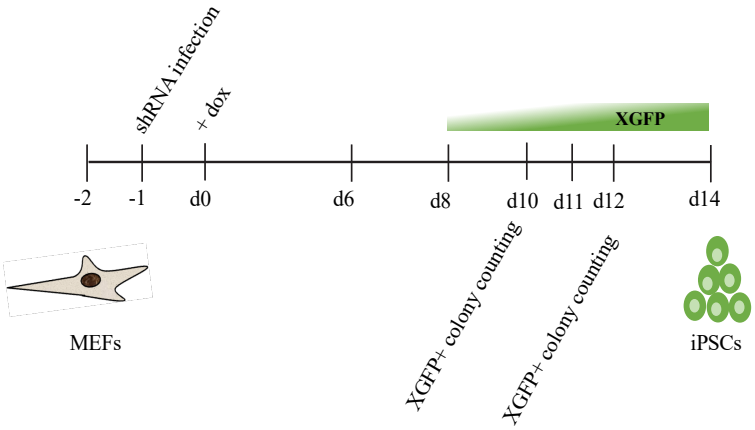

Figure R9 Schematic representation of the lentiviral infection and reprogramming time course. Day 10 and day 12 as timepoints to score the number of XGFP positive colonies.

We focused on those factors whose knockdown caused reduced *XGFP*-reactivation indicating a role in the process. In **Fig. R10** and **R11** we show for batch1 and batch2 respectively, two different graphs: the combined graph with total number of colonies (red line) and the relative number of XGFP positive colonies (green bars). The factors have been ordered according to the number of XGFP positive colonies **(Fig. R10a and R11a)**. In the second graph we show the X Chromosome Reactivation efficiency scored at day 10 of reprogramming and we normalized according to the one scored for LacZ shRNA as our negative control **(Fig. R10b and R11b)**.

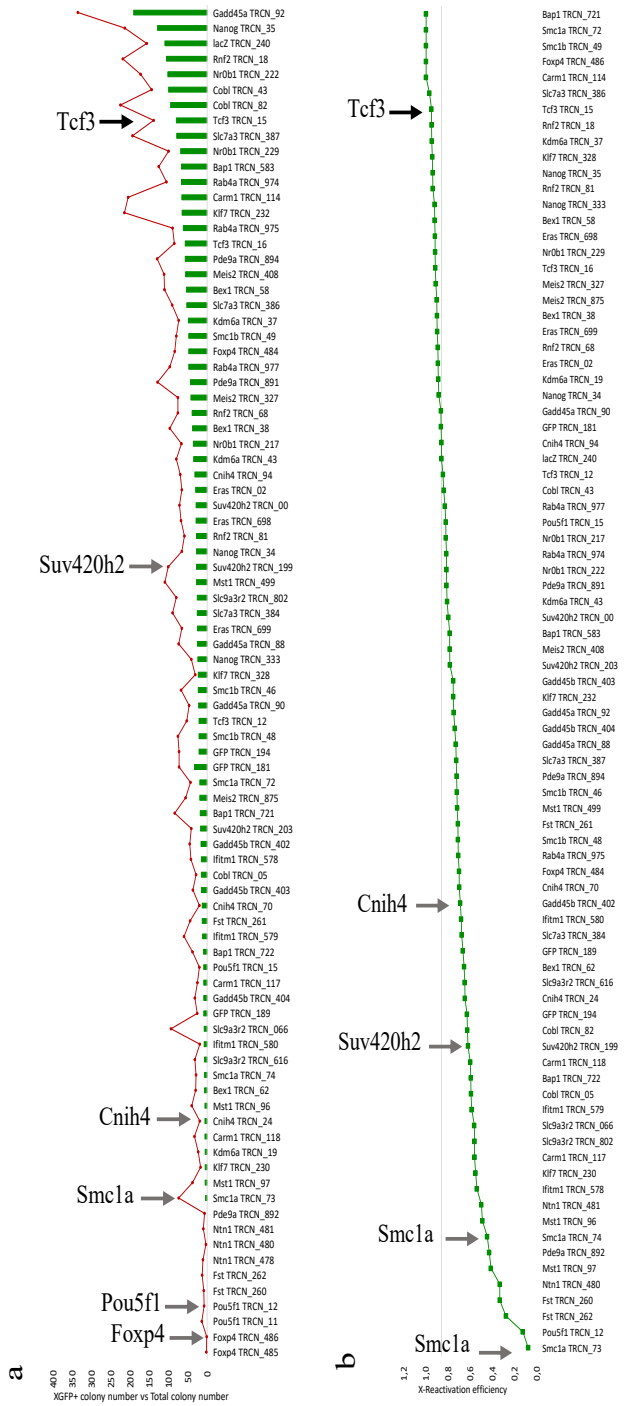

Figure R10 Impact of candidate knockdown on XCR efficiency (Batch1). a) The graph shows both total colony number (red line) and XGFP+ colonies (green bars). b) XCR efficiency scored as ratio between XGFP positive colony number and total colony number. *x*-axis set as the value of LacZ shRNA control. In both graphs grey arrows point out factors with low number of XGFP+ colonies or XCR efficiency whereas black arrows highlight factors with higher number of XGFP+ colonies or XCR efficiency.

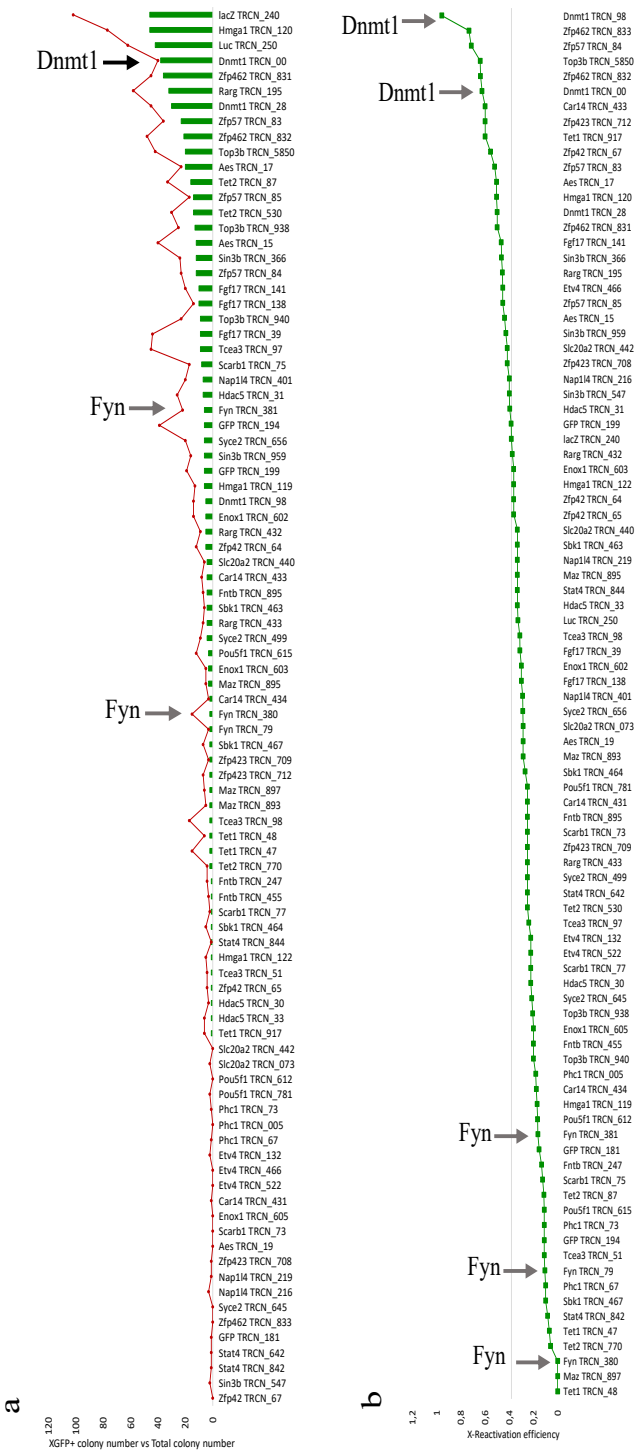

Figure R11 Impact of candidate knockdown on XCR efficiency (Batch2). a) The graph shows both total colony number (red line) and XGFP+ colonies (green bars). b) XCR efficiency scored as ratio between XGFP positive colony number and total colony number. x-axis set as the value of LacZ shRNA control. In both graphs grey arrows point out factors with low number of XGFP+ colonies or XCR efficiency whereas black arrows highlight factors with higher number of XGFP+ colonies or XCR efficiency.

We identified six factors that might play a specific role in XCR as potential enhancers. We included factors for which at least two shRNAs showed a similar effect in reducing the reactivation of the XGFP comparable to the effect that we assessed upon *GFP* transgene expression knockdown.

Among the candidates we highlighted in **Fig. R10a**, CNIH4 (Sauvageau et al. 2014), a GPCR-interacting protein, whose knockdown showed a decrease in the total colony number as *Oct4* knockdown as well. But concomitantly there was a decrease in *XGFP* reactivation as shown in **Fig. R10b** where the scored ratio for this factor is similar to the value of the negative control LacZ shRNA. This suggests that *Cnih4* knockdown affects the reprogramming efficiency and might as a consequence have an effect on XCR, for which pluripotency is a prerequisite. Therefore, in this case the two processes, XCR and pluripotency, are coupled.

However, we were mainly interested in factors specifically involved in XCR. Among the six factors that we identified, there was SUV420H2, a histone methyltransferase required to di- and tri-methylate lysine 20 of histone H4 (H4K20me2/3) (Schotta 2004). In **Fig. R10a** it is highlighted as one of the factors that showed a discrepancy between the total colony number, that was not affected upon knockdown and the number of XGFP positive colonies that, on the contrary, was reduced. This is scored in a low reactivation efficiency ratio **(Fig. R10b)**, suggesting that it might play a specific role in XCR.

Another interesting factor, that belongs to the category of chromatin remodelers, was a cohesin complex component, SMC1A (Minajigi et al. 2015). In fact, in terms of XCR, we saw a dramatic decrease in *XGFP*

reactivation upon knockdown **(Fig. R10a-b)**. However, the reprogramming efficiency seemed not to be affected by *Smc1a* knockdown, suggesting a specific role in X-Chromosome Reactivation **(Fig.R10a)**.

Furthermore, we saw an effect on XCR after knocking down the expression of FYN, a novel factor, that belongs to the Src-family kinases and which has been described in literature as important for the completion of meiosis in mouse oocytes (McGinnis, Kinsey, and Albertini 2009). In our screen its knockdown showed a specific decrease of *XGFP* reactivation without affecting iPSC colony formation in general **(Fig. R11a-b)**.

In **Fig R12a**, the graph specifically shows the X-Reactivation efficiency of the factors mentioned until now as potential players in XCR. On the other hand, as a confirmation of the adequacy of our system for monitoring XCR kinetics, we saw that knocking down the DNA methyltransferase DNMT1 showed a clear increase of *XGFP* reactivation in accordance with its role during maintenance of X-inactivation (T Sado et al. 2000; Csankovszki, Nagy, and Jaenisch 2001).

In blastocyst, looking at the expression profile of the factors described as specific for XCR, we saw them to be up-regulated in the epiblast between E4.25 and E4.5 when XCR occurs in anti-correlation with *Xist* expression profile. In primitive endoderm and in the epiblast at E3.5 when *Xist* is expressed their expression is low **(Fig. R12b)**.

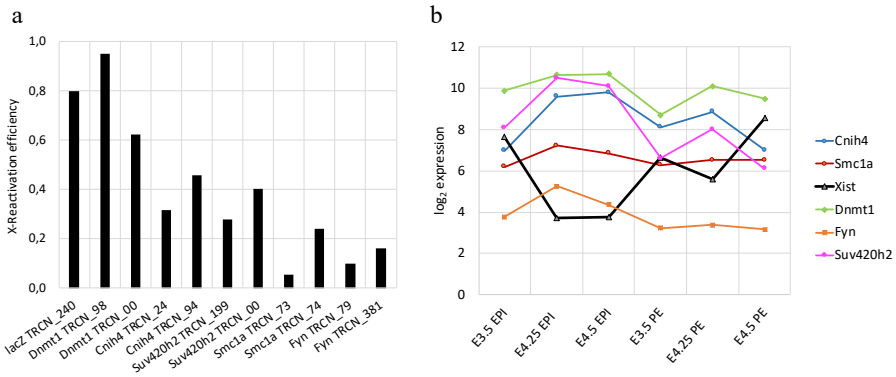

Figure R12. Selected candidates with a role in XCR. a) The graph shows the XCR efficiency scored upon knockdown of DNMT1, CNIH4, SUV420H2, SMC1A and FYN with 2 different shRNAs compared to LacZ control shRNA set to 1. b) Expression profile of *Dnmt1, Cnih4, Suv420h2, Smc1a* and *Fyn* in Epiblast (EPI) and primitive endoderm (PE) of E3.5 and E4.5 blastocysts in comparison with *Xist* expression (black line).

In order to analyze XCR more quantitatively, we looked at the bulk population by FACS. We stained the cells with two surface markers for pluripotency: SSEA1 and EpCAM1 to define the reprogrammed cells (Polo et al. 2012) and then we checked the percentage of SSEA1+/EpCAM1+ double-positive cells that were also GFP-positive **(Fig. R13)**.

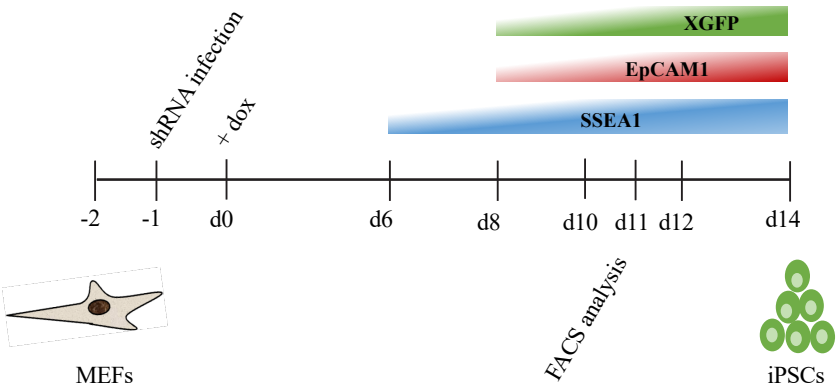

Figure R13. Schematic representation of lentiviral infection and reprogramming time course. Flow cytometry analysis was performed at day 12 of the reprogramming by staining iPSCs with SSEA1 and EpCAM1 and checking the percentage of XGFP positive cells within the pluripotent population.

In line with our results obtained by colony scoring **(Fig. R10b and R11b)**, flow cytometry analysis **(Fig. R14a-b)** confirmed that factors previously highlighted such as CNIH4, SMC1A and FYN show a reduction of around 10%, in terms of XGFP within the pluripotent population in comparison with LacZ shRNA control (25% *XGFP* reactivation). On the other hand, DNMT1, as expected, showed high percentage of XGFP cells, around 30% and 45%, within the EpCAM1+SSEA1+ population.

Figure R14 Flow cytometry analysis. a-b) FACS analysis by staining the cells at d11 of the reprogramming with two surface markers EpCAM1 and SSEA1 and scoring the percentage of XGFP-positive cells within the pluripotent population. x-axis is set at the value score for LacZ shRNA (red arrows). Gray arrows highlight factors whose knockdown decreases the percentage of XGFP+ cells. Black arrow points out a control such as Dnmt1. (a: batch1; b: batch2).

4. Characterization of top candidates

In order to narrow down the number of factors for follow up analysis after the RNAi screen, we looked at the knockdown efficiency of the different hairpins and their toxicity. Therefore, we infected MEFs with different lentiviral vectors carrying shRNAs and after 24h we analyzed which ones were impairing cell proliferation, leading to cell death. That led us to conclude that in some cases the low reprogramming efficiency was linked to the toxic effect of some hairpins on cell growth rate. Indeed, we excluded 19 hairpins for their toxicity (data not shown).

The next step was to check the knockdown efficiency information of each shRNA provided by the Broad Institute from where we have purchased them. We set a threshold, excluding those hairpins whose knockdown efficiency was lower than 50% in agreement with the data reported by the provider. In this case we excluded 6 hairpins.

Indeed, as shown in **Fig. R15a**, we selected 31 candidates out of 60 by looking at:

a) the primary screen results;
b) the likelihood of involvement in reprogramming and/or XCR according to the scientific literature;
c) hairpin toxicity;
d) remaining transcripts expression (Broad Institute).

We classified them based on their GO-term function and as shown in the pie chart in **Fig R15b**, the majority acts as transcriptional regulator such as pluripotency factors (ZFP42, OCT4, NANOG), followed by the other two main categories: chromatin factors (SUV420H2, KDM6A/UTX, SMC1A) and cell cycle regulators (SMC1A). However, there are also factors whose function is not known as for example CNIH4.

As next step we checked the knockdown efficiency of the selected factors in our cell line, as for the secondary screen three different hairpins have been used for each factor. We infected MEFs with homemade lentiviral preparations and 24h later we induced reprogramming by addition of dox. The main purpose was to maintain the same conditions as in our screen. Setting expression levels for each gene to 1 in our LacZ shRNA negative knockdown control, we set a threshold around 0.5 as successful knockdown in order to exclude hairpins where remaining transcript levels were higher **(Fig. R15c)**.

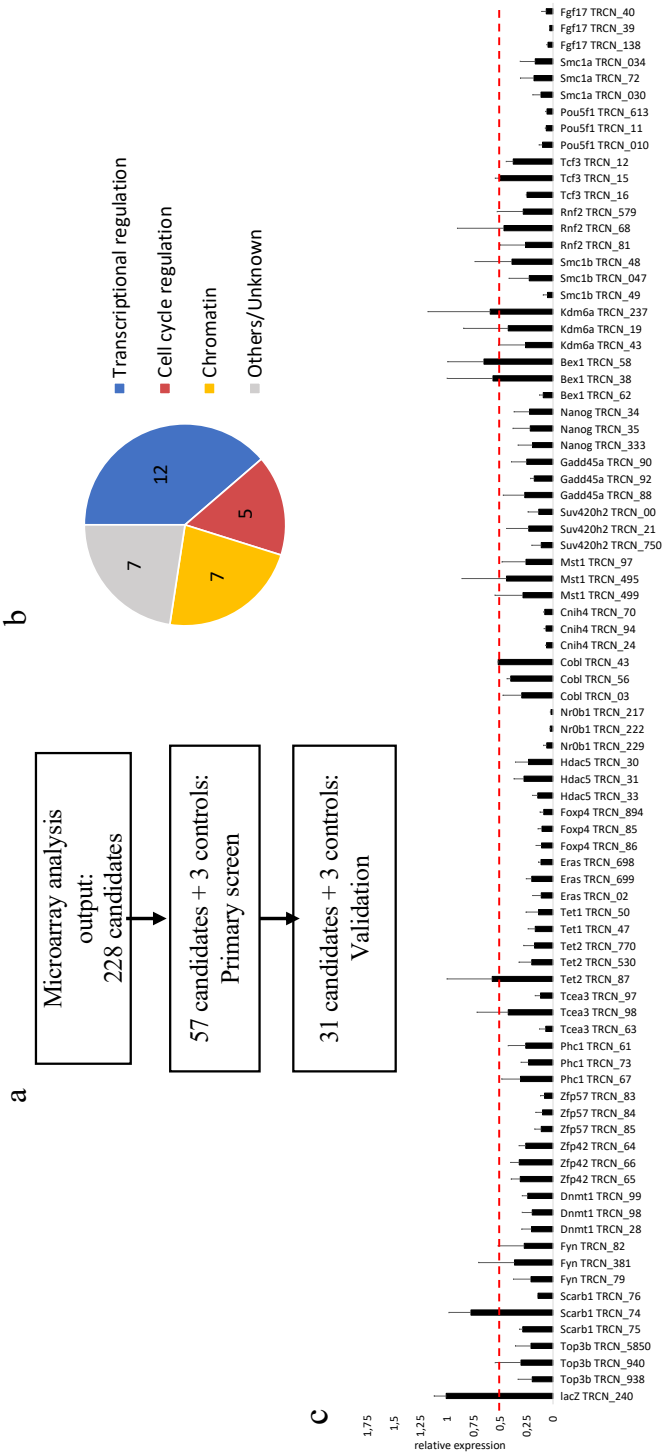

Figure R15 Validation of top candidates from the first screen. a) Schematic representation of the different steps of the screen. b) Pie chart of candidates-related pathways. c) Assessment of mRNA levels upon knockdown of 31 candidates by Real time PCR (LacZ shRNA used as 1) The red line shows our threshold at 0.5. (Error bars=SEM).

4.1 Effect of candidate knockdown on pluripotency and XCR

In order to validate the candidates identified in the shRNA reprogramming screen, we repeated the experiment using the system used previously. In this case we are able to narrow down the number of candidates according to the outcome, the knockdown efficiency values and by replacing some hairpins that were not working in the previous experiments. First of all, after knocking down the expression of the selected candidates, we counted the number of total colonies at different time points and then we scored the reprogramming efficiency, using LacZ-control set as 1 to normalize the data. Confirming our first screen, the majority of the candidates had an effect on pluripotency in accordance with their up-regulation in the epiblast tissue **(Fig. R16a)**. For instance, ERas, FOXP4 and ZFP42 showed a decrease in terms of reprogramming efficiency after knocking down their expression. Whereas for DNMT1 and TCF3, as expected, there was a higher number of colonies when their expression was reduced by shRNA knockdown.

In terms of XCR, we looked at the efficiency of the process by scoring the ratio between the number of colonies XGFP positive and the total colony number **(Fig. R16b)**. On one hand we have factors whose knock down is affecting the reprogramming efficiency, and thereby also indirectly affects XCR. This is the case for ZFP42, FOXP4 and CNIH4. On the other hand, we have factors such as SMC1A, SUV420H2 and FYN, whose decreased expression is not affecting the capability of the cells to reprogram but to reactivate X-Chromosome based on *XGFP*-reactivation.

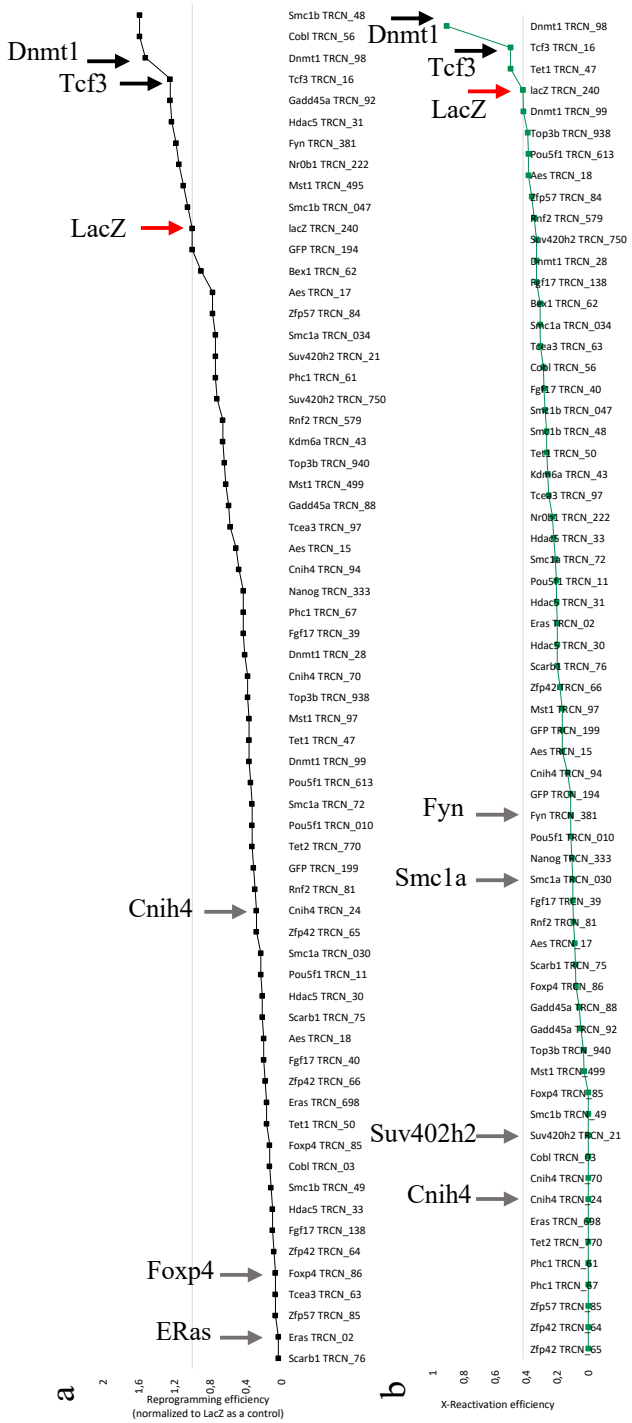

Figure R16 Validation top candidates. a) The graph shows the reprogramming efficiency upon knockdown. LacZ shRNA as negative control is set as 1 (red arrow). Gray arrows highlight factors whose knockdown decreases reprogramming efficiency in line with primary screen. b) It has shown the XCR efficiency upon knockdown. X-axis is set at the value scored for LacZ shRNA (red arrow). Gray arrows point out factors whose knockdown decreases XCR efficiency as shown in the primary screen. Black arrows show Tcf3(a) and Dnmt1 (b) as controls.

Therefore, according to the outcome, we highlighted the candidates that give a consistent phenotype in line with first screen by grouping them into two different categories:

I. Factors that have an effect on both iPSC and XCR.
II. Factors that have a specific effect on XCR;

In **Fig. R17** the results are shown in a Venn diagram.

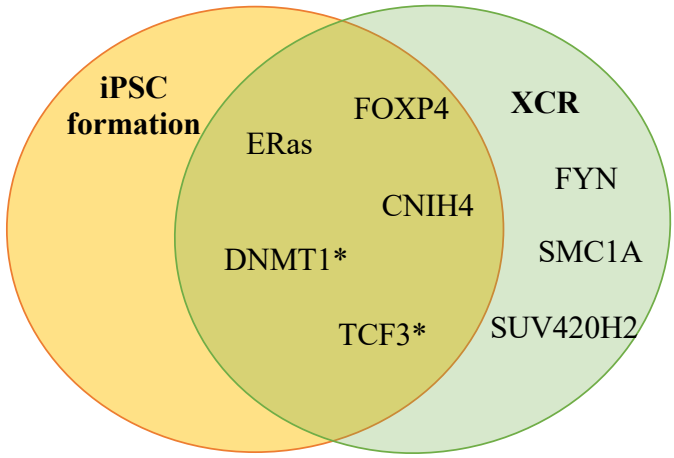

Figure R17. Top candidates. Venn diagram shows two different groups of factors: factors that have an effect on reprogramming and XCR and factors that have a specific role in XCR.

In the following **Table R1** the top candidates are listed for function and potential role.

Factors	Function	Literature	Potential role
CNIH4	GPCR protein	Sauvageau et al. 2014	Reprogramming enhancer
ERAS	Small GTPase Protein	Yu et al. 2014	Reprogramming enhancer
FYN	Src kinase	McGinnis et al. 2009	XCR
FOXP4	Transcription factor	Li et al. 2004; Kim et al. 2008	Reprogramming enhancer
SMC1A	Chromatin factor	Minajigi et al. 2015	XCR
SUV420H2	Histone methyltransferase	Schotta 2004	XCR
DNMT1*	DNA methylase	Mikkelsen et al. 2008	XCR
TCF3*	Transcription factor	Lluis et al. 2011	Reprogramming repressor

Table R1 shows a list of the top candidates, their known function and their potential role according to our screen. (*) factors used as controls which show the expected phenotype.

4.2 Effect on endogenous X-linked gene: *Hprt*

So far, we have shown the kinetics of reactivation of the *XGFP* located on the X-Chromosome as a simple and useful tool to follow XCR. However, as *XGFP* is a transgene inserted into the X-chromosome by random

integration (Hadjantonakis et al. 2001), we were not looking at an endogenous gene on the X. Therefore, in order to confirm that *XGFP* reactivation corresponds also to the reactivation of endogenous X-linked genes, we analyzed the *Hprt* locus. We took advantage from the fact that our reprogrammable cell line, besides carrying an *XGFP* transgene, also has a mutation in the *Hprt* allele on the opposite X-Chromosome (Eggan et al. 2000). In fact, if we grow the cells in 6-thio-guanine (6-TG) medium, only the cells with a mutated *Hprt* gene on the Xa and the wildtype allele on the Xi can survive. Those also carry the *XGFP* transgene on the Xi **(Fig.R18)**.

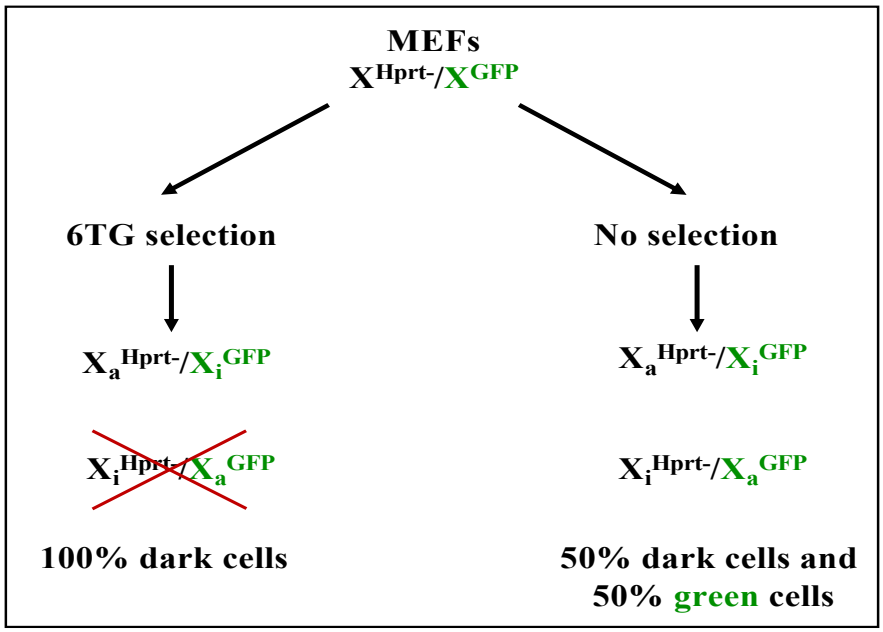

Figure R18 6TG selection scheme. Drug selection scheme for obtaining populations of MEFs with a predeterminate X-Inactivation state.

So, this particular feature makes it possible to apply a drug selection scheme after reprogramming. Specifically, we performed the same reprogramming experiment by knocking down the expression of the candidates at the beginning and following the reprogramming until day10. At this point we trypsinized the colonies and we seeded them on *Hprt* (-) feeders, able to survive in 6TG medium and we applied the selection for 6 days.

The aim was to analyze by flow cytometry the iPS cells able to survive upon selection, as only cells which did not reactivate the *Hprt* allele would survive in 6TG medium (Xa^{Hprt-}/Xi^{GFP}), while cells, which have reactivated *Hprt* on the X would be selectively killed (Xa^{Hprt-}/Xa^{GFP}) (**Fig.R19a)**. As expected, only the *XGFP*-negative colonies were able to survive because of the presence on the same chromosome of the wildtype Hprt allele, indicating that *XGFP*-reactivation is a good proxy for reactivation of endogenous X-linked genes like *Hprt*. The outcome confirmed some of the candidates that came out in the previous screen as potentially important for XCR such as SMC1A, FYN and SUV420H2 **(Fig R19b)**. In fact, upon knockdown of those factors, a percentage of colonies failed to reactivate the X, remaining XGFP negative. As expected, in the case of DNMT1, whose knockdown causes an increase of XCR, none of the iPSCs survive, and the same for those factors such as TCF3, that causes an increase of the reprogramming efficiency and XCR as well.

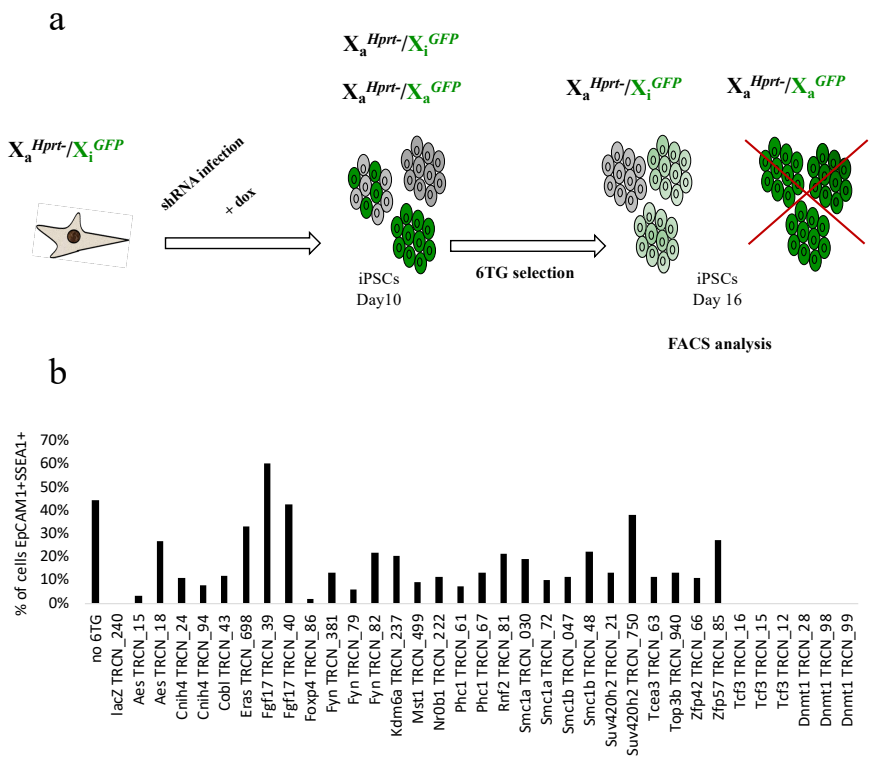

Figure R19. Reactivation of endogenous X-linked gene *Hprt*. a) 6TG selection scheme upon knockdown and reprogramming induction. At day 10 6TG drug is added to the iPS cells and maintained for 6 days. At day 16 FACS analysis is performed by staining the iPS cells with SSEA1 and EpCAM1. b) The graph shows the percentage of pluripotent cells stained by EpCAM1 and SSEA1, which survived upon 6TG selection. The more cells survive, the bigger is the effect on XCR by candidate knockdown.

4.3 Do candidate factors for XCR act through *Xist* or not?

Downregulation of Xist RNA, the master-regulator of X-inactivation, is an essential hallmark of XCR (Maherali et al., 2007, Payer et al. 2013, Pasque et al. 2014). Therefore, we wanted to understand, if the function of our candidate factors was repression of *Xist* during XCR, as we initially identified them by anticorrelated expression to *Xist* in mouse blastocysts. To do so, we decided to knock down the expression of the candidate factors in ESCs, where *Xist* is not expressed and observe, if that would lead to de-repression and upregulation of *Xist*.

24h after lentiviral shRNA infection, we put the cells under puromycin selection for 48h to select infected cells and then extracted RNA for RT-PCR analysis. First, we assessed the knockdown efficiency of our candidates and after excluding non-functional hairpins, we checked *Xist* expression. Overall, we did not see a clear effect on *Xist* expression except after knocking down factors, whose role in *Xist* repression has been already described such as *Nanog* and *Oct4* **(Fig. R20a)** (P. Navarro et al. 2008; Nesterova et al. 2011). Then, we checked the expression of *Rnf12*, a positive regulator of *Xist* (Barakat et al. 2011), and we only saw an increase of *Rnf12* expression when we knocked down *Oct4*, a known repressor of *Rnf12* **(Fig. R20b)** (Pablo Navarro et al. 2011).

Furthermore, we looked at *Tsix* expression, which is a negative regulator of *Xist* and which has been implicated in XCR in mouse blastocysts (Payer et al. 2013). We only observed reduced *Tsix* expression after knocking down *Zfp42/Rex1*, which is a known activator of *Tsix* (Navarro et al. 2010) **(Fig. R21)**.

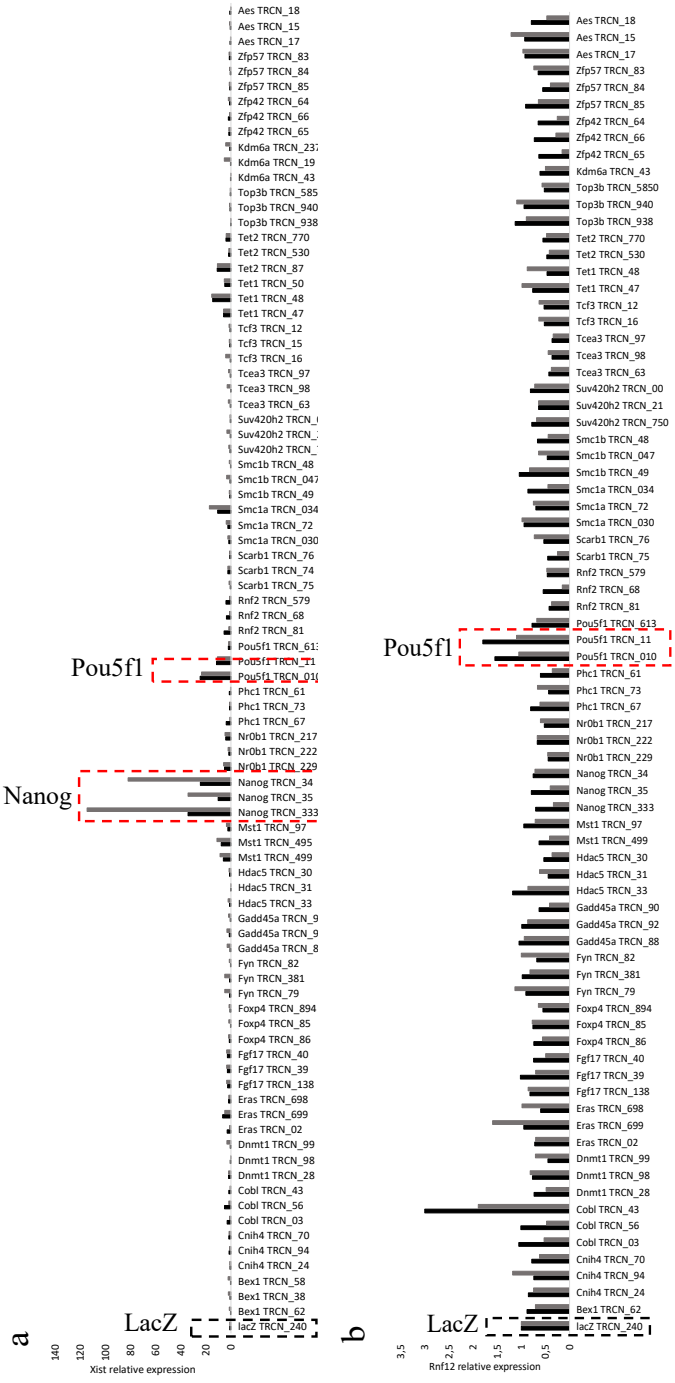

Figure R20 Impact of candidate knockdown expression of *Xist* and its regulator *Rnf12*. a) Xist mRNA levels in female ESCs upon knockdown of the top screened candidates. b) Rnf12 mRNA levels upon knockdown of the top screened candidates. In both graphs black and gray bars indicate two biological replicates. LacZ shRNA is set as 1.

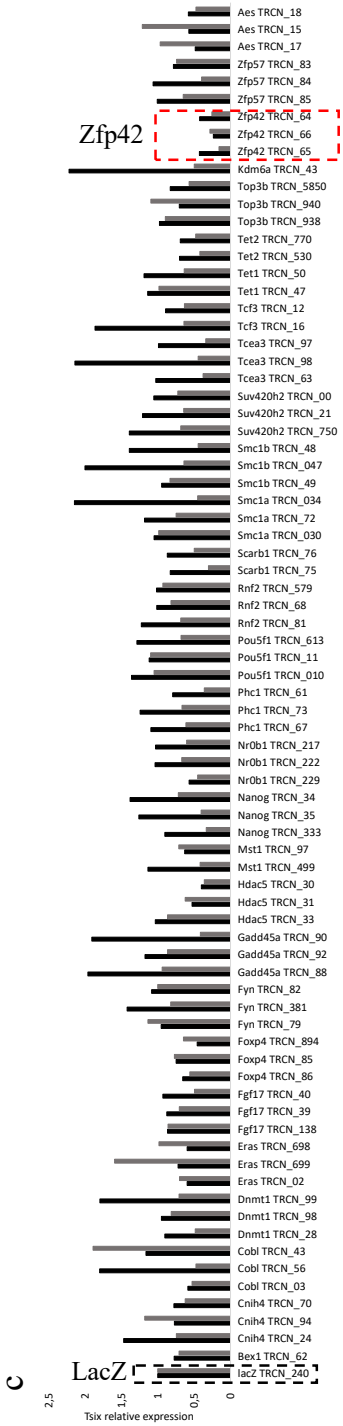

Figure R21 Impact of candidate knockdown expression *of Tsix.* *c*) Tsix mRNA levels in female ESCs upon knockdown of the top screened candidates. Black and gray bars indicate two biological replicates. LacZ shRNA is set as 1.

In conclusion, despite the fact that one of the criteria to select our candidates from the microarray was their anti-correlation with *Xist* expression, none of our novel candidates seems to control XCR by acting through *Xist* or its regulators, but rather do so through other unknown mechanisms. On the other hand, we performed the same experiment during the iPS cell reprogramming to check *Xist* expression upon knockdown of our candidates at different timepoints before and after X-Chromosome Reactivation. However, this experiment needs to be repeated because the result was not conclusive mainly due to its technical complexity.

5. Cohesin is a pluripotency-independent regulator of XCR

The validation screen allowed us to narrow down the number of factors from 31 to 6 that have shown a consistent phenotype either in pluripotency and/or XCR (ERas, CNIH4, FOXP4) or XCR-specific (SMC1A, FYN, SUV420H2).

Among them we decided to focus our attention on the cohesin complex member SMC1A, due to its implication in regulation of X-chromosome 3D-structure (Minajigi et al. 2015) **(Fig. R22)**.

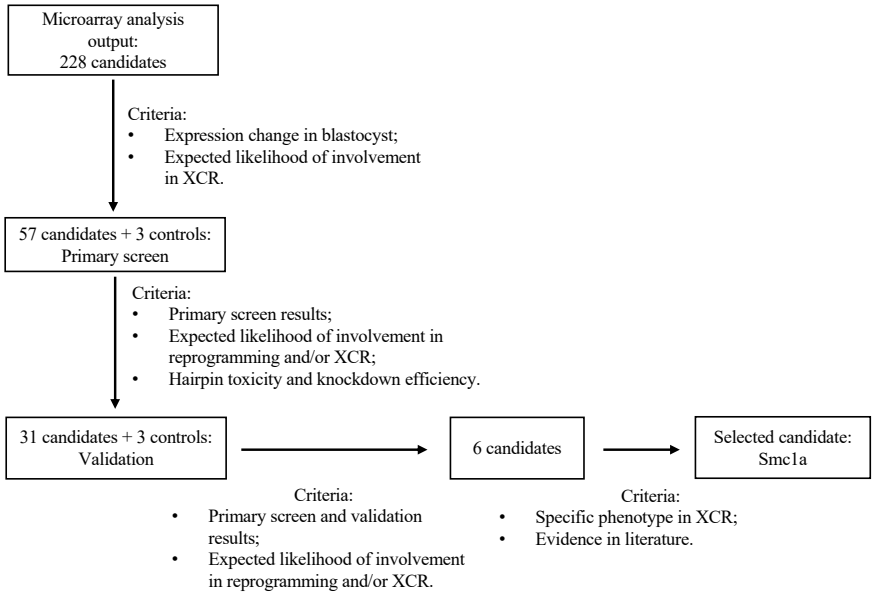

Figure R22. Schematic representation of the different steps of the screen.

Throughout the different screening runs, SMC1A showed consistently a potential role in XCR. By imaging we could see that colony formation was not impaired after its knockdown, whereas *XGFP* reactivation was affected **(Fig. R23a)**. As shown in **Fig. R23b**, knocking down *Smc1a* expression with two different hairpins, decreased XCR efficiency, on average, by around 80% compared to the lacZ control shRNA.

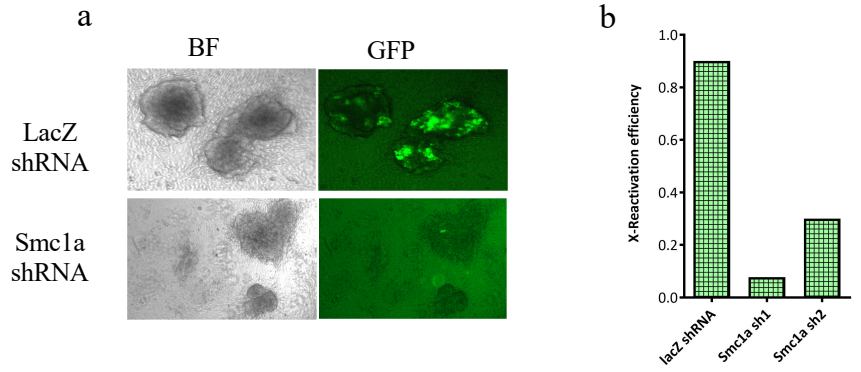

Figure R23 *Smc1a* knockdown effect on XCR. a) Images of iPSC colonies with (bottom, shRNA) or without (top, LacZ shRNA) knocking down *Smc1a*. BF, bright field; GFP, *XGFP* expression. c) XCR efficiency upon Smc1a knockdown with two different shRNAs compared to LacZ control shRNA.

This effect of *Smc1a* knockdown became even more evident by FACS analysis. We induced reprogramming after knocking down Smc1a and lacZ shRNA and then stained iPS cells by EpCAM1 and SSEA1 pluripotency markers at day 11. **In Fig. R24a** FACS plots for both LacZ shRNA control and Smc1a knockdown are shown. We did not detect any difference in terms of the EpCAM1+SSEA1+ pluripotent cell population, which, was between 46% and 40% respectively of total live cells. However, when we looked at the percentage of XGFP-positive cells within the EpCAM1+SSEA1+ double-positive population, we could see a drastic difference. At day 11 in the LacZ shRNA control the percentage of pluripotent cells XGFP+ was around 23% whereas in *Smc1a* knockdown the percentage decreased down to 4%. This leads us to hypothesize that Smc1a might be a specific XCR regulator and that this process can be

uncoupled from the emergence of pluripotency, as it was not affected after *Smc1a* knockdown **(Fig. R24b)**

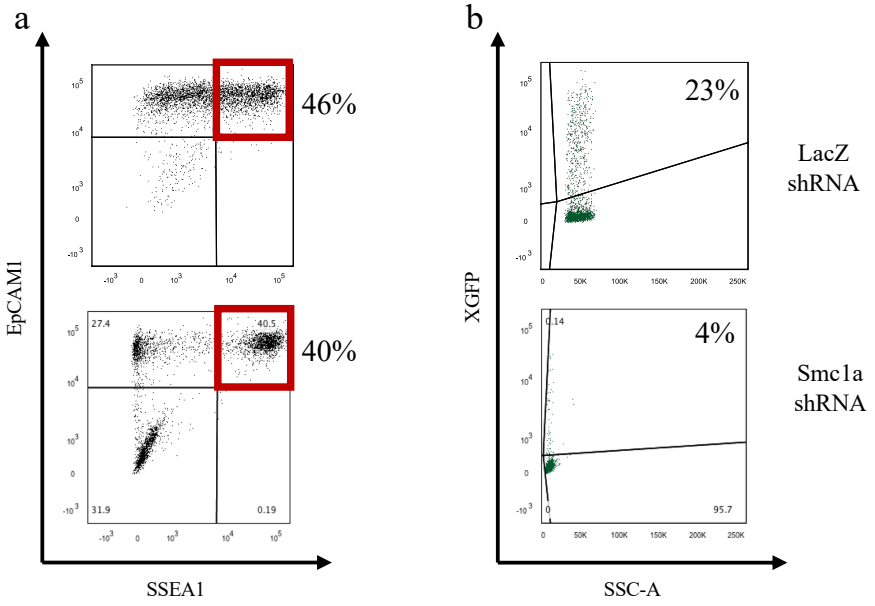

Figure R24: Flow cytometry analysis of *Smc1a* knockdown. a) iPSC colonies w/wo *Smc1a* knockdown stained by EpCAM1 and SSEA1 at d11 of the reprogramming. b) XGFP percentage scored within pluripotent population (EpCAM1 and SSEA1 double-positive cells). SSC-A, side scatter.

5.1 How is *Smc1a* affecting XCR?

SMC1A is known to play a role in chromosome architecture and particularly has been described as important in maintaining autosome-like TAD-structures on the active X Chromosome. On the inactive X-chromosome TADs are nearly absent, as SMC1A is repelled by Xist RNA (Minajigi et al. 2015). Therefore, in order to understand how SMC1A

could play a role in XCR we focused our attention on X chromosome structure.

In collaboration with Marie Victoire Neguembor, a Postdoc in Maria Pia Cosma lab (CRG), we performed an experiment of Super Resolution Stochastic Optical Reconstruction Microscopy (STORM) in MEFs with and without knocking down *Smc1a* expression (Ricci et al. 2015). Specifically, we performed immuno-DNA FISH experiments, using sequentially an X-Paint to identify by DNA FISH the whole two X chromosomes in the nucleus followed by immunofluorescence. We stained the cells with H3K27me3 antibody to discriminate the two X-chromosomes by marking the inactive X in combination with an antibody able to recognize the cohesin SMC1A. Representative images are shown in **Fig. R25**. In MEFs LacZ shRNA control sample, as expected, there was a distinct nuclear distribution of SMC1A when imaged by conventional microscopy. The pattern was much more defined in super resolution as it allowed to identify single protein localizations within the nucleus. Furthermore, even by conventional imaging we could see how the inactive X chromosome looked much more compact compared to the active X, in agreement with published data (Giorgetti et al. 2014; Teller et al. 2011a; Naughton et al. 2010a).

In MEFs with shRNA against SMC1A the reduced amount of cohesin was evident in the nucleus and super resolution imaging confirmed almost complete absence of single localizations of SMC1A protein, with just few spots remaining.

Regarding the two X Chromosomes, we could see how the conformation of the active X looked much more compact than expected, similar to the Xi after knocking down *Smc1a*.

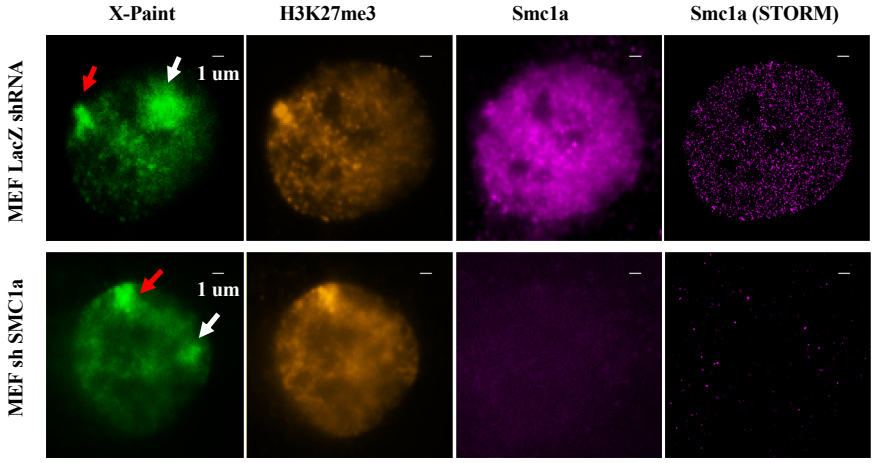

Figure R25 The X-Chromosome and Smc1a (I). Experiment of Immuno-DNA FISH in combination with Super resolution microscopy (STORM). MEFs w/wo Smc1a knockdown stained by X-Paint (green), H3K27me3 (orange) and SMC1A (magenta). The arrows point out the two X-Chromosomes (red=inactive X; white=active X) (bar=1um).

By overlapping the localization of SMC1A in super resolution on top of the two X chromosomes, we could see how the amount of cohesin appeared to be higher on the active X than the inactive one in LacZ shRNA control sample which is in agreement with published ChIP-Seq data (Minajigi et al. 2015). Whereas in the SMC1A shRNA sample both X chromosomes appeared more compacted and showed few Smc1a localizations **(Fig. R26)**.

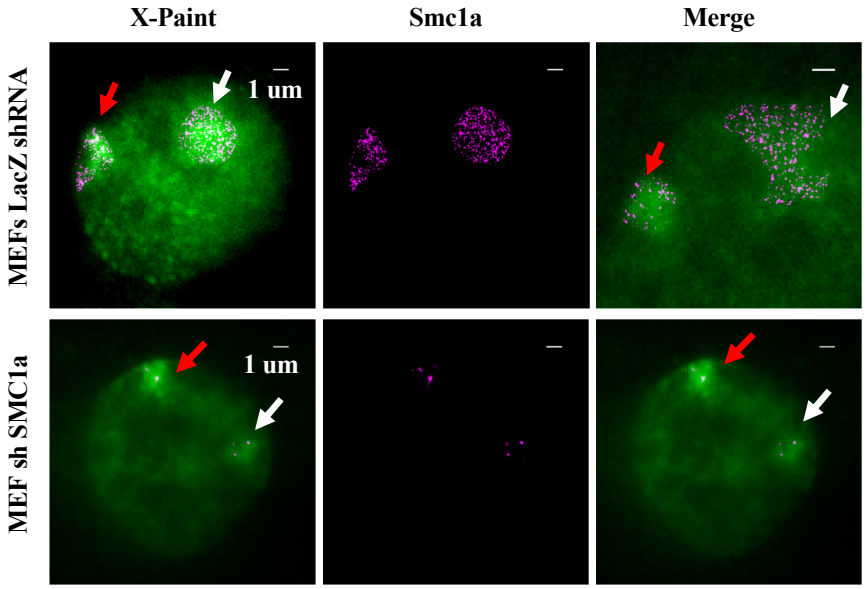

Figure R26 The X-Chromosome and SMC1A (II). Overlap of SMC1A protein localizations (magenta) and X-Chromosomes (green). The arrows point out the two X-Chromosomes (red=inactive X; white=active X) (bar=1um).

After collecting different images for both conditions, we analyzed them by:

a) selecting the area of the active and inactive X chromosomes;

b) scoring the number of SMC1A localizations;

c) performing a protein localization cluster analysis;

d) and comparing active versus inactive X chromosome.

Our first analysis was based on the comparison of the area of the active versus inactive X chromosome in both conditions upon LacZ shRNA and

Smc1a shRNA. In agreement with the literature, in the control sample (LacZ shRNA) the area occupied by the active X is significant bigger than the area occupied by the inactive X that results more compact **(Fig. R27a)**. On the contrary, upon knockdown of *Smc1a*, no significant differences are detected between the two X chromosomes. In particular the active X, on average, has a reduced area, similar to the inactive X **(Fig. R27b)**. This result is in line with what observed by imaging **(Fig. R25),** suggesting an increase of compaction upon Smc1a knockdown on the active X.

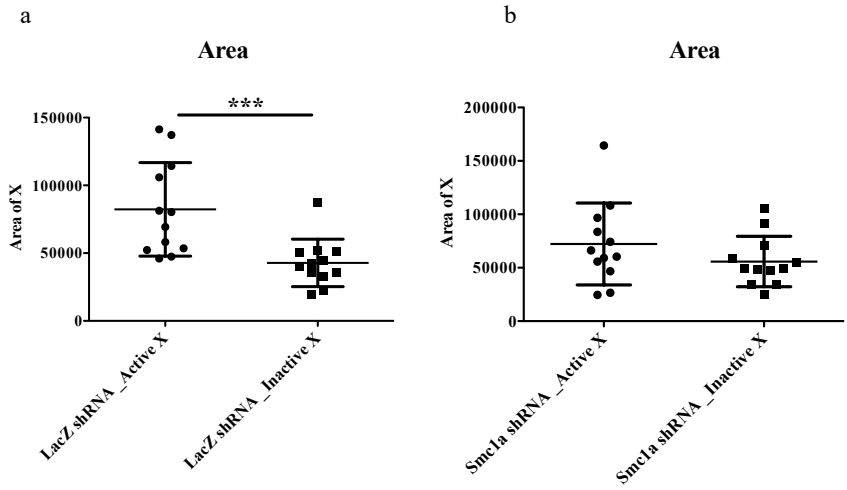

Figure R27 Active X area bigger than Inactive X. a) The graph shows the comparison of the X-Chromosome area between active and inactive in the control. b) Xa versus Xi area comparison upon *Smc1a* knockdown.
For all plots Mean+/- SD is displayed. Stars indicate P-values (***$P \leq 0.001$) for two-tailed paired t-test.

The **Fig. R28a** shows the average number of localizations per locus comparing both conditions, control and knockdown, active and inactive X. There was a significant and preferential SMC1A enrichment on the Xa in LacZ shRNA control compared to the Xi in the same sample. Upon knockdown, there was a substantial SMC1A reduction on both chromosomes. Looking at the median number of localizations per cluster, the cluster size between Xi and Xa was comparable in LacZ shRNA control. A cluster size reduction occurred upon Smc1a knockdown showing comparable levels between Xa and Xi **(Fig. R28b)**.

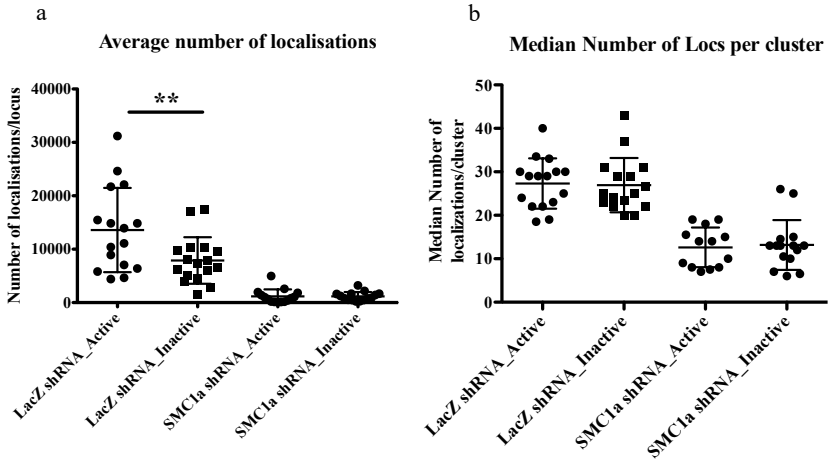

Figure R28 Preferential SMC1A enrichment on the Xa in scramble control MEFs. a) Average number of Smc1a localizations in scramble control and Smc1a knockdown MEFs for both active and inactive X Chromosomes. b) Median number of SMC1A localizations per cluster w/wo *Smc1a* knockdown. For all plots Mean ± SD is displayed. Stars indicate P-values (**$P \leq 0.01$) for two-tailed paired t-test.

By scoring the ratio between Xa and Xi within the same nucleus, there was a preferential Smc1a enrichment on the Xa compared to its respective Xi in terms of number of localizations and number of clusters in the sample control **(Fig. R29a-b)**. A drastic reduction and not significant difference in terms of localization and clusters number between active and inactive X have shown in shRNA *Smc1a* sample **(Fig. R29a-b)**.

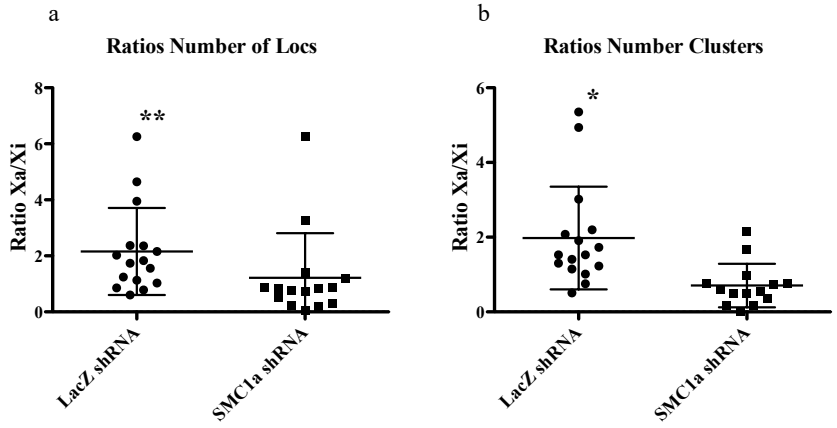

Figure R29 Preferential SMC1A enrichment in Xa compared to its respective Xi. a) Ratio Xa\Xi scored per number of localizations.
b) Ratio Xa\Xi per number of clusters of SMC1A localizations. For all plots Mean ± SD is displayed. Stars indicate P-values (**$P \leq 0.01$ and *$P \leq 0.05$) for one sample t-test.

Indeed, we observed a preferential enrichment of SMC1A on the active compared to inactive X, suggesting a role in shaping the Xa structure. Therefore, we conclude that cohesin-mediated changes in X-chromosome structure are a key step during the XCR process.

Discussion

Single cell microarray expression profile in blastocyst.

As a starting point of my project I used the data generated by a single cell microarray in blastocyst that has been previously performed by my supervisor (Bernhard Payer, unpublished).

According to the dynamics of the process *in vivo*, the reactivation of the inactive X chromosome (XCR) occurs in the epiblast cell lineage of the late blastocyst (Huynh and Lee 2003a) whereas in the extra embryonic tissues such as primitive endoderm (PE) and trophectoderm (TE) the imprinted X-inactivation form is maintained (Nobuo Takagi and Sasaki 1975). Therefore, in order to identify factors playing a role in XCR, the microarray has been performed considering different developmental stages of the blastocyst in order to cover the entire process. Specifically, at the E (embryonic day) 3.5, E4.25 and E4.5 which means before, during and after X-Reactivation respectively.

This was based on the hypothesis that potential factors actively involved in the process could be up-regulated between E4.25 and E4.5 when XCR occurs. In particular, they could thereby show an anti-correlation with Xist, the master regulator of the opposite XCI process, whose expression is down-regulated at that stage. In fact, one of the candidates that came out from the microarray screen was Tsix, a long non-coding RNA expressed during X-Reactivation in the mouse epiblast. Tsix is known for its role as antisense Xist repressor on the active X during X-inactivation (J T Lee and Lu 1999) and has been implicated in the XCR process in blastocysts (Payer et al. 2013).

Therefore, out of 228 candidates that came out from the microarray, 57 were selected according to their expression change and their expected likelihood involvement in the process. In this regard, we selected chromatin modifiers such as histone deacetylases methyltransferase, DNA

methylases and demethylases that might play a role in epigenetic remodeling of the process. Nevertheless, chromatin factors involved in XCR, not necessarily have to show a change in expression as they might be specifically recruited during XCR. We also selected transcription factors, which due to their Xist anti-correlation might act as Xist-repressors similar to Tsix or pluripotency factors like PRDM14, NANOG and OCT4 (P. Navarro et al. 2008; Donohoe et al. 2009; Ma et al. 2011; Nesterova et al. 2011).

Are the screened factors acting on Xist-regulation?

One of the main criteria we used to select our candidates from the microarray was their anti-correlated expression with Xist. Therefore, we were wondering whether they could potentially act as Xist repressors. To answer this question, we performed an experiment in ESCs, where Xist is downregulated, by knocking down the expression of our candidates and see if the consequence was a de-repression or up-regulation of Xist.

Thus, we looked at Xist expression levels and we could not detect any significant change except for known pluripotency factors such as NANOG and OCT4. In fact, as described in the literature, upon their knockdown Xist is up-regulated in ESCs (P. Navarro et al. 2008; Nesterova et al. 2011). One of the reasons why we could not see an effect on Xist levels for the screened factors might be the involvement of other factors in repressing Xist. It is known that *Xist* intron 1 is bound by multiple pluripotency factors, presumably recruiting repressive histone modifications. However, it has been shown that even the deletion of this region is not sufficient to induce an up-regulation of Xist (Minkovsky et al. 2013). This suggests that Xist de-repression might require a balance between down-regulation of repressors such as Tsix and pluripotency

factors and an up-regulation of its *Xist* activators as RNF12 and Jpx. Therefore, we also looked at the expression of those activators and repressors upon knockdown of our candidates. In the first case we checked Rnf12 expression and we could not detect any major effect on its expression except upon knocking down its known repressor OCT4 (Pablo Navarro et al. 2011).
In the same manner for Tsix we could not see a correlation between its expression levels and the knockdown of our candidates. We could only detect a decreased expression after knocking down ZFP42/REX1, known to be its activator (Pablo Navarro et al. 2010). Indeed, we could not conclude that our candidates were acting on XCR through Xist or its regulators but probably did so through other mechanisms.

We also hypothesized that in a transition state it would have been easier to detect a change in Xist expression. Therefore, we tried to assess the down-regulation of Xist during reprogramming. We knocked down our candidates and followed reprogramming and XGFP reactivation dynamics up to day 10 when Xist should be down-regulated. Then, we sorted for each candidate the iPSCs into two groups: XGFP+ (reactivated population) and XGFP- (no reactivated population) and checked Xist expression in both. We could see that in our negative control LacZ shRNA Xist levels were higher in XGFP negative cells as expected, because no reactivation occurred. However, due to a lower knockdown efficiency, our positive control NANOG was not showing a difference in Xist expression between the two populations. Therefore, we could not obtain a conclusive result from this experiment. However, our plan is to repeat this experiment improving the condition of the experiment and minimizing the technical complexity. We think that in a transition state and checking different time points of the reactivation process we might

get a more conclusive answer about the role of the anti-correlation of our candidates with Xist.

Pluripotency and X-dosage.

Female cells undergo X-Chromosome Reactivation in the mouse inner cell mass (ICM) resulting in two active X chromosomes and this state is maintained in reprogrammed iPSCs (Maherali et al. 2007), thereby coupling pluripotency and X-Reactivation. The reprogramming of somatic cells into iPSCs is an important system to study the erasure of epigenetic memory and pluripotency.

XaXa gives to mouse ESCs/iPSCs a double dose of X-linked genes compared to male (XY) cells and shifts them to a naïve pluripotent state. Recent studies suggest that X-Chromosome dosage can modulate the properties of ESCs/iPSCs (Choi, Clement, et al. 2017; Schulz et al. 2014; Song et al. 2018). In fact, two active X chromosomes stabilize the pluripotency network, blocking the exit from the pluripotent state, delaying the differentiation (Schulz et al. 2014). This is further supported by the fact that the loss of one X in female ESCs/iPSCs leads to a loss of sex-dependent differences (Choi, Huebner, et al. 2017; Schulz et al. 2014).

Female ESCs display global DNA hypomethylation (Zvetkova et al. 2005) and recent work confirmed this in iPSCs as well (Milagre et al. 2017). Differences in global DNA methylation have been also attributed to X-Chromosome dosage. In fact, female XaXa ESCs/iPSCs display a global DNA hypomethylation but in case they lose one X (XO), they display a male-like methylation level (Schulz et al. 2014; Choi, Clement, et al. 2017; Song et al. 2018).

It has been shown that at the molecular level X-dosage affects three pathways that regulate pluripotency and differentiation: the MAPK/Erk, GSK3 and Pi3K/AKT. The MAPK/Erk pathway downregulates *Nanog* whereas GSK3 mediated WNT signaling represses pluripotency factors such as ESRRB, NANOG and KLF2 via β-catenin and TCF3. Pi3K/AKT signaling promotes pluripotency and blocks differentiation (Lanner and Rossant 2010; Welham et al. 2011). Specifically, the presence of two XaXa inhibits MAPK/Erk and Gsk3 signaling, which increases activity of Pi3K/AKT pathway and decreases the global DNA methylation in ESCs/iPSCs. These X dosage effects are likely attributed to one of more X-linked genes, present in higher dose in XX female cells compare to male XY.

A recent study indicates that the X-linked gene ERK phosphatase, DUSP9, modulates DNA hypomethylation in female ESCs/iPSCs (Choi, Clement, et al. 2017). In fact, the heterozygous deletion of *Dusp9* in female ESCs/iPSCs causes an increase in global methylation while its overexpression in male cells induces partial hypomethylation. It has also been shown that *Dusp9* deletion causes up-regulation of MAPK/Erk target genes (Choi, Clement, et al. 2017; Song et al. 2018). In our screen among the candidates we focused on an X-linked gene, ERas, as potential enhancer in iPSC reprogramming (Welham et al. 2011). Indeed, upon ERas knockdown we saw a decrease in reprogramming efficiency. This is in line with what has been reported in the literature about its role in sustaining pluripotency. In fact, ERas is expressed at high levels in ESCs and is an activator of the Pi3K/AKT pathway (Welham et al. 2011). It has been shown that it increases the levels of Erk phosphorylation in female ESCs/iPSCs compared to male promoting the activation downstream of key pluripotency factors such as NANOG and SOX2. However, how ERas might mediate an increase of AKT

signaling in XX ESCs/iPSCs remains to elucidate. Notably, ERas was included in the original list of 24 factors screened for the ability to generate iPSC by the Yamanaka group (Takahashi and Yamanaka 2006a). At that time, it showed a marginal effect on reprogramming, however, the screening strategies were different, and have been improved substantially since then (Blelloch et al. 2007; Okita, Ichisaka, and Yamanaka 2007; Meissner, Wernig, and Jaenisch 2007).

Our hypothesis is also supported by a study showing that the pathway ERas-Akt-FoxO1 can play a role in somatic cell reprogramming (Yu et al. 2014). The enhancing role of ERas in reprogramming is also consistent with another study, where this factor was selected out by expression profiling during iPS cell reprogramming (Polo et al. 2012).

Other potential players in iPSCs reprogramming.

Another factor that came out from our screen was the transcription factor FOXP4 (S. Li, Weidenfeld, and Morrisey 2004). In our study upon its knockdown, we obtained a drastic reduction of iPSC colony formation. This result was consistent through the different reprogramming runs and was obtained with two different hairpins. Thus, FOXP4 might play a novel role in somatic cell reprogramming. However, very little is known about this factor. FOXP4 belongs to the FOXP family, forkhead transcription proteins, which play a key role in embryonic development and cell cycle regulation (Teufel et al. 2003). So far, it has not been described to have a role either in pluripotency or iPS cell reprogramming but has been described to have functions in heart and neural development (S. Li, Weidenfeld, and Morrisey 2004; Rousso et al. 2012). However, in a study on the OCT4 interaction network in embryonic stem cells, which revealed interactors with

documented roles in self-renewal such as ESRRB and DAX1, FOXP4 has been identified as OCT4 partner (van den Berg et al. 2010). Indeed, it might be worth to further characterize this factor by exploring also the function for its interaction with OCT4.

Among the novel unexpected factors we pointed out, there is CNIH4, a GPCR-protein about which very little is known from the literature (Sauvageau et al. 2014). In our screen upon knockdown of this candidate, we observed a decrease in terms of colony formation and X-Reactivation efficiency. Our hypothesis is that as a signaling protein CNIH4 might act through a specific pathway such as ERas thereby possibly affecting the activation of the pluripotency network. Further work will be needed to investigate CNIH4's exact role during reprogramming.

X-Reactivation and pluripotency can be uncoupled.

We were interested in studying the XCR process that occurs in the epiblast cell lineage in the inner cell mass of the late blastocyst to revert imprinted X-inactivation (Huynh and Lee 2003a). To do that we used as *in vitro* system iPS cell reprogramming. However, this system does not mimic exactly the reactivation of the paternal X-Chromosome in blastocyst. In fact, MEFs are somatic cells characterized by random X-inactivation and the reactivation of the X occurs as late event and concomitantly with endogenous Nanog gene up-regulation. *In vivo*, the reactivation of the Xp in blastocyst occurs in 24 hours and without cell division (Mak et al. 2004; I. Okamoto et al. 2004; L. H. Williams et al. 2011; Payer et al. 2013). Moreover, imprinted XCI is less stringently maintained than random XCI, because of less involvement of DNA

methylation as additional layer of silencing (T Sado et al. 2000). In fact, in extra-embryonic tissues, where imprinted XCI is maintained, X-linked genes can sporadically reactivate (Corbel et al. 2013; Dubois et al. 2014; Hadjantonakis et al. 2001). Nevertheless, using terminally differentiated cells to induce the reprogramming to iPS cells gave us the big advantage of a complete and stable XCI as starting point to study the XCR process. As described in the literature, pluripotency is a prerequisite in order to achieve XCR. Indeed, in our screen we could see how that factors with negative effects on iPS cell reprogramming had consequences on XCR efficiency as well. However, one of the most interesting findings in our study is that it is possible to uncouple the two processes. In other words, XCR is not a prerequisite for pluripotency. In fact, there are factors whose knockdown has a specific effect for the XCR without affecting the reprogramming.

SUV420H2, a histone methyltransferase for XCR.

One of the features of XCI is the enrichment of H4K20me1 on the inactive X where it acts as repressive mark (Kohlmaier et al. 2004). In *C. elegans* many studies have described the mechanism underlying the presence of this repressive mark on the X chromosomes (Liu et al. 2011; Vielle et al. 2012; Wells et al. 2012; Kramer et al. 2015). It has been shown that there is a correlation between the presence of H4K20me1 on the X and its condensed state (Oda et al. 2009b). Indeed, a recent study showed that the enrichment of H4K20me1 controls X chromosome topology by facilitating compaction and therefore, reducing gene expression (Brejc et al. 2017; Bian et al. 2017).

There are different methyltransferase and demethylases that regulate H4K20me1. PRSET-7 converts H4K20me into H4K20me1 which then can be further methylated by Suv420h1/2 into H4K20me2/me3

(Pannetier et al. 2008; Schotta 2004). Recently, a novel H4K20me2 Jumonji demethylase has been identified in *C. elegans*, DPY-21 which converts H4K20me2 into H4K20me1. Interestingly, it has been shown that mutants of DPY-21 present low levels of H4K20me1 and an increase in X-linked gene expression, suggesting its role in X chromosome silencing by enriching H4K20me1 on the X (Lau, Nabeshima, and Csankovszki 2014).

The histone methyltransferase SUV420H2 is one of the top candidates that came out from our screen. Its knockdown shows an effect on XCR by decreasing its efficiency without affecting the iPSCs formation. This suggests that SUV420H2 might play a specific role in XCR. It has been observed that SUV420H2 overexpression leads to a decrease in H4K20me1 and an increase of H4K20me3 in facultative heterochromatic regions on the X chromosome (Tsang, Hu, and Underhill 2010). Another study in *C. elegans* shows that the inhibition of a SUV420 ortholog, SET-4, might be responsible for H4K20me1 enrichment on the X (Vielle et al. 2012). In line with what has been described in the literature, we think that SUV420H2 might act by erasing the enrichment of H4K20me1 on the inactive X. As a consequence, this leads to a change in X chromosome topology by releasing the compaction and promoting reactivation of X-linked genes.

SMC1A: a candidate with specific effect on X-Reactivation.

We focused on a candidate, SMC1A, that could have a specific role in X-Reactivation. SMC1Ais a part of the cohesin complex and plays many key

roles in cell cycle, DNA repair and genome organization (Haering et al. 2002; Guacci, Koshland, and Strunnikov 1997; Michaelis, Ciosk, and Nasmyth 1997; H. Xu et al. 2010).

In our screen, we detected a decrease in X-Reactivation efficiency upon SMC1A knockdown as the number of XGFP-positive colonies was reduced compared to control. This result was confirmed by FACS analysis. In fact, while the control was showing at day 10 of reprogramming, a percentage of XGFP positive cells of around 25%, in the SMC1A knockdown sample this percentage decreased down to 4%. This suggested that SMC1A could have a role in XGFP reactivation. Besides that, another interesting aspect to point out is that in terms of percentage of reprogrammed cells there was no a significant difference between the control cells and SMC1A knock down cells. In fact, in both cases the percentage of SSEA1/EpCAM1-positive cells was the same of around 40%. This observation suggested that the two processes, pluripotency and X-Reactivation, can be uncoupled. We further checked if the effect of SMC1A knockdown was evident only for GFP-transgene reactivation or if it could also affect endogenous X-linked genes. To address that question, we checked the reactivation of *Hprt*, an X-linked gene, after selecting our reprogrammed cells in 6-TG (Eggan et al. 2000). From this experiment we assessed that upon knock down of SMC1A, iPS cells were able to survive in 6-TG medium, which were all XGFP-negative. This result suggested that not only the GFP transgene, but also the endogenous *Hprt* gene was not reactivated upon SMC1A knockdown showing that SMC1A plays a general role in reactivating X-linked genes.

What role can SMC1A play in X-Reactivation?

We decided to focus our attention on SMC1A and try to find out how this factor was able to have an effect on X-Chromosome reactivation. As mentioned earlier, cohesins play roles in different biological processes.
In recent years, it has been shown that cohesin is important in mediating architectural chromatin loops and topologically associated domains (TADs) and how this important function defines genome topology in association with CTCF (Wendt et al. 2008; Parelho et al. 2008; Rubio et al. 2008).
Related to X-Chromosome structure, it is known that the two Xs have a different topology. The active X has a pretty well-organized structure divided in TADs similar to autosomes, while the inactive X is almost devoid of TADs and is characterized by two megadomains separated by a hinge within the microsatellite repeat Dxz4 (Naughton et al. 2010b; Teller et al. 2011b; Giorgetti et al. 2014; Rao et al. 2014). Regarding the role of cohesin on the X chromosome, a recent paper showed how SMC1A binds the active X differently than the inactive one (Minajigi et al. 2015). In fact, it seems that cohesin binds the X in a specific manner that favors the Xa conformation. There are specific binding sites on the Xa that are not present on the Xi and that help to maintain the organized TAD structure. On the inactive X are only few specific Smc1a binding sites and when the X is coated by Xist RNA during inactivation, SMC1A is largely displaced from the X that then acquires a disorganized structure. When Xist is ablated from the inactive X, Xa-specific SMC1A binding sites are restored and the Xi acquires an Xa-like structure.
Therefore, our hypothesis was that SMC1A could have a role in X-Reactivation by shaping the structure of the X chromosome. In order to investigate that aspect, we started a collaboration with M. Victoire Neguembore from M. Pia Cosma lab, where we used a Super Resolution

Microscopy (STORM) approach. We chose this strategy to have a single cell read-out due to the high resolution of the technique in order to look at the global structure of the X chromosome, its compaction and single cohesin localizations on the X.

First, we performed an experiment in MEFs, where by random inactivation the cells have one active and one inactive X. We stained the two X chromosomes with a DNA Paint, identifying the inactive X by its characteristic H3K27me3 mark and compared the SMC1A localization on the two X-chromosomes. We performed the experiment with and without knocking down SMC1A. It is important to mention that even when upon knockdown the amount of cohesin was greatly reduced in the nucleus, the cells were perfectly viable. As shown in the literature, the active X showed a greater area than the inactive X which was more compacted (Naughton et al. 2010a; Teller et al. 2011c; Giorgetti et al. 2014). In agreement with published ChIP-seq data (Minajigi et al. 2015), we observed a preferential and significant enrichment of SMC1A binding on the Xa compared to the Xi in control cells. Upon knockdown we saw a drastic reduction of SMC1A on both chromosomes and the size of cohesin localizations, defined clusters, was comparable between the Xi and Xa. In particular, upon knockdown, the area of the two chromosomes was comparable displaying an Xi-like compacted configuration even on the Xa. This was an indication that SMC1A can have a role in shaping the X Chromosome into an active Xa structure and its depletion could affect it thereby as a consequence causing reduced X-Reactivation during iPSC reprogramming. However, these are only preliminary data and in order to prove that hypothesis, we will need to perform further experiments.

Future outlook

In summary we could identified through our screen potential players in both processes, pluripotency **(Fig.D1a)** and XCR **(Fig.D1b)**.

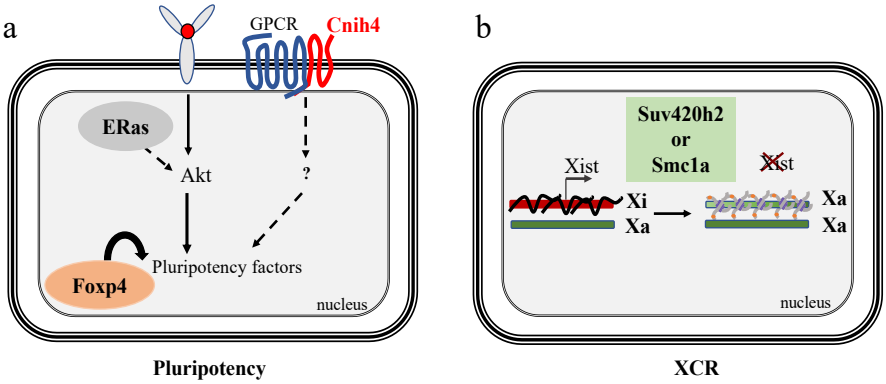

Figure D1 Schematic representation describing potential pathways of our top screen candidates related to pluripotency and XCR.

This opens up to the opportunity of developing different projects in the lab to characterize some of those factors and try to understand their molecular mechanism. We are now focusing on the follow up of SMC1A and SUV420H2 as XCR-specific factors.

Regarding SMC1A we are now performing the same experiment realized in MEFs, during the reprogramming at different time points. Our aim will be to follow the changes in X-Chromosome structure upon cohesin knockdown and possibly to see how TADs formation is affected.

For SUV420H2 we would like to confirm the exchange between H4K20me1 and H4K20me3 on the inactive X during X Chromosome Reactivation process. Furthermore, we will investigate possible changes of the chromosome structure across the transition from one histone

modification to the other. Another interesting question to answer is what happens if we knock down or knock out our candidates *in vivo* at the blastocyst stage when XCR occurs. Thereby we could study the effect on XCR function *in vivo* and also on cell fate and embryo development.

Conclusions

Main Conclusions

- Established screening conditions in iPS cells.
- RNAi screen for 60 selected candidates in iPSCs.
- Some factors show a phenotype in both Pluripotency and X-Reactivation.
- ERas, FOXP4 and CNIH4 show an effect on Pluripotency
- X-Reactivation can be uncoupled from Pluripotency.
- SUV420H2 and SMC1A as XCR-specific factors.
- SMC1A shows a preferential enrichment on the active X compared to the inactive one.

Material and Methods

Material and methods

1. Cell culture

1.1 Cell lines

The following cell lines have been used in this work:

- MEFs: wild-type female or male mouse embryonic fibroblasts were derived from E14.5 embryos. The sex was determined by genotyping for *Ube1*. Female MEFs containing a single polycistronic, DOX-inducible cassette carrying the four reprogramming factors *Oct4*, *Sox2*, *Klf4*, and *c-Myc* in the *Col1A* locus and the reverse tet-transactivator M2rtTA in the R26 locus were derived as described before (Stadtfeld et al. 2010). Cells also carry an XGFP transgene on the X-chromosome and a mutation on one of the two Hprt allele. X^{GFP}/Y males are crossed with homozygous hypoxanthine guanin phosphoribosyl transferase (*Hprt–*) mutant females (X^{Hprt-}/X^{Hprt-}) and mouse embryonic fibroblasts are derived from daughters carrying the transgene (X^{Hprt-}/X^{GFP}). Xi^{GFP}/Xa^{Hprt} (Hadjantonakis et al. 2001).
- EL16.7: Mouse embryonic stem cell line 16.7 (40XX, 129 ×[*M.castaneus* × 129) (J T Lee and Lu 1999) .
- HEK-293T: epithelial cell line derived from human embryonic kidney transformed with the SV40 virus large T antigen.

MEFs were cultured at 37°C in a 5% CO_2 and 5%O_2, waterlogged atmosphere using Dulbecco's Modified Eagle's Medium (DMEM, GIBCO®, Invitrogen), supplemented with 10% fetal bovine serum (FBS) (Life Tech.), penicillin/streptomycin (Ibian Tech), sodium pyruvate

(1mM, Invitrogen), Hepes (30mM, Life Tech), non-essential amino acid (NEAA) (Life Tech), 2-mercaptoethanol (0,1mM, Life Tech).
EL16.7 (ESCs) were maintained in gelatin (reference)-coated plates with DMEM supplemented with 15% ES-Cell fetal bovine serum (ES-FBS) (Life Tech), penicillin/streptomycin (Ibian Tech), sodium pyruvate (1mM, Life Tech), Hepes (30mM, Life Tech), non-essential amino acid (NEAA) (Life Tech), 2-mercaptoethanol (0,1mM, Life Tech) and LIF (0,01g/ml, Orf Genetics).
Both EL16.7 and HEK293T were cultured at 37°C in a 5% CO_2 waterlogged atmosphere.

1.2 iPSC induction

The reprogramming experiment of female OKSM-MEFs were routinely conducted on a feeder layer of male MEFs that were inactivated by irradiation, in the ESC culture medium supplemented with 15% fetal bovine serum (ES-cell FBS), with doxycycline (1ug/ml, Biogen Cientifica), ascorbic acid (25ug/ml, Sigma-Aldrich) and LIF (0,01ug/ml, Orf Genetics). After addition of dox, the medium was changed after 4 days and every two days from then. After Dox withdrawal at day 12, iPSCs were cultured in the ESC medium supplemented with ascorbic acid and LIF.

1.3 Plasmids

Short hairpin targeting the 60 genes cloned into pLKO-vector were purchased by the Broad Institute. A list of shRNAs divided in two batches is provided in **Table MM1** (Batch1) and **Table MM2** (Batch2).

Table MM1. List shRNAs Batch1

Gene	Clone ID	Target sequence
Bap1	TRCN0000030721	CCCACAACTATGACGAGTTTA
Bap1	TRCN0000030722	CGTCTGTGATTGATGATGATA
Bap1	TRCN0000315583	CCCTCAGTATTACCATGTCTT
Bex1	TRCN0000249062	CTGCCTTGTGATGTACAAATT
Bex1	TRCN0000257858	TTATGTAGATCTCTCCCTGTT
Bex1	TRCN0000257838	AGCCCATCGCTCACTATAGAT
Carm1	TRCN0000039114	GCCATGAAGATGTGTGTGTTT
Carm1	TRCN0000039118	CCCGACCAACACCATGCACTA
Carm1	TRCN0000039117	CCACGATTTCTGTTCTTTCTA
Cnih4	TRCN0000174324	CGTCTACTTCATCATTACATT
Cnih4	TRCN0000176170	GATTACATTAACGCCAGATCA
Cnih4	TRCN0000173594	GCTATACTACACACTGCACAA
Cobl	TRCN0000177543	CCAAGTATCATCACTTTAGAA
Cobl	TRCN0000182082	CGAAACAGACACTCCACCTAT
Cobl	TRCN0000177705	CCACAGTTACATCACTTGTTT
Eras	TRCN0000077699	GACTCACCAATGCTTCGTGAA
Eras	TRCN0000077698	GTCTCATGTCAAGGTGACAAT
Eras	TRCN0000077702	GCTTGGGCACAGTGCAAAGAT
Foxp4	TRCN0000071485	CCGCAGGAGAAGTAATGACAA
Foxp4	TRCN0000071486	CAGAGCTGGAAACGATGAGAT
Foxp4	TRCN0000071484	CCCTCCTTCACTTAAGTTATT
	TRCN0000274894	CCAGTTTATCAAACACCTCAA
Fst	TRCN0000066260	TGTCGAATGAACAAGAAGAAT
Fst	TRCN0000066262	GAGGAGGATGTGAACGACAAT
Fst	TRCN0000066261	GCAACTCCATCTCGGAAGAAA
Gadd45a	TRCN0000054690	CCTGCCTTAAGTCAACTTATT
Gadd45a	TRCN0000054688	CCCACATTCATCACAATGGAA
Gadd45a	TRCN0000054692	GCTCGGAGTCAGCGCACCATT

Gadd45b	TRCN0000234403	TGAAGAGAGCAGAGGCAATAA
Gadd45b	TRCN0000234402	CACGAACTGTCATACAGATTC
Gadd45b	TRCN0000234404	GACCCACTCCAAACATCTAAA
GFP	TRCN0000072181	ACAACAGCCACAACGTCTATA
GFP	TRCN0000072189	CCTACGGCGTGCAGTGCTTCA
GFP	TRCN0000072194	CCACATGAAGCAGCACGACTT
Ifitm1	TRCN0000066579	GTCATCGTTGTCTGTGCCATT
Ifitm1	TRCN0000066580	CACAATCAACATGCCTGAGAT
Ifitm1	TRCN0000066578	CCTGTTCAATACACTCTTCAT
Kdm6a	TRCN0000096243	CCTTCTCCTAAGTCCACTGAA
Kdm6a	TRCN0000331919	GCTACGAATCTCTAATCTTAA
Kdm6a	TRCN0000305237	TGGACTTGCAGCACGAATTAA
Klf7	TRCN0000084230	CTCAACGCAGTGACCTCATTA
Klf7	TRCN0000084232	CCCATGCATTGAGGAGAGCTT
Klf7	TRCN0000232328	TAACGGGTGCCGGAAAGTTTA
LacZ	TRCN0000072240	TCGTATTACAACGTCGTGACT
Luciferase	TRCN0000072256	ACGCTGAGTACTTCGAAATGT
Meis2	TRCN0000301408	CCACGAACTATGTGATAACTT
Meis2	TRCN0000301327	CCCACAATGTTAAATTCTGTA
Meis2	TRCN0000310875	TCTATGGGCACCCGTTGTTTC
Mst1	TRCN0000220496	CCAGGAATGTAACACGAAGTA
	TRCN0000308495	CCCGAATGTTGAGCGAGAATT
Mst1	TRCN0000220497	CGGACCTGCATTATGGACAAT
Mst1	TRCN0000220499	CCCGAATGTTGAGCGAGAATT
Nanog	TRCN0000075333	GCCAACCTGTACTATGTTTAA
Nanog	TRCN0000075334	GCCAGTGATTTGGAGGTGAAT
Nanog	TRCN0000075335	CCTGAGCTATAAGCAGGTTAA
Nr0b1	TRCN0000026217	CATCCTCTACAATCTACTGAT
Nr0b1	TRCN0000026229	CGCAGCTATGTGTGCGGTGAA
Nr0b1	TRCN0000026222	CCAGGCCATCAAGAGTTTCTT
Ntn1	TRCN0000071478	CGGAAGACTGTGATTCCTATT

Ntn1	TRCN0000071480	GTGGAAGTTCACCGTGAACAT
Ntn1	TRCN0000071481	GACCTATGTGAGCCTGCAATT
Pde9a	TRCN0000114892	CCACCTTTGATGTCTGGCTTT
Pde9a	TRCN0000114891	GACCTGCTACAGACCATGTTT
Pde9a	TRCN0000114894	GCTGAGCTGTTTAGAACATAT
Pou5f1	TRCN0000009611	GCCGACAACAATGAGAACCTT
Pou5f1	TRCN0000009612	CCTACAGCAGATCACTCACAT
	TRCN0000430010	CCACTTCACCACACTCTACTC
Pou5f1	TRCN0000009615	CAAGGGAGGTAGACAAGAGAA
Rab4a	TRCN0000088974	GATAATAAATGTCGGTGGTAA
Rab4a	TRCN0000088975	AGATGACTCAAATCATACCAT
Rab4a	TRCN0000088977	CTCAAATCATACCATAGGAAT
Rnf2	TRCN0000218768	GTAATCTGTGCCATAAGATTT
Rnf2	TRCN0000040581	CCATGACTACAAAGGAGTGTT
Rnf2	TRCN0000226018	TGAGAAGCAGTACACCATTTA
	TRCN0000040579	CCCATCCAACTCTTATGGAAA
Slc7a3	TRCN0000079384	CCGTACTACTAACTGTTCTTT
Slc7a3	TRCN0000079386	GCCCAAACTATAGACCTTGAT
Slc7a3	TRCN0000079387	GCCCGCTACTTGGTGGCTATT
Slc9a3r2	TRCN0000314066	CTCCACATGTTTCTAGTTAAT
Slc9a3r2	TRCN0000068616	CCAGGTGGTACAGAGGATCAA
Slc9a3r2	TRCN0000317802	GCGAGAGATCTTCAGCAACTT
Smc1a	TRCN0000324672	ACTCTATCTTCTTGTCTGGAT
Smc1a	TRCN0000324674	GCTTCAAATGCGGCTGAAGTA
	TRCN0000109030	ACTCTATCTTCTTGTCTGGAT
Smc1a	TRCN0000324673	GCAGGCATTTGAACAGATAAA
	TRCN0000109034	GCTTCAAATGCGGCTGAAGTA
Smc1b	TRCN0000109048	GCCTCAGTACATTAAGGCTAA
Smc1b	TRCN0000109046	CCATTGTTGTAGCCTCAGAAA
	TRCN0000109047	GCTCCATTCTTTGTATTAGAT
Smc1b	TRCN0000109049	GCTGAAGAAGATGCACAATTT

Suv420h2	TRCN0000039199	CCACTCCTGATTTCATCCCTA
	TRCN0000375750	AGAGCTGATCCTTGTTCTATG
Suv420h2	TRCN0000039203	CCGTGCTTGGAAGAAGAATGA
	TRCN0000340221	GAATGGAGTGCAGAGTCTATC
Suv420h2	TRCN0000039200	GAGAAGAATGAGCACTGTGAA
Tcf3	TRCN0000233416	GCACATCGTGCCTAAGCATTT
Tcf3	TRCN0000233412	TTTGACCCTAGCCGGACATAC
Tcf3	TRCN0000233415	CTGCACCTCAAGTCGGATAAG

Table MM2. List shRNAs Batch2**.**

Gene	Clone ID	Target sequence
Aes	TRCN0000097717	TGACGGAGAGAAGTCGGATTA
Aes	TRCN0000097719	CGACTCCTGTGACCGCATCAA
	TRCN0000097718	AGGCATTACGTCATGTACTAT
Aes	TRCN0000097715	CCCAGAATGTACACAACGCTA
Car14	TRCN0000114434	GAGACTGAGAATCCAGCTTAT
Car14	TRCN0000114431	CTGCTAGGTAACCCTCTCTAT
Car14	TRCN0000114433	CCTTTGGATCTACACAATAAT
Dnmt1	TRCN0000039028	GCAAAGAGTATGAGCCAATAT
Dnmt1	TRCN0000225698	TATATGAAGACCTGATCAATA
Dnmt1	TRCN0000225700	ACCAAGCTGTGTAGTACTTTG
	TRCN0000225699	CTATCGCATCGGTCGGATAAA
Enox1	TRCN0000248603	TGTGCCTTTGAAGGAATTAAA
Enox1	TRCN0000248602	AGCGCAAGAACATAGACATTT
Enox1	TRCN0000248605	CCAGACCTGTCCCTATGAATA
Etv4	TRCN0000295522	TCGGCCACAGAGGTGGATATT
Etv4	TRCN0000295466	TGGAGGCAGGCCAAATCTAAA
Etv4	TRCN0000055132	GTGATGGGTTATGGCTATGAA
Fgf17	TRCN0000067138	CCTGTGCTTGCAGCTATTGAT

Fgf17	TRCN0000067141	CATCGTGGAGACAGATACATT
	TRCN0000067140	CCACTTCATCAAGCGCCTCTA
Fgf17	TRCN0000067139	GAGCGAGAAGTACATCTGTAT
Fntb	TRCN0000190455	GTACAACATTGGACCTGAGAA
Fntb	TRCN0000340247	CCTCAAGAAGGAACGTTCTTT
Fntb	TRCN0000200895	CCAATGCTGAAATGGAAGATA
Fyn	TRCN0000023379	GCTCGGTTGATTGAAGACAAT
Fyn	TRCN0000023380	CCTGTATGGAAGGTTCACAAT
	TRCN0000023382	GCTCTGAAGTTGCCAAACCTT
Fyn	TRCN0000023381	CCTTTGGAAACCCAAGAGGTA
GFP	TRCN0000072199	TGACCCTGAAGTTCATCTGCA
GFP	TRCN0000072181	ACAACAGCCACAACGTCTATA
GFP	TRCN0000072194	CCACATGAAGCAGCACGACTT
Hdac5	TRCN0000238233	GACGCCTCCCTCCTACAAATT
Hdac5	TRCN0000238231	CCGTAGCCATCACAGCTAAAC
Hdac5	TRCN0000238230	CATCGCTGAGAACGGCTTTAC
Hmga1	TRCN0000235120	GACCAAAGGGAAGCAAGAATA
Hmga1	TRCN0000235119	GTGAAGTGCCAACTCCGAAGA
Hmga1	TRCN0000235122	AGTGATCACCACTCGCAGTGC
LacZ	TRCN0000072240	TCGTATTACAACGTCGTGACT
Luc	TRCN0000072250	AGAATCGTCGTATGCAGTGAA
Maz	TRCN0000238895	TCTGTGAGCTCTGCAACAAAG
Maz	TRCN0000238893	GATGCTGAGCTCGGCTTATAT
Maz	TRCN0000238897	GAGTAAGGTTGGGTGGTTAAA
Nap1l4	TRCN0000110216	CCCAACGACTACTTCACCAAT
Nap1l4	TRCN0000309401	GCAGTTCAGAATAGGAGATTA
Nap1l4	TRCN0000110219	GCAGCTTTGCAGGAACGTCTT
Phc1	TRCN0000273067	CACCTGAACCAACCTCTAAAC
Phc1	TRCN0000273005	GCCTGGCTGTTCAGGTTATAA
	TRCN0000012561	GCTTATTAGCTCAGCCACATA

Phc1	TRCN0000321173	CAACCTAATGCGGCTCAATAT
Pou5f1	TRCN0000426781	CAAGTTGGCGTGGAGACTTTG
	TRCN0000009613	CGTTCTCTTTGGAAAGGTGTT
Pou5f1	TRCN0000009612	CCTACAGCAGATCACTCACAT
Pou5f1	TRCN0000009615	CAAGGGAGGTAGACAAGAGAA
Rarg	TRCN0000222432	GCTCAGCATTGCCGACCAGAT
Rarg	TRCN0000279195	AGCCTGGGTCTAGACTCTAAA
Rarg	TRCN0000222433	CAATGACAAGTCTTCTGGCTA
Sbk1	TRCN0000088467	CTGCGTATGTTCCAGCGGCTT
Sbk1	TRCN0000088464	CCCGAGAATGTGCTGCTGTTT
Sbk1	TRCN0000088463	CCCTACAGTATTCCATCCAAA
Scarb1	TRCN0000066573	CGTCTCTGCTATGTCACTGAA
Scarb1	TRCN0000066575	CCCTTTCTACTTGTCTGTCTA
Scarb1	TRCN0000066577	CCTGTGTTGTCAGAAGCTGTT
Pde9a	TRCN0000114891	GACCTGCTACAGACCATGTTT
Pde9a	TRCN0000114894	GCTGAGCTGTTTAGAACATAT
Sin3b	TRCN0000287547	CCGTATAGACATTCCCAAGAA
Sin3b	TRCN0000294959	AGATGGTGTTCATCGTCAATT
Sin3b	TRCN0000039366	CCGCACCTTATCTTCGTGTAT
Slc20a2	TRCN0000317073	CCACAGCTCATCTTCCAGAAT
Slc20a2	TRCN0000068440	CCCATCTCCAATGGTACATTT
Slc20a2	TRCN0000068442	GAGTTACACAAGAAGCTGCTA
Stat4	TRCN0000235842	ACGGTGCAAACGGACACTTTA
Stat4	TRCN0000081642	CGCTGCAAGAAATGCTTAATA
Stat4	TRCN0000235844	AGCAATATTGGACCTAATTAA
Syce2	TRCN0000200645	CAGGAAAGACTACAAGAATTT
Syce2	TRCN0000201499	CCATGCACTTATGACCAACTT
Syce2	TRCN0000190656	GCTTCCATCTCAATGTGAGAA
Tcea3	TRCN0000084851	GAAGCTGAACAGTTGCCAGAT
	TRCN0000301963	GAAGCTGAACAGTTGCCAGAT

Tcea3	TRCN0000301898	CCATATCTATCAAGAACTCAA
Tcea3	TRCN0000301897	GCCTCAGAAATAGAAGACCAT
Tet1	TRCN0000341847	CAACTTGCATCCACGATTAAT
Tet1	TRCN0000341848	TTTCAACTCCGACGTAAATAT
Tet1	TRCN0000341917	TCTAACCAGTGTGCTAATATA
	TRCN0000341850	CCTACGGGAAGCGACCATAAT
Tet2	TRCN0000201087	CGCTGGACATTTGTCTTGAAA
Tet2	TRCN0000217530	CTTGTACTGTATAGGCATAAG
Tet2	TRCN0000192770	CCAACTCATGGGTCAATTCTT
Top3b	TRCN0000366938	TGGGAAGTGCCATCGATTTAT
Top3b	TRCN0000366940	ACTATGTCCCTACTGCTATAA
Top3b	TRCN0000375850	ATATCTGCCAGCGCAACTATG
Zfp42	TRCN0000096365	GCTCGAAACTAAAGCGACATT
Zfp42	TRCN0000096364	GCAGTAGTCAACAAATGAATA
Zfp42	TRCN0000096367	GTGTGTACTGTGGTGTCTTAT
	TRCN0000096366	AGCTCGAAACTAAAGCGACAT
Zfp423	TRCN0000084712	CGTGGAAGATGAGTCAATTTA
Zfp423	TRCN0000084709	CGGTGCATTACATGACTACAT
Zfp423	TRCN0000084708	CCCTGAATGTAACGTGAAGTT
Zfp462	TRCN0000095831	CGCAACATGATCGACCACATA
Zfp462	TRCN0000095832	GCAGGAACGAAATCCATACAA
Zfp462	TRCN0000095833	CCCTTAAAGAGCGAAACAGTA
Zfp57	TRCN0000256685	ATGTCAGATCCAACTCTATTA
Zfp57	TRCN0000256684	TAGCTCAGATCTGCAAGATAA

1.4 Virus preparation and cell infection

For MEF infection, lentiviral particles were produced following the RNA interference Consortium (TRC) instructions for lentiviral particle

production and infection in 6-well plates (http://www.broadinstitute.org.rnai.public/). Briefly, $5x10^5$ HEL293T cells/well were seeded in 6-well plates in DMEM, supplemented with 10% fetal bovine serum (FBS), without penicillin and streptomycin. The day after plating, the cells were co-transfected with 500ng of pLKO-shRNA for each factor, 500ng pCMV-dR8.9 and 25ng pCMV-VSV-G, using TransiT-LT1 as transfectant reagent (Mirus Bio). The day after transfection, the HEK293T medium was replaced with fresh one. The lentiviral-containing medium was harvested from HEK293T cells at 48h and 72h after transfection, filtered, concentrated with Lenti-X-Concentrator (Clontech). After concentration, the lentiviral-containing medium was centrifugated at 1500g for 45min at 4°C, the pellet resuspended in 500ul DMEM and stored at -80°C. Then $3x10^3$ MEFs/well were plated on 96-well plate. After 24h, cells were infected with 4ul of virus in combination with polybrene (Merk Chemicals and Life Science) at the concentration of 8ug/mml and centrifugated at 2250rpm for 30min at room temperature. The day after infection, these MEFs were washed in PBS, trypsinised and seeded on feeders in reprogramming medium.

1.5 Flow cytometry

For analysis and/or sorting, cells were trypsinised, washed in PBS and resuspended in PBS with 2% FBS and 1% Pen/Strep. Those harvested cells were incubated with antibodies against SSEA1 (APC, 1:20, eBioscience) and EpCAM1 (PE, 1:50, eBioscience) for 30min on ice, washed twice in PBS and stained with DAPI (1:1000, Biogen Cientifica) for viability. Then they were sorted or analyzed as indicated. Unstained cells were used as negative staining control.

1.6 RNA extraction and quantitative PCR detection of mRNA

RNA was extracted and purified using RNeasy kits (Qiagen), according to manufacturer instructions. Total RNA was treated with DNAse I (Qiagen) to prevent DNA contamination.

The cDNA was produced with High Capacity RNA-to-cDNA kit (Life Technologies) starting from 100ng RNA. Real-time quantitative PCR reactions from 10ng of cDNA were set up in triplicate using Power SYBR green PCR Master Mix (Thermo Fisher Scientific). The RT-PCR has been run with Viia 7 Real-Time PCR system (Applied Biosystem). For oligo sequences see **Table MM3**.

Table MM3. RT Primers sequences.

Target	Forward	Reverse
Aes	CCTCAGCAGCTCAAGTTCACC	CTTCAGGCTGTGATACTGCG
Bex1 (Rex3)	TAGATGGGACCTGATGCAGA	GAAGCTGGTAACAGGGAGAGA
Carm1	TGACATCAGTATTGTGGCACAG	CTGAGGAGCCTAAGGGAATCA
Cnih4	TCTCGCTCCTCGACTGTTG	CGGGATCACCCACTTGTTTAAT
Cobl	CTTAGGGGGAAGCTATGGACT	ACACATCCCTGTCATAACACCT
Dnmt1	GGCCATGGCTGACACTAAGCTG	CACCTGCACAGTGGCAGATCTG
Eras	TGCCTACAAAGTCTAGCATCTTG	CTTTTACCAACACCACTTGCAC
Fgf17	GCTGCCTAACCTTACCCTGTG	CCTGGTCCCTCACGTACTG
Foxp4	ATGATGGTGGAGTCTGCATCG	AGAGCCTGTTGCTGTTGGAAG
Fyn	ACCTCCATCCCGAACTACAAC	CGCCACAAACAGTGTCACTC
Gadd45a	CCGAAAGGATGGAC	TTATCGGGGTCTACGTTG

	ACGGTG	AGC
Gapdh	ATGAATACGGCTACAGCAACAGG	CTCTTGCTCAGTGTCCTTGCTG
Hdac5	TGCAGCACGTTTTGCTCCT	TGCAGCACGTTTTGCTCCT
Kdm6a (Utx)	CGGGCGGACAAAAGAAGAAC	CATAGACTTGCATCAGATCCTCC
Jpx	TTAGCCAGGCAGCTAGAGGA	AGCCGTATTCCTCCATGGTT
Mst1	CTCACCACTGAATGACTTCCAG	AAGGCCCGACAGTCCAGAA
Nanog	CTTTCACCTATTAAGGTGCTTGC	TGGCATCGGTTCATCATGGTAC
Nr0b1	GGTCCCTCTTGTACCGCTG	TCTTCTCCGCAGAAACAACAG
Oct4 (Pou5f1)	ACATCGCCAATCAGCTTGG	AGAACCATACTCGAACCACATCC
Phc1	TAGCACAGATGTCCCTGTATGA	TTGCTGGAGCATGAACTGGTG
Prdm14	ACAGCCAAGCAATTTGCACTAC	TTACCTGGCATTTTCATTGCTC
Rnf2	GAGTTACAACGAACACCTCAGG	CAATCCGCGCAAAACCGATG
Rnf12 (Rlim)	GGTCCACCACCACAGAGC	TGACCACTTCTTGTTGTATTTCC
Scarb1	TTTGGAGTGGTAGTAAAAAGGGC	TGACATCAGGGACTCAGAGTAG
Smc1a	CCATTCCGTGGCATGTCTGA	CAGGTGCTCCATGTATCAGGT
Smc1b	TCGGACCATTTCAGAGGTTTACC	CAGGTTTTCCAGTATGTGCTCC
Sox2	ACAGATGCAACCGATGCACC	TGGAGTTGTACTGCAGGGCG
Suv420h2	GAGAATTTCAAGTCGTGGCGA	ACAGGCAGTATTCCCATCTGA
Tcea3	GCAGAGCTGCGTGAAGAGG	GCAGCCGCTTCCAGTTTTTAAT
Tcf3	GGGTGCCAGCGAGATCAAG	ATGAGCAGTTTGGTCTGCGG
Tet1	ACACAGTGGTGCTAATGCAG	AGCATGAACGGGAGAATCGG
Tet2	AGAGAAGACAATCGAGAAGTCGG	CCTTCCGTACTCCCAAACTCAT
Top3b	GGGTGGAGGCTACAAGCAG	GACCTTTCCAAGGGCGGTT
Tsix	TGGGTCATTGGCAT	CCCAGGGTGTCTGATCTC

	CTTAGTC	TT
Zfp42 (Rex1)	ATGGCAGCTAGGAA ACAGTCT	TGGTAAAGGGTCTTCTGT GTAGA
Zfp57	CCCTCGACAGACTG ACCCTAA	TCGGGGCTAATCTCACTT TCAT
Xist	CCCGCTGCTGAGTG TTTGATATG	CAGAGTAGCGAGGACTTG AAGAG

1.7 Fluorescence in situ hybridization (FISH)

$5x10^4$ cells were grown in 8-well Lab-Tek chamber slides (Thermo Fisher Scientifc) and fixed in 4% paraformaldehyde for 10min at room temperature. Then, washed three times in PBS. Fixed cells were permeabilized in 0,5% Triton X-100 (Sigma- Aldrich) in PBS buffer for 10min at room temperature. And then washed in PBST (PBS with 0.1% Tween (Sigma-Aldrich)) and incubated for 2min at RT. Then the cells were incubated with 0.1N HCL for 5min at RT and washed twice in 2xSSCT for 1min each time at RT. Then washed in 2xSSCT+ 50% Formamide (Panreac AppliChem) for 2min at RT and stored in the same buffer at 4°C for up to 2 weeks.

For DNA-FISH 2xSSCT+ 50% Formamide was aspirated and any excess liquid was dried off.

10ul of X-Chromosome Paint (Metasystem) mix were added to the cells. Cells and the probe were denaturated at 78°C for 3min on a hot plate. A cover was placed over the hot plate to protect form the light during denaturation. The following step was the incubation of cells with the probe at 37°C overnight in a light-tight humidified chamber. To humidify, paper towels were placed in a light-tight box and dampen with water.

The day after cells were washed twice in 2xSSCT+50% Formamide at 45°C for 5min and then washed in 2xSSCT at 45°C for 5min. Another wash was done in 2XSSCT at RT for 5min. Then, the cells were incubated

in 2xSSCT + DAPI (1:1000) at RT for 5min and washed in PBS for 5min before immunofluorescence.

1.8 Immunofluorescence staining

As described earlier, $5x10^4$ cells were grown in 8-well Lab-Tek chamber slides and DNA-FISH was performed. Once aspirated the PBS, cells were incubated in blocking solution containing 10% bovine serum albumin (BSA, Sigma) and 0.01% Triton X-100 for 1h at room temperature. The cells were then left at 4°C overnight in blocking solution containing the primary antibody. The next day, the cells were washed three times in PBS and then, incubated with the secondary antibody for 45min at room temperature. The primary antibodies used are given in Table 2. Goat anti-mouse IgG, goat anti-rabbit IgG and anti-chicken IgG (1:500, Life Technologies) conjugated to Alexa Fluor-488, Alexa Fluor-555, Alexa Fluor-647, Alexa Fluor-TRITC were used as secondary antibodies. For STORM as secondary antibody has been used an AF405-AF647 dye pair (Ricci et al. 2015). Nuclear staining was performed with DAPI (1:1000, Biogen Cientifica).

1.9 Super Resolution Microscopy (STORM)

Immuno-FISH images were acquired in a N-STORM 4.0 microscope (Nikon) with an iXon Ultra 897 camera (Andor), a CFI HP Apochromat TIRF 100X 1.49 oil objective (Nikon), a Quad-band filter and TIRF/Hilo inclined illumination mode. X chromosome FISH, H3K27me3 and SMC1a signals were detected with 488 nm, 560 nm and 647 nm lasers respectively. Diffraction limited fluorescence images were taken at the beginning of each imaging cycle for all previously mentioned signals and were used as reference to identify the position and areas occupied by Xa

and Xi chromosomes. SMC1a STORM signal was acquired for 60 000 frames at 10 ms frame rate using sequential activation regime, meaning alternating one frame of 405 nm activation with three frames of 647 nm reporter. 405 nm activation was gradually increased over the imaging duration while 647 nm was maintained constant at 70% power over the whole acquisition. In order to allow proper blinking of molecules, imaging buffer was changed regularly, every hour. Imaging buffer was composed by 100 mM Cysteamine MEA (#30070, Sigma-Aldrich)—1% Glox Solution (0.5 mg/ml glucose oxidase, 40 mg/ml catalase (#G2133 and #C100, Sigma-Aldrich))—5% Glucose (#G8270, Sigma-Aldrich) in PBS.SMC1 signal was analyzed and rendered in Insight3 (Bates et al. 2007; Rust, Bates, and Zhuang 2006). Localizations were identified based on a minimum intensity threshold of 1200 and fit to a simple Gaussian with a width between 200 and 400 nm and a maximum axial ratio of 1.5. Images were rendered with localizations represented as uniform Gaussian peaks having a width of 9 nm and the same contrast parameters were applied to each image. In order to selectively analysis SMC1a signal belonging to X chromosomes, the area occupied by Xa and Xi (X paint signal) was manually drawn in Fiji and used as masks to select the overlapping SMC1a localizations. Chromosome selected localizations were analyzed with FindCluster (Ricci et al. 2015) a Matlab based code that identifies clusters of SMC1a signal and provide quantitative information regarding their size and distribution. Values obtained from FindCluster were plotted and analysed statistically with Graphpad Prism7.

2. Statistical analysis

Average from two independent experiments were calculated for most of the shown experiments. Two tailed paired t-test or one sample t-test.
$p < 0.05$ defined statistical significance.

Table MM4. *List of 57 candidates and controls (*).*

Factor	Function	Potential role	Reference
AES/ GRG5	Transcriptional corepressor		
BAP1	Deubiquitylase		
BEX1	Signaling molecule		
CAR14	Zinc metalloenzyme		
CARM1	Chromatin modifier	Role in pluripotency maintenance	(Q. Wu et al. 2009)
CNIH4	GPCR coupled protein		
COBL	Actin-binding protein		
DNMT1*	DNA methyltransferase	Reprogramming repressor, role in XCR	(Mikkelsen et al. 2008; T Sado et al. 2000)
ENOX1	NADH oxidase		
ERAS	GTPase	Role in reprogramming	(Yu et al. 2014)
ETV4	Transcriptional factor	Upregulated in vivo iPS	(Abad et al. 2013)
FGF17	Growth factor		
FNTB	Farnesyltransferase		
FOXP4	Transcription factor		
FST	Activin-binding protein		
FYN	Kinase protein	Function in oocyte meiosis	(McGinnis, Kinsey, and Albertini 2009)
GADD45A	Nuclear protein	Role in DNA demethylation/ Reprogramming enhancer	(K. Chen et al. 2016; Z. Li et al. 2015)
GADD45B	Nuclear protein	Role in DNA demethylation	(Sultan et al. 2012)
HDAC5	Histone deacetylase		
HMGA1	Architectural factor	Role in reprogramming/Xist promoter binding in vole	(Shah et al. 2012; Orishchenko et al. 2012)

IFITM1	Transmembrane protein	Role in PGCs repulsion	(Tanaka et al. 2005)
KDM6A/ UTX*	H3k27me3 demethylase	Somatic cell reprogramming regulator	(Mansour et al. 2012)
KLF7	Transcription factor		
MAZ	Transcription factor		
MEIS2	Transcription regulator		
MST1	Kinase protein		
NANOG*	Pluripotency factor	Role in pluripotency and reprogramming	(Jose Silva et al. 2009)
NAP1L4	Histone chaperone		
NR0B1	Nuclear receptor	Required for testis determination	(Meeks, Weiss, and Jameson 2003)
NTN1	Signaling molecule		
PDE9A	Phosphodiesterase		
PHC1		Component of Polycomb repressive complex 1	(Isono et al. 2005)
OCT4*	Pluripotency factor	Role in pluripotency and reprogramming	(Takahashi and Yamanaka 2006a)
RAB4A	GTPase		
RARG	Receptor	Reprogramming enhancer	(W. Wang et al. n.d.)
RNF2	E3 ubiquitin-protein ligase	Essential to stably maintain an undifferentiated state of mouse ES cells	(van der Stoop et al. 2008)
SBK1	Kinase protein		
SCARB1	Receptor	Infertility and exencephaly in females	(Santander et al. 2013)
SIN3B	Transcription regulator		
SLC20A2	Receptor	Female specific growth defect	(Wallingford, Gammill, and Giachelli 2016)
SLC7A3	Protein transport		

SLC9A3R2	Scaffold protein		
SMC1A	Cohesin	Chromosome structure	(Minajigi et al. 2015)
SMC1B	Cohesin	Sister chromatid cohesion in meiosis of human oocytes	(Garcia-Cruz et al. 2010)
STAT4	Transcription factor		
SUV420H2	H4K20me3 methylase	Chromatin remodeler	(Tsang, Hu, and Underhill 2010)
SYCE2	Synaptonemal complex	Necessary for XY body formation, spermatogenesis and oogenesis	(Bolcun-Filas et al. 2007)
TCEA3	Transcription factor	Self-renewal and/or pluripotent differentiation potential control	(Park et al. 2013)
TCF3*	Transcription factor	Reprogramming repressor	(Lluis et al. 2011)
TET1*	Dioxygenase	DNA demethylation/ reprogramming enhancer or repressor	(Esteban et al. 2010)
TET2*	Dioxygenase	DNA demethylation/reprogramming enhancer	(Costa et al. 2013)
TOP3B	DNA topoisomerase	Role in meiosis and XY body	(Kwan, Moens, and Wang 2003)
ZFP42/ REX1	Pluripotency factor	Rex1, repressor of xist, activator of tsix	(Pablo Navarro et al. 2010)
ZFP423	Transcription factor		
ZFP462	Zinc finger protein		
ZFP57	Transcriptional repressor	Involved in imprinting	(X. Li et al. 2008)

Abbreviations

Abbreviations

6TG 6-Tio-Guanine

AP Alkaline Phosphatase

CTCF CCCTC-binding factor

E Embryonic day of development

EPI Epiblast

ESCs Embryonic stem cells

FACS Fluorescence-activated cell sorting

FISH Fluorescent in situ hybridization

HAT Hypoxanthine-aminopterin-thymidine

ICM Inner Cell Mass

iPSCs Induced Pluripotent Stem Cells

KD Knockdown

lncRNA long non-coding RNA

MEFs Mouse embryonic fibroblasts

OKSM Oct4-Klf4-Sox2-c-Myc

PE Primitive Endoderm

PGCs Primordial Germ Cells

RT-PCR Real time PCR

shRNA short hairpin RNA

STORM Stochastic Optical Reconstruction Microscopy

TAD Topologically Associated Domain

TE Trophectoderm

Xa Active X-Chromosome

Xi Inactive X-Chromosome

Xic X-Inactivation Center

XCI X-Chromosome Inactivation

XCR X-Chromosome Reactivation

Xm Maternally Inherited X-Chromosome

Xp Paternally Inherited X-Chromosome

Xist X-Inactive Specific Transcript

YY1 Yin Yang 1

References

References

Abad, María, Lluc Mosteiro, Cristina Pantoja, Marta Cañamero, Teresa Rayon, Inmaculada Ors, Osvaldo Graña, et al. 2013. "Reprogramming in Vivo Produces Teratomas and IPS Cells with Totipotency Features." *Nature* 502 (7471): 340–45. https://doi.org/10.1038/nature12586.

Agger, Karl, Paul A. C. Cloos, Jesper Christensen, Diego Pasini, Simon Rose, Juri Rappsilber, Irina Issaeva, Eli Canaani, Anna Elisabetta Salcini, and Kristian Helin. 2007. "UTX and JMJD3 Are Histone H3K27 Demethylases Involved in HOX Gene Regulation and Development." *Nature* 449 (7163): 731–34. https://doi.org/10.1038/nature06145.

Alipour, Elnaz, and John F Marko. 2012. "Self-Organization of Domain Structures by DNA-Loop-Extruding Enzymes." *Nucleic Acids Research* 40 (22): 11202–12. https://doi.org/10.1093/nar/gks925.

Almeida, Mafalda, Greta Pintacuda, Osamu Masui, Yoko Koseki, Michal Gdula, Andrea Cerase, David Brown, et al. 2017. "PCGF3/5-PRC1 Initiates Polycomb Recruitment in X Chromosome Inactivation." *Science (New York, N.Y.)* 356 (6342): 1081–84. https://doi.org/10.1126/science.aal2512.

Ang, Yen-Sin, Su-Yi Tsai, Dung-Fang Lee, Jonathan Monk, Jie Su, Kajan Ratnakumar, Junjun Ding, et al. 2011. "Wdr5 Mediates Self-Renewal and Reprogramming via the Embryonic Stem Cell Core Transcriptional Network." *Cell* 145 (2): 183–97. https://doi.org/10.1016/j.cell.2011.03.003.

Anguera, Montserrat C, Weiyuan Ma, Danielle Clift, Satoshi Namekawa, Raymond J Kelleher, and Jeannie T Lee. 2011. "Tsx Produces a Long Noncoding RNA and Has General Functions in the Germline,

Stem Cells, and Brain." Edited by Gregory S. Barsh. *PLoS Genetics* 7 (9): e1002248. https://doi.org/10.1371/journal.pgen.1002248.

Bar-Nur, Ori, Justin Brumbaugh, Cassandra Verheul, Effie Apostolou, Iulian Pruteanu-Malinici, Ryan M Walsh, Sridhar Ramaswamy, and Konrad Hochedlinger. 2014. "Small Molecules Facilitate Rapid and Synchronous IPSC Generation." *Nature Methods* 11 (11): 1170–76. https://doi.org/10.1038/nmeth.3142.

Barakat, Tahsin Stefan, Nilhan Gunhanlar, Cristina Gontan Pardo, Eskeatnaf Mulugeta Achame, Mehrnaz Ghazvini, Ruben Boers, Annegien Kenter, Eveline Rentmeester, J Anton Grootegoed, and Joost Gribnau. 2011. "RNF12 Activates Xist and Is Essential for X Chromosome Inactivation." Edited by Wolf Reik. *PLoS Genetics* 7 (1): e1002001. https://doi.org/10.1371/journal.pgen.1002001.

Barakat, Tahsin Stefan, Friedemann Loos, Selma van Staveren, Elvira Myronova, Mehrnaz Ghazvini, J Anton Grootegoed, and Joost Gribnau. 2014. "The Trans-Activator RNF12 and Cis-Acting Elements Effectuate X Chromosome Inactivation Independent of X-Pairing." *Molecular Cell* 53 (6): 965–78. https://doi.org/10.1016/j.molcel.2014.02.006.

BARR, M L, and E G BERTRAM. 1949. "A Morphological Distinction between Neurones of the Male and Female, and the Behaviour of the Nucleolar Satellite during Accelerated Nucleoprotein Synthesis." *Nature* 163 (4148): 676. http://www.ncbi.nlm.nih.gov/pubmed/18120749.

Bates, M., B. Huang, G. T. Dempsey, and X. Zhuang. 2007. "Multicolor Super-Resolution Imaging with Photo-Switchable Fluorescent Probes." *Science* 317 (5845): 1749–53. https://doi.org/10.1126/science.1146598.

Beletskii, A, Y K Hong, J Pehrson, M Egholm, and W M Strauss. 2001. "PNA Interference Mapping Demonstrates Functional Domains in

the Noncoding RNA Xist." *Proceedings of the National Academy of Sciences of the United States of America* 98 (16): 9215–20. https://doi.org/10.1073/pnas.161173098.

Bell, A C, A G West, and G Felsenfeld. 1999. "The Protein CTCF Is Required for the Enhancer Blocking Activity of Vertebrate Insulators." *Cell* 98 (3): 387–96. http://www.ncbi.nlm.nih.gov/pubmed/10458613.

Belote, J M, and J C Lucchesi. 1980. "Male-Specific Lethal Mutations of Drosophila Melanogaster." *Genetics* 96 (1): 165–86. http://www.ncbi.nlm.nih.gov/pubmed/6781985.

Berg, Debbie L C van den, Tim Snoek, Nick P Mullin, Adam Yates, Karel Bezstarosti, Jeroen Demmers, Ian Chambers, and Raymond A Poot. 2010. "An Oct4-Centered Protein Interaction Network in Embryonic Stem Cells." *Cell Stem Cell* 6 (4): 369–81. https://doi.org/10.1016/j.stem.2010.02.014.

Berletch, Joel B., Fan Yang, Jun Xu, Laura Carrel, and Christine M. Disteche. 2011. "Genes That Escape from X Inactivation." *Human Genetics* 130 (2): 237–45. https://doi.org/10.1007/s00439-011-1011-z.

BEUTLER, E, M YEH, and V F FAIRBANKS. 1962. "The Normal Human Female as a Mosaic of X-Chromosome Activity: Studies Using the Gene for C-6-PD-Deficiency as a Marker." *Proceedings of the National Academy of Sciences of the United States of America* 48 (January): 9–16. http://www.ncbi.nlm.nih.gov/pubmed/13868717.

Bian, Qian, Erika C Anderson, Katjuša Brejc, and Barbara J Meyer. 2017. "Dynamic Control of Chromosome Topology and Gene Expression by a Chromatin Modification." *Cold Spring Harbor Symposia on Quantitative Biology* 82: 279–91. https://doi.org/10.1101/sqb.2017.82.034439.

Bischoff, A, J Albers, I Kharboush, E Stelzer, T Cremer, and C Cremer.

1993. “Differences of Size and Shape of Active and Inactive X-Chromosome Domains in Human Amniotic Fluid Cell Nuclei.” *Microscopy Research and Technique* 25 (1): 68–77. https://doi.org/10.1002/jemt.1070250110.

Blelloch, Robert, Monica Venere, Jonathan Yen, and Miguel Ramalho-Santos. 2007. “Generation of Induced Pluripotent Stem Cells in the Absence of Drug Selection.” *Cell Stem Cell* 1 (3): 245–47. https://doi.org/10.1016/j.stem.2007.08.008.

Blewitt, Marnie E, Anne-Valerie Gendrel, Zhenyi Pang, Duncan B Sparrow, Nadia Whitelaw, Jeffrey M Craig, Anwyn Apedaile, et al. 2008. “SmcHD1, Containing a Structural-Maintenance-of-Chromosomes Hinge Domain, Has a Critical Role in X Inactivation.” *Nature Genetics* 40 (5): 663–69. https://doi.org/10.1038/ng.142.

Bolcun-Filas, Ewelina, Yael Costa, Robert Speed, Mary Taggart, Ricardo Benavente, Dirk G De Rooij, and Howard J Cooke. 2007. “SYCE2 Is Required for Synaptonemal Complex Assembly, Double Strand Break Repair, and Homologous Recombination.” *The Journal of Cell Biology* 176 (6): 741–47. https://doi.org/10.1083/jcb.200610027.

Bonora, G., X. Deng, H. Fang, V. Ramani, R. Qiu, J. B. Berletch, G. N. Filippova, et al. 2018. “Orientation-Dependent Dxz4 Contacts Shape the 3D Structure of the Inactive X Chromosome.” *Nature Communications* 9 (1): 1445. https://doi.org/10.1038/s41467-018-03694-y.

Borensztein, Maud, Ikuhiro Okamoto, Laurène Syx, Guillaume Guilbaud, Christel Picard, Katia Ancelin, Rafael Galupa, et al. 2017. “Contribution of Epigenetic Landscapes and Transcription Factors to X-Chromosome Reactivation in the Inner Cell Mass.” *Nature Communications* 8 (1): 1297. https://doi.org/10.1038/s41467-017-

01415-5.

Brejc, Katjuša, Qian Bian, Satoru Uzawa, Bayly S Wheeler, Erika C Anderson, David S King, Philip J Kranzusch, Christine G Preston, and Barbara J Meyer. 2017. "Dynamic Control of X Chromosome Conformation and Repression by a Histone H4K20 Demethylase." *Cell* 171 (1): 85–102.e23. https://doi.org/10.1016/j.cell.2017.07.041.

Brown, C J, B D Hendrich, J L Rupert, R G Lafrenière, Y Xing, J Lawrence, and H F Willard. 1992. "The Human XIST Gene: Analysis of a 17 Kb Inactive X-Specific RNA That Contains Conserved Repeats and Is Highly Localized within the Nucleus." *Cell* 71 (3): 527–42. http://www.ncbi.nlm.nih.gov/pubmed/1423611.

Brown, Carolyn J., Andrea Ballabio, James L. Rupert, Ronald G. Lafreniere, Markus Grompe, Rossana Tonlorenzi, and Huntington F. Willard. 1991. "A Gene from the Region of the Human X Inactivation Centre Is Expressed Exclusively from the Inactive X Chromosome." *Nature* 349 (6304): 38–44. https://doi.org/10.1038/349038a0.

Carrel, Laura, and Huntington F Willard. 2005. "X-Inactivation Profile Reveals Extensive Variability in X-Linked Gene Expression in Females." *Nature* 434 (7031): 400–404. https://doi.org/10.1038/nature03479.

Chadwick, Brian P, and Huntington F Willard. 2004. "Multiple Spatially Distinct Types of Facultative Heterochromatin on the Human Inactive X Chromosome." *Proceedings of the National Academy of Sciences of the United States of America* 101 (50): 17450–55. https://doi.org/10.1073/pnas.0408021101.

Chan, Yun-Shen, Jonathan Göke, Xinyi Lu, Nandini Venkatesan, Bo Feng, I-Hsin Su, and Huck-Hui Ng. 2013. "A PRC2-Dependent Repressive Role of PRDM14 in Human Embryonic Stem Cells and Induced Pluripotent Stem Cell Reprogramming." *STEM CELLS* 31

(4): 682–92. https://doi.org/10.1002/stem.1307.

Chaumeil, Julie, Patricia Le Baccon, Anton Wutz, and Edith Heard. 2006. "A Novel Role for Xist RNA in the Formation of a Repressive Nuclear Compartment into Which Genes Are Recruited When Silenced." *Genes & Development* 20 (16): 2223–37. https://doi.org/10.1101/gad.380906.

Cheloufi, Sihem, Ulrich Elling, Barbara Hopfgartner, Youngsook L Jung, Jernej Murn, Maria Ninova, Maria Hubmann, et al. 2015. "The Histone Chaperone CAF-1 Safeguards Somatic Cell Identity." *Nature* 528 (7581): 218–24. https://doi.org/10.1038/nature15749.

Chen, C.-K., M. Blanco, C. Jackson, E. Aznauryan, N. Ollikainen, C. Surka, A. Chow, A. Cerase, P. McDonel, and M. Guttman. 2016. "Xist Recruits the X Chromosome to the Nuclear Lamina to Enable Chromosome-Wide Silencing." *Science* 354 (6311): 468–72. https://doi.org/10.1126/science.aae0047.

Chen, Jiekai, Lin Guo, Lei Zhang, Haoyu Wu, Jiaqi Yang, He Liu, Xiaoshan Wang, et al. 2013. "Vitamin C Modulates TET1 Function during Somatic Cell Reprogramming." *Nature Genetics* 45 (12): 1504–9. https://doi.org/10.1038/ng.2807.

Chen, Keshi, Qi Long, Tao Wang, Danyun Zhao, Yanshuang Zhou, Juntao Qi, Yi Wu, et al. 2016. "Gadd45a Is a Heterochromatin Relaxer That Enhances IPS Cell Generation." *EMBO Reports* 17 (11): 1641–56. https://doi.org/10.15252/embr.201642402.

Chen, Tong, Ya-Juan Hao, Ying Zhang, Miao-Miao Li, Meng Wang, Weifang Han, Yongsheng Wu, et al. 2015. "M(6)A RNA Methylation Is Regulated by MicroRNAs and Promotes Reprogramming to Pluripotency." *Cell Stem Cell* 16 (3): 289–301. https://doi.org/10.1016/j.stem.2015.01.016.

Choi, Jiho, Kendell Clement, Aaron J Huebner, Jamie Webster, Christopher M Rose, Justin Brumbaugh, Ryan M Walsh, et al. 2017.

"DUSP9 Modulates DNA Hypomethylation in Female Mouse Pluripotent Stem Cells." *Cell Stem Cell* 20 (5): 706–719.e7. https://doi.org/10.1016/j.stem.2017.03.002.

Choi, Jiho, Aaron J Huebner, Kendell Clement, Ryan M Walsh, Andrej Savol, Kaixuan Lin, Hongcang Gu, et al. 2017. "Prolonged Mek1/2 Suppression Impairs the Developmental Potential of Embryonic Stem Cells." *Nature* 548 (7666): 219–23. https://doi.org/10.1038/nature23274.

Chu, Ci, Qiangfeng Cliff Zhang, Simão Teixeira da Rocha, Ryan A Flynn, Maheetha Bharadwaj, J Mauro Calabrese, Terry Magnuson, Edith Heard, and Howard Y Chang. 2015. "Systematic Discovery of Xist RNA Binding Proteins." *Cell* 161 (2): 404–16. https://doi.org/10.1016/j.cell.2015.03.025.

Chureau, Corinne, Sophie Chantalat, Antonio Romito, Angélique Galvani, Laurent Duret, Philip Avner, and Claire Rougeulle. 2011. "Ftx Is a Non-Coding RNA Which Affects Xist Expression and Chromatin Structure within the X-Inactivation Center Region." *Human Molecular Genetics* 20 (4): 705–18. https://doi.org/10.1093/hmg/ddq516.

Chuva de Sousa Lopes, Susana M., Katsuhiko Hayashi, Tanya C. Shovlin, Will Mifsud, M. Azim Surani, and Anne McLaren††. 2008. "X Chromosome Activity in Mouse XX Primordial Germ Cells." *PLoS Genetics* 4 (2): e30. https://doi.org/10.1371/journal.pgen.0040030.

Cifuentes-Rojas, Catherine, Alfredo J. Hernandez, Kavitha Sarma, and Jeannie T. Lee. 2014. "Regulatory Interactions between RNA and Polycomb Repressive Complex 2." *Molecular Cell* 55 (2): 171–85. https://doi.org/10.1016/j.molcel.2014.05.009.

Cohen, Dena E, Lance S Davidow, Jennifer A Erwin, Na Xu, David Warshawsky, and Jeannie T Lee. 2007. "The DXPas34 Repeat Regulates Random and Imprinted X Inactivation." *Developmental*

Cell 12 (1): 57–71. https://doi.org/10.1016/j.devcel.2006.11.014.

Cooper, Sarah, Anne Grijzenhout, Elizabeth Underwood, Katia Ancelin, Tianyi Zhang, Tatyana B Nesterova, Burcu Anil-Kirmizitas, et al. 2016. "Jarid2 Binds Mono-Ubiquitylated H2A Lysine 119 to Mediate Crosstalk between Polycomb Complexes PRC1 and PRC2." *Nature Communications* 7 (November): 13661. https://doi.org/10.1038/ncomms13661.

Corbel, Catherine, Patricia Diabangouaya, Anne-Valerie Gendrel, Jennifer C Chow, and Edith Heard. 2013. "Unusual Chromatin Status and Organization of the Inactive X Chromosome in Murine Trophoblast Giant Cells." *Development (Cambridge, England)* 140 (4): 861–72. https://doi.org/10.1242/dev.087429.

Costa, Yael, Junjun Ding, Thorold W Theunissen, Francesco Faiola, Timothy A Hore, Pavel V Shliaha, Miguel Fidalgo, et al. 2013. "NANOG-Dependent Function of TET1 and TET2 in Establishment of Pluripotency." *Nature* 495 (7441): 370–74. https://doi.org/10.1038/nature11925.

Costanzi, Carl, and John R. Pehrson. 1998. "Histone MacroH2A1 Is Concentrated in the Inactive X Chromosome of Female Mammals." *Nature* 393 (6685): 599–601. https://doi.org/10.1038/31275.

Csankovszki, G, A Nagy, and R Jaenisch. 2001. "Synergism of Xist RNA, DNA Methylation, and Histone Hypoacetylation in Maintaining X Chromosome Inactivation." *The Journal of Cell Biology* 153 (4): 773–84. http://www.ncbi.nlm.nih.gov/pubmed/11352938.

Csankovszki, G, B Panning, B Bates, J R Pehrson, and R Jaenisch. 1999. "Conditional Deletion of Xist Disrupts Histone MacroH2A Localization but Not Maintenance of X Inactivation." *Nature Genetics* 22 (4): 323–24. https://doi.org/10.1038/11887.

Darrow, Emily M, Miriam H Huntley, Olga Dudchenko, Elena K Stamenova, Neva C Durand, Zhuo Sun, Su-Chen Huang, et al. 2016.

"Deletion of DXZ4 on the Human Inactive X Chromosome Alters Higher-Order Genome Architecture." *Proceedings of the National Academy of Sciences of the United States of America* 113 (31): E4504-12. https://doi.org/10.1073/pnas.1609643113.

Darrow, Emily M, Andrew P Seberg, Sunny Das, Debbie M Figueroa, Zhuo Sun, Shawn C Moseley, and Brian P Chadwick. 2014. "A Region of Euchromatin Coincides with an Extensive Tandem Repeat on the Mouse (Mus Musculus) Inactive X Chromosome." *Chromosome Research : An International Journal on the Molecular, Supramolecular and Evolutionary Aspects of Chromosome Biology* 22 (3): 335–50. https://doi.org/10.1007/s10577-014-9424-x.

Davidson, Iain F, Daniela Goetz, Maciej P Zaczek, Maxim I Molodtsov, Pim J Huis in 't Veld, Florian Weissmann, Gabriele Litos, et al. 2016. "Rapid Movement and Transcriptional Re-localization of Human Cohesin on DNA." *The EMBO Journal* 35 (24): 2671–85. https://doi.org/10.15252/embj.201695402.

DAVIDSON, R G, H M NITOWSKY, and B CHILDS. 1963. "DEMONSTRATION OF TWO POPULATIONS OF CELLS IN THE HUMAN FEMALE HETEROZYGOUS FOR GLUCOSE-6-PHOSPHATE DEHYDROGENASE VARIANTS." *Proceedings of the National Academy of Sciences of the United States of America* 50 (September): 481–85. http://www.ncbi.nlm.nih.gov/pubmed/14067093.

Dekker, Job, Karsten Rippe, Martijn Dekker, and Nancy Kleckner. 2002. "Capturing Chromosome Conformation." *Science (New York, N.Y.)* 295 (5558): 1306–11. https://doi.org/10.1126/science.1067799.

Deng, Xinxian, Wenxiu Ma, Vijay Ramani, Andrew Hill, Fan Yang, Ferhat Ay, Joel B. Berletch, et al. 2015. "Bipartite Structure of the Inactive Mouse X Chromosome." *Genome Biology* 16 (1): 152. https://doi.org/10.1186/s13059-015-0728-8.

Dietzel, S, R Eils, K Sätzler, H Bornfleth, A Jauch, C Cremer, and T Cremer. 1998. “Evidence against a Looped Structure of the Inactive Human X-Chromosome Territory.” *Experimental Cell Research* 240 (2): 187–96. https://doi.org/10.1006/excr.1998.3934.

Dixon, Jesse R., Siddarth Selvaraj, Feng Yue, Audrey Kim, Yan Li, Yin Shen, Ming Hu, Jun S. Liu, and Bing Ren. 2012. “Topological Domains in Mammalian Genomes Identified by Analysis of Chromatin Interactions.” *Nature* 485 (7398): 376–80. https://doi.org/10.1038/nature11082.

Donohoe, Mary E, Susana S Silva, Stefan F Pinter, Na Xu, and Jeannie T Lee. 2009. “The Pluripotency Factor Oct4 Interacts with Ctcf and Also Controls X-Chromosome Pairing and Counting.” *Nature* 460 (7251): 128–32. https://doi.org/10.1038/nature08098.

Dubois, Agnès, Jane Lynda Deuve, Pablo Navarro, Sarra Merzouk, Sylvain Pichard, Pierre-Henri Commere, Anne Louise, Danielle Arnaud, Philip Avner, and Céline Morey. 2014. “Spontaneous Reactivation of Clusters of X-Linked Genes Is Associated with the Plasticity of X-Inactivation in Mouse Trophoblast Stem Cells.” *Stem Cells (Dayton, Ohio)* 32 (2): 377–90. https://doi.org/10.1002/stem.1557.

Eggan, K, H Akutsu, K Hochedlinger, W Rideout, R Yanagimachi, and R Jaenisch. 2000. “X-Chromosome Inactivation in Cloned Mouse Embryos.” *Science (New York, N.Y.)* 290 (5496): 1578–81. http://www.ncbi.nlm.nih.gov/pubmed/11090356.

Eils, R, S Dietzel, E Bertin, E Schröck, M R Speicher, T Ried, M Robert-Nicoud, C Cremer, and T Cremer. 1996. “Three-Dimensional Reconstruction of Painted Human Interphase Chromosomes: Active and Inactive X Chromosome Territories Have Similar Volumes but Differ in Shape and Surface Structure.” *The Journal of Cell Biology* 135 (6 Pt 1): 1427–40.

http://www.ncbi.nlm.nih.gov/pubmed/8978813.

Engreitz, Jesse M, Amy Pandya-Jones, Patrick McDonel, Alexander Shishkin, Klara Sirokman, Christine Surka, Sabah Kadri, et al. 2013. "The Xist LncRNA Exploits Three-Dimensional Genome Architecture to Spread across the X Chromosome." *Science (New York, N.Y.)* 341 (6147): 1237973. https://doi.org/10.1126/science.1237973.

Esteban, Miguel Angel, Tao Wang, Baoming Qin, Jiayin Yang, Dajiang Qin, Jinglei Cai, Wen Li, et al. 2010. "Vitamin C Enhances the Generation of Mouse and Human Induced Pluripotent Stem Cells." *Cell Stem Cell* 6 (1): 71–79. https://doi.org/10.1016/j.stem.2009.12.001.

Evans, M J, and M H Kaufman. 1981. "Establishment in Culture of Pluripotential Cells from Mouse Embryos." *Nature* 292 (5819): 154–56. http://www.ncbi.nlm.nih.gov/pubmed/7242681.

Forejt, J, J R Saam, S Gregorová, and S M Tilghman. 1999. "Monoallelic Expression of Reactivated Imprinted Genes in Embryonal Carcinoma Cell Hybrids." *Experimental Cell Research* 252 (2): 416–22. https://doi.org/10.1006/excr.1999.4627.

Froberg, John E, Stefan F Pinter, Andrea J Kriz, Teddy Jegu, and Jeannie T Lee. 2018. "Megadomains and Superloops Form Dynamically but Are Dispensable for X Chromosome Inactivation and Gene Escape." *BioRxiv*, July, 364893. https://doi.org/10.1101/364893.

Fudenberg, Geoffrey, Maxim Imakaev, Carolyn Lu, Anton Goloborodko, Nezar Abdennur, and Leonid A Mirny. 2016. "Formation of Chromosomal Domains by Loop Extrusion." *Cell Reports* 15 (9): 2038–49. https://doi.org/10.1016/j.celrep.2016.04.085.

Furlan, Giulia, Nancy Gutierrez Hernandez, Christophe Huret, Rafael Galupa, Joke Gerarda van Bemmel, Antonio Romito, Edith Heard, Céline Morey, and Claire Rougeulle. 2018a. "The Ftx Noncoding

Locus Controls X Chromosome Inactivation Independently of Its RNA Products." *Molecular Cell* 70 (3): 462–472.e8. https://doi.org/10.1016/j.molcel.2018.03.024.

———. 2018b. "The Ftx Noncoding Locus Controls X Chromosome Inactivation Independently of Its RNA Products." *Molecular Cell* 70 (3): 462–472.e8. https://doi.org/10.1016/j.molcel.2018.03.024.

Garcia-Cruz, R, M A Brieño, I Roig, M Grossmann, E Velilla, A Pujol, L Cabero, A Pessarrodona, J L Barbero, and M Garcia Caldés. 2010. "Dynamics of Cohesin Proteins REC8, STAG3, SMC1 Beta and SMC3 Are Consistent with a Role in Sister Chromatid Cohesion during Meiosis in Human Oocytes." *Human Reproduction (Oxford, England)* 25 (9): 2316–27. https://doi.org/10.1093/humrep/deq180.

Gayen, Srimonta, Emily Maclary, Emily Buttigieg, Michael Hinten, and Sundeep Kalantry. 2015. "A Primary Role for the Tsix LncRNA in Maintaining Random X-Chromosome Inactivation." *Cell Reports* 11 (8): 1251–65. https://doi.org/10.1016/j.celrep.2015.04.039.

Gdula, Michal R, Tatyana B Nesterova, Greta Pintacuda, Jonathan Godwin, Ye Zhan, Hakan Ozadam, Michael McClellan, et al. 2018. "The Non-Canonical SMC Protein SmcHD1 Antagonises TAD Formation on the Inactive X Chromosome." *BioRxiv*, June, 342147. https://doi.org/10.1101/342147.

Gendrel, Anne-Valerie, Anwyn Apedaile, Heather Coker, Ausma Termanis, Ilona Zvetkova, Jonathan Godwin, Y Amy Tang, et al. 2012. "Smchd1-Dependent and -Independent Pathways Determine Developmental Dynamics of CpG Island Methylation on the Inactive X Chromosome." *Developmental Cell* 23 (2): 265–79. https://doi.org/10.1016/j.devcel.2012.06.011.

Giorgetti, Luca, Rafael Galupa, Elphège P Nora, Tristan Piolot, France Lam, Job Dekker, Guido Tiana, and Edith Heard. 2014. "Predictive Polymer Modeling Reveals Coupled Fluctuations in Chromosome

Conformation and Transcription." *Cell* 157 (4): 950–63. https://doi.org/10.1016/j.cell.2014.03.025.

Giorgetti, Luca, Bryan R. Lajoie, Ava C. Carter, Mikael Attia, Ye Zhan, Jin Xu, Chong Jian Chen, et al. 2016. "Structural Organization of the Inactive X Chromosome in the Mouse." *Nature* 535 (7613): 575–79. https://doi.org/10.1038/nature18589.

Goloborodko, Anton, John F. Marko, and Leonid A. Mirny. 2016. "Chromosome Compaction by Active Loop Extrusion." *Biophysical Journal* 110 (10): 2162–68. https://doi.org/10.1016/j.bpj.2016.02.041.

Grant, Jennifer, Shantha K. Mahadevaiah, Pavel Khil, Mahesh N. Sangrithi, Hélène Royo, Janine Duckworth, John R. McCarrey, et al. 2012. "Rsx Is a Metatherian RNA with Xist-like Properties in X-Chromosome Inactivation." *Nature* 487 (7406): 254–58. https://doi.org/10.1038/nature11171.

Guacci, V, D Koshland, and A Strunnikov. 1997. "A Direct Link between Sister Chromatid Cohesion and Chromosome Condensation Revealed through the Analysis of MCD1 in S. Cerevisiae." *Cell* 91 (1): 47–57. http://www.ncbi.nlm.nih.gov/pubmed/9335334.

Hacisuleyman, Ezgi, Loyal A Goff, Cole Trapnell, Adam Williams, Jorge Henao-Mejia, Lei Sun, Patrick McClanahan, et al. 2014. "Topological Organization of Multichromosomal Regions by the Long Intergenic Noncoding RNA Firre." *Nature Structural & Molecular Biology* 21 (2): 198–206. https://doi.org/10.1038/nsmb.2764.

Hacisuleyman, Ezgi, Chinmay J Shukla, Catherine L Weiner, and John L Rinn. 2016. "Function and Evolution of Local Repeats in the Firre Locus." *Nature Communications* 7 (March): 11021. https://doi.org/10.1038/ncomms11021.

Hadjantonakis, A K, L L Cox, P P Tam, and A Nagy. 2001. "An X-

Linked GFP Transgene Reveals Unexpected Paternal X-Chromosome Activity in Trophoblastic Giant Cells of the Mouse Placenta." *Genesis (New York, N.Y. : 2000)* 29 (3): 133–40. http://www.ncbi.nlm.nih.gov/pubmed/11252054.

Haering, Christian H, Jan Löwe, Andreas Hochwagen, and Kim Nasmyth. 2002. "Molecular Architecture of SMC Proteins and the Yeast Cohesin Complex." *Molecular Cell* 9 (4): 773–88. http://www.ncbi.nlm.nih.gov/pubmed/11983169.

Handoko, Lusy, Han Xu, Guoliang Li, Chew Yee Ngan, Elaine Chew, Marie Schnapp, Charlie Wah Heng Lee, et al. 2011. "CTCF-Mediated Functional Chromatin Interactome in Pluripotent Cells." *Nature Genetics* 43 (7): 630–38. https://doi.org/10.1038/ng.857.

Hasegawa, Yuko, Neil Brockdorff, Shinji Kawano, Kimiko Tsutui, Ken Tsutui, and Shinichi Nakagawa. 2010. "The Matrix Protein HnRNP U Is Required for Chromosomal Localization of Xist RNA." *Developmental Cell* 19 (3): 469–76. https://doi.org/10.1016/j.devcel.2010.08.006.

Hayashi, K., S. Ogushi, K. Kurimoto, S. Shimamoto, H. Ohta, and M. Saitou. 2012. "Offspring from Oocytes Derived from in Vitro Primordial Germ Cell-like Cells in Mice." *Science* 338 (6109): 971–75. https://doi.org/10.1126/science.1226889.

He, Y.-F., B.-Z. Li, Z. Li, P. Liu, Y. Wang, Q. Tang, J. Ding, et al. 2011. "Tet-Mediated Formation of 5-Carboxylcytosine and Its Excision by TDG in Mammalian DNA." *Science* 333 (6047): 1303–7. https://doi.org/10.1126/science.1210944.

Hendrich, B D, C J Brown, and H F Willard. 1993. "Evolutionary Conservation of Possible Functional Domains of the Human and Murine XIST Genes." *Human Molecular Genetics* 2 (6): 663–72. http://www.ncbi.nlm.nih.gov/pubmed/8353487.

Hong, Sunhwa, Young-Wook Cho, Li-Rong Yu, Hong Yu, Timothy D

Veenstra, and Kai Ge. 2007. “Identification of JmjC Domain-Containing UTX and JMJD3 as Histone H3 Lysine 27 Demethylases.” *Proceedings of the National Academy of Sciences of the United States of America* 104 (47): 18439–44. https://doi.org/10.1073/pnas.0707292104.

Horakova, Andrea H, J Mauro Calabrese, Christine R McLaughlin, Deanna C Tremblay, Terry Magnuson, and Brian P Chadwick. 2012. “The Mouse DXZ4 Homolog Retains Ctcf Binding and Proximity to Pls3 despite Substantial Organizational Differences Compared to the Primate Macrosatellite.” *Genome Biology* 13 (8): R70. https://doi.org/10.1186/gb-2012-13-8-r70.

Horakova, Andrea H, Shawn C Moseley, Christine R McLaughlin, Deanna C Tremblay, and Brian P Chadwick. 2012. “The Macrosatellite DXZ4 Mediates CTCF-Dependent Long-Range Intrachromosomal Interactions on the Human Inactive X Chromosome.” *Human Molecular Genetics* 21 (20): 4367–77. https://doi.org/10.1093/hmg/dds270.

Hu, Xiao, Lei Zhang, Shi-Qing Mao, Zheng Li, Jiekai Chen, Run-Rui Zhang, Hai-Ping Wu, et al. 2014. “Tet and TDG Mediate DNA Demethylation Essential for Mesenchymal-to-Epithelial Transition in Somatic Cell Reprogramming.” *Cell Stem Cell* 14 (4): 512–22. https://doi.org/10.1016/j.stem.2014.01.001.

Huynh, Khanh D., and Jeannie T. Lee. 2003a. “Inheritance of a Pre-Inactivated Paternal X Chromosome in Early Mouse Embryos.” *Nature* 426 (6968): 857–62. https://doi.org/10.1038/nature02222.

Huynh, Khanh D, and Jeannie T Lee. 2003b. “Inheritance of a Pre-Inactivated Paternal X Chromosome in Early Mouse Embryos.” *Nature* 426 (6968): 857–62. https://doi.org/10.1038/nature02222.

Isono, K.-i., Y.-i. Fujimura, J. Shinga, M. Yamaki, J. O-Wang, Y. Takihara, Y. Murahashi, Y. Takada, Y. Mizutani-Koseki, and H.

Koseki. 2005. “Mammalian Polyhomeotic Homologues Phc2 and Phc1 Act in Synergy To Mediate Polycomb Repression of Hox Genes.” *Molecular and Cellular Biology* 25 (15): 6694–6706. https://doi.org/10.1128/MCB.25.15.6694-6706.2005.

Jansz, Natasha, Andrew Keniry, Marie Trussart, Heidi Bildsoe, Tamara Beck, Ian D. Tonks, Arne W. Mould, et al. 2018. “Smchd1 Regulates Long-Range Chromatin Interactions on the Inactive X Chromosome and at Hox Clusters.” *Nature Structural & Molecular Biology* 25 (9): 766–77. https://doi.org/10.1038/s41594-018-0111-z.

Jeon, Yesu, and Jeannie T Lee. 2011. “YY1 Tethers Xist RNA to the Inactive X Nucleation Center.” *Cell* 146 (1): 119–33. https://doi.org/10.1016/j.cell.2011.06.026.

Jonkers, Iris, Tahsin Stefan Barakat, Eskeatnaf Mulugeta Achame, Kim Monkhorst, Annegien Kenter, Eveline Rentmeester, Frank Grosveld, J. Anton Grootegoed, and Joost Gribnau. 2009. “RNF12 Is an X-Encoded Dose-Dependent Activator of X Chromosome Inactivation.” *Cell* 139 (5): 999–1011. https://doi.org/10.1016/j.cell.2009.10.034.

Kagey, Michael H, Jamie J Newman, Steve Bilodeau, Ye Zhan, David A Orlando, Nynke L van Berkum, Christopher C Ebmeier, et al. 2010. “Mediator and Cohesin Connect Gene Expression and Chromatin Architecture.” *Nature* 467 (7314): 430–35. https://doi.org/10.1038/nature09380.

Kim, Jonghwan, Jianlin Chu, Xiaohua Shen, Jianlong Wang, and Stuart H. Orkin. 2008. “An Extended Transcriptional Network for Pluripotency of Embryonic Stem Cells.” *Cell* 132 (6): 1049–61. https://doi.org/10.1016/j.cell.2008.02.039.

Kim, Joomyeong, Angela Kollhoff, Anne Bergmann, and Lisa Stubbs. 2003. “Methylation-Sensitive Binding of Transcription Factor YY1 to an Insulator Sequence within the Paternally Expressed Imprinted

Gene, Peg3." *Human Molecular Genetics* 12 (3): 233–45. http://www.ncbi.nlm.nih.gov/pubmed/12554678.

Koche, Richard P, Zachary D Smith, Mazhar Adli, Hongcang Gu, Manching Ku, Andreas Gnirke, Bradley E Bernstein, and Alexander Meissner. 2011. "Reprogramming Factor Expression Initiates Widespread Targeted Chromatin Remodeling." *Cell Stem Cell* 8 (1): 96–105. https://doi.org/10.1016/j.stem.2010.12.001.

Kohlmaier, Alexander, Fabio Savarese, Monika Lachner, Joost Martens, Thomas Jenuwein, and Anton Wutz. 2004. "A Chromosomal Memory Triggered by Xist Regulates Histone Methylation in X Inactivation." Edited by Peter Becker. *PLoS Biology* 2 (7): E171. https://doi.org/10.1371/journal.pbio.0020171.

Kramer, Maxwell, Anna-Lena Kranz, Amanda Su, Lara H. Winterkorn, Sarah Elizabeth Albritton, and Sevinc Ercan. 2015. "Developmental Dynamics of X-Chromosome Dosage Compensation by the DCC and H4K20me1 in C. Elegans." Edited by Erica Larschan. *PLOS Genetics* 11 (12): e1005698. https://doi.org/10.1371/journal.pgen.1005698.

Kueng, Stephanie, Björn Hegemann, Beate H. Peters, Jesse J. Lipp, Alexander Schleiffer, Karl Mechtler, and Jan-Michael Peters. 2006a. "Wapl Controls the Dynamic Association of Cohesin with Chromatin." *Cell* 127 (5): 955–67. https://doi.org/10.1016/j.cell.2006.09.040.

Kueng, Stephanie, Björn Hegemann, Beate H Peters, Jesse J Lipp, Alexander Schleiffer, Karl Mechtler, and Jan-Michael Peters. 2006b. "Wapl Controls the Dynamic Association of Cohesin with Chromatin." *Cell* 127 (5): 955–67. https://doi.org/10.1016/j.cell.2006.09.040.

Kung, Johnny T, Barry Kesner, Jee Young An, Janice Y Ahn, Catherine Cifuentes-Rojas, David Colognori, Yesu Jeon, et al. 2015. "Locus-

Specific Targeting to the X Chromosome Revealed by the RNA Interactome of CTCF." *Molecular Cell* 57 (2): 361–75. https://doi.org/10.1016/j.molcel.2014.12.006.

Kurimoto, K., Yukihiro Yabuta, Yasuhide Ohinata, Yukiko Ono, Kenichiro D Uno, Rikuhiro G Yamada, Hiroki R Ueda, and Mitinori Saitou. 2006. "An Improved Single-Cell CDNA Amplification Method for Efficient High-Density Oligonucleotide Microarray Analysis." *Nucleic Acids Research* 34 (5): e42–e42. https://doi.org/10.1093/nar/gkl050.

Kurimoto, Kazuki, Yukihiro Yabuta, Yasuhide Ohinata, and Mitinori Saitou. 2007. "Global Single-Cell CDNA Amplification to Provide a Template for Representative High-Density Oligonucleotide Microarray Analysis." *Nature Protocols* 2 (3): 739–52. https://doi.org/10.1038/nprot.2007.79.

Kwan, Kelvin Y, Peter B Moens, and James C Wang. 2003. "Infertility and Aneuploidy in Mice Lacking a Type IA DNA Topoisomerase III Beta." *Proceedings of the National Academy of Sciences of the United States of America* 100 (5): 2526–31. https://doi.org/10.1073/pnas.0437998100.

Lan, Fei, Peter E Bayliss, John L Rinn, Johnathan R Whetstine, Jordon K Wang, Shuzhen Chen, Shigeki Iwase, et al. 2007. "A Histone H3 Lysine 27 Demethylase Regulates Animal Posterior Development." *Nature* 449 (7163): 689–94. https://doi.org/10.1038/nature06192.

Lanner, Fredrik, and Janet Rossant. 2010. "The Role of FGF/Erk Signaling in Pluripotent Cells." *Development (Cambridge, England)* 137 (20): 3351–60. https://doi.org/10.1242/dev.050146.

Lau, Alyssa C, and Györgyi Csankovszki. 2015. "Balancing up and Downregulation of the C. Elegans X Chromosomes." *Current Opinion in Genetics & Development* 31 (April): 50–56. https://doi.org/10.1016/j.gde.2015.04.001.

Lau, Alyssa C, Kentaro Nabeshima, and Györgyi Csankovszki. 2014. "The C. Elegans Dosage Compensation Complex Mediates Interphase X Chromosome Compaction." *Epigenetics & Chromatin* 7 (1): 31. https://doi.org/10.1186/1756-8935-7-31.

Lee, J T. 2000. "Disruption of Imprinted X Inactivation by Parent-of-Origin Effects at Tsix." *Cell* 103 (1): 17–27. http://www.ncbi.nlm.nih.gov/pubmed/11051544.

Lee, J T, L S Davidow, and D Warshawsky. 1999. "Tsix, a Gene Antisense to Xist at the X-Inactivation Centre." *Nature Genetics* 21 (4): 400–404. https://doi.org/10.1038/7734.

Lee, J T, and N Lu. 1999. "Targeted Mutagenesis of Tsix Leads to Nonrandom X Inactivation." *Cell* 99 (1): 47–57. http://www.ncbi.nlm.nih.gov/pubmed/10520993.

Lee, Jeannie T., William M. Strauss, Jessica A. Dausman, and Rudolf Jaenisch. 1996. "A 450 Kb Transgene Displays Properties of the Mammalian X-Inactivation Center." *Cell*. https://doi.org/10.1016/S0092-8674(00)80079-3.

Leeb, Martin, and Anton Wutz. 2007. "Ring1B Is Crucial for the Regulation of Developmental Control Genes and PRC1 Proteins but Not X Inactivation in Embryonic Cells." *The Journal of Cell Biology* 178 (2): 219–29. https://doi.org/10.1083/jcb.200612127.

Li, Shanru, Joel Weidenfeld, and Edward E Morrisey. 2004. "Transcriptional and DNA Binding Activity of the Foxp1/2/4 Family Is Modulated by Heterotypic and Homotypic Protein Interactions." *Molecular and Cellular Biology* 24 (2): 809–22. http://www.ncbi.nlm.nih.gov/pubmed/14701752.

Li, Xiajun, Mitsuteru Ito, Fen Zhou, Neil Youngson, Xiaopan Zuo, Philip Leder, and Anne C Ferguson-Smith. 2008. "A Maternal-Zygotic Effect Gene, Zfp57, Maintains Both Maternal and Paternal Imprints." *Developmental Cell* 15 (4): 547–57.

https://doi.org/10.1016/j.devcel.2008.08.014.

Li, Zheng, Tian-Peng Gu, Alain R Weber, Jia-Zhen Shen, Bin-Zhong Li, Zhi-Guo Xie, Ruichuan Yin, et al. 2015. "Gadd45a Promotes DNA Demethylation through TDG." *Nucleic Acids Research* 43 (8): 3986–97. https://doi.org/10.1093/nar/gkv283.

Liang, Gaoyang, Jin He, and Yi Zhang. 2012. "Kdm2b Promotes Induced Pluripotent Stem Cell Generation by Facilitating Gene Activation Early in Reprogramming." *Nature Cell Biology* 14 (5): 457–66. https://doi.org/10.1038/ncb2483.

Lieberman-Aiden, Erez, Nynke L van Berkum, Louise Williams, Maxim Imakaev, Tobias Ragoczy, Agnes Telling, Ido Amit, et al. 2009a. "Comprehensive Mapping of Long-Range Interactions Reveals Folding Principles of the Human Genome." *Science (New York, N.Y.)* 326 (5950): 289–93. https://doi.org/10.1126/science.1181369.

———. 2009b. "Comprehensive Mapping of Long-Range Interactions Reveals Folding Principles of the Human Genome." *Science (New York, N.Y.)* 326 (5950): 289–93. https://doi.org/10.1126/science.1181369.

Liu, T., A. Rechtsteiner, T. A. Egelhofer, A. Vielle, I. Latorre, M.-S. Cheung, S. Ercan, et al. 2011. "Broad Chromosomal Domains of Histone Modification Patterns in C. Elegans." *Genome Research* 21 (2): 227–36. https://doi.org/10.1101/gr.115519.110.

Lluis, Frederic, Luigi Ombrato, Elisa Pedone, Stefano Pepe, Bradley J Merrill, and Maria Pia Cosma. 2011. "T-Cell Factor 3 (Tcf3) Deletion Increases Somatic Cell Reprogramming by Inducing Epigenome Modifications." *Proceedings of the National Academy of Sciences of the United States of America* 108 (29): 11912–17. https://doi.org/10.1073/pnas.1017402108.

Luikenhuis, S., A. Wutz, and R. Jaenisch. 2001. "Antisense Transcription through the Xist Locus Mediates Tsix Function in Embryonic Stem

Cells." *Molecular and Cellular Biology* 21 (24): 8512–20. https://doi.org/10.1128/MCB.21.24.8512-8520.2001.

LYON, M F. 1961. "Gene Action in the X-Chromosome of the Mouse (Mus Musculus L.)." *Nature* 190 (April): 372–73. http://www.ncbi.nlm.nih.gov/pubmed/13764598.

———. 1962. "Sex Chromatin and Gene Action in the Mammalian X-Chromosome." *American Journal of Human Genetics* 14 (2): 135–48. http://www.ncbi.nlm.nih.gov/pubmed/14467629.

Ma, Ziyang, Tomek Swigut, Anton Valouev, Alvaro Rada-Iglesias, and Joanna Wysocka. 2011. "Sequence-Specific Regulator Prdm14 Safeguards Mouse ESCs from Entering Extraembryonic Endoderm Fates." *Nature Structural & Molecular Biology* 18 (2): 120–27. https://doi.org/10.1038/nsmb.2000.

Maclary, Emily, Emily Buttigieg, Michael Hinten, Srimonta Gayen, Clair Harris, Mrinal Kumar Sarkar, Sonya Purushothaman, and Sundeep Kalantry. 2014. "Differentiation-Dependent Requirement of Tsix Long Non-Coding RNA in Imprinted X-Chromosome Inactivation." *Nature Communications* 5 (1): 4209. https://doi.org/10.1038/ncomms5209.

Madl, J. E., and R. K. Herman. 1979. "Polyploids and Sex Determination in Caenorhabditis Elegans." *Genetics*.

Maherali, Nimet, Rupa Sridharan, Wei Xie, Jochen Utikal, Sarah Eminli, Katrin Arnold, Matthias Stadtfeld, et al. 2007. "Directly Reprogrammed Fibroblasts Show Global Epigenetic Remodeling and Widespread Tissue Contribution." *Cell Stem Cell* 1 (1): 55–70. https://doi.org/10.1016/j.stem.2007.05.014.

Mak, W., Tatyana B Nesterova, Mariana de Napoles, Ruth Appanah, Shinya Yamanaka, Arie P Otte, and Neil Brockdorff. 2004. "Reactivation of the Paternal X Chromosome in Early Mouse Embryos." *Science* 303 (5658): 666–69.

https://doi.org/10.1126/science.1092674.

Mansour, Abed AlFatah, Ohad Gafni, Leehee Weinberger, Asaf Zviran, Muneef Ayyash, Yoach Rais, Vladislav Krupalnik, et al. 2012. "The H3K27 Demethylase Utx Regulates Somatic and Germ Cell Epigenetic Reprogramming." *Nature* 488 (7411): 409–13. https://doi.org/10.1038/nature11272.

Marahrens, Y, B Panning, J Dausman, W Strauss, and R Jaenisch. 1997. "Xist-Deficient Mice Are Defective in Dosage Compensation but Not Spermatogenesis." *Genes & Development* 11 (2): 156–66. http://www.ncbi.nlm.nih.gov/pubmed/9009199.

McGinnis, Lynda K., William H. Kinsey, and David F. Albertini. 2009. "Functions of Fyn Kinase in the Completion of Meiosis in Mouse Oocytes." *Developmental Biology* 327 (2): 280–87. https://doi.org/10.1016/j.ydbio.2008.11.038.

McHugh, Colleen A, Chun-Kan Chen, Amy Chow, Christine F Surka, Christina Tran, Patrick McDonel, Amy Pandya-Jones, et al. 2015. "The Xist LncRNA Interacts Directly with SHARP to Silence Transcription through HDAC3." *Nature* 521 (7551): 232–36. https://doi.org/10.1038/nature14443.

Meeks, Joshua J., Jeffrey Weiss, and J. Larry Jameson. 2003. "Dax1 Is Required for Testis Determination." *Nature Genetics* 34 (1): 32–33. https://doi.org/10.1038/ng1141.

Meissner, Alexander, Marius Wernig, and Rudolf Jaenisch. 2007. "Direct Reprogramming of Genetically Unmodified Fibroblasts into Pluripotent Stem Cells." *Nature Biotechnology* 25 (10): 1177–81. https://doi.org/10.1038/nbt1335.

Mermoud, J E, C Costanzi, J R Pehrson, and N Brockdorff. 1999. "Histone MacroH2A1.2 Relocates to the Inactive X Chromosome after Initiation and Propagation of X-Inactivation." *The Journal of Cell Biology* 147 (7): 1399–1408.

http://www.ncbi.nlm.nih.gov/pubmed/10613899.

Meyer, Barbara J., and Lawrence P. Casson. 1986. "Caenorhabditis Elegans Compensates for the Difference in X Chromosome Dosage between the Sexes by Regulating Transcript Levels." *Cell*. https://doi.org/10.1016/0092-8674(86)90802-0.

Michaelis, C, R Ciosk, and K Nasmyth. 1997. "Cohesins: Chromosomal Proteins That Prevent Premature Separation of Sister Chromatids." *Cell* 91 (1): 35–45. http://www.ncbi.nlm.nih.gov/pubmed/9335333.

Mikkelsen, Tarjei S, Jacob Hanna, Xiaolan Zhang, Manching Ku, Marius Wernig, Patrick Schorderet, Bradley E Bernstein, Rudolf Jaenisch, Eric S Lander, and Alexander Meissner. 2008. "Dissecting Direct Reprogramming through Integrative Genomic Analysis." *Nature* 454 (7200): 49–55. https://doi.org/10.1038/nature07056.

Milagre, Inês, Thomas M Stubbs, Michelle R King, Julia Spindel, Fátima Santos, Felix Krueger, Martin Bachman, et al. 2017. "Gender Differences in Global but Not Targeted Demethylation in IPSC Reprogramming." *Cell Reports* 18 (5): 1079–89. https://doi.org/10.1016/j.celrep.2017.01.008.

Minajigi, Anand, John Froberg, Chunyao Wei, Hongjae Sunwoo, Barry Kesner, David Colognori, Derek Lessing, et al. 2015. "Chromosomes. A Comprehensive Xist Interactome Reveals Cohesin Repulsion and an RNA-Directed Chromosome Conformation." *Science (New York, N.Y.)* 349 (6245): aab2276-aab2276. https://doi.org/10.1126/science.aab2276.

Minkovsky, Alissa, Tahsin Stefan Barakat, Nadia Sellami, Mark Henry Chin, Nilhan Gunhanlar, Joost Gribnau, and Kathrin Plath. 2013. "The Pluripotency Factor-Bound Intron 1 of Xist Is Dispensable for X Chromosome Inactivation and Reactivation in Vitro and in Vivo." *Cell Reports* 3 (3): 905–18. https://doi.org/10.1016/j.celrep.2013.02.018.

Minor, Emily A., Brenda L. Court, Juan I. Young, and Gaofeng Wang. 2013. “Ascorbate Induces Ten-Eleven Translocation (Tet) Methylcytosine Dioxygenase-Mediated Generation of 5-Hydroxymethylcytosine.” *Journal of Biological Chemistry* 288 (19): 13669–74. https://doi.org/10.1074/jbc.C113.464800.

Miyanari, Yusuke, and Maria-Elena Torres-Padilla. 2012. “Control of Ground-State Pluripotency by Allelic Regulation of Nanog.” *Nature* 483 (7390): 470–73. https://doi.org/10.1038/nature10807.

Moffat, Jason, Dorre A. Grueneberg, Xiaoping Yang, So Young Kim, Angela M. Kloepfer, Gregory Hinkle, Bruno Piqani, et al. 2006. “A Lentiviral RNAi Library for Human and Mouse Genes Applied to an Arrayed Viral High-Content Screen.” *Cell* 124 (6): 1283–98. https://doi.org/10.1016/j.cell.2006.01.040.

Moindrot, Benoit, Andrea Cerase, Heather Coker, Osamu Masui, Anne Grijzenhout, Greta Pintacuda, Lothar Schermelleh, Tatyana B Nesterova, and Neil Brockdorff. 2015. “A Pooled ShRNA Screen Identifies Rbm15, Spen, and Wtap as Factors Required for Xist RNA-Mediated Silencing.” *Cell Reports* 12 (4): 562–72. https://doi.org/10.1016/j.celrep.2015.06.053.

Monfort, Asun, Giulio Di Minin, Andreas Postlmayr, Remo Freimann, Fabiana Arieti, Stéphane Thore, and Anton Wutz. 2015. “Identification of Spen as a Crucial Factor for Xist Function through Forward Genetic Screening in Haploid Embryonic Stem Cells.” *Cell Reports* 12 (4): 554–61. https://doi.org/10.1016/j.celrep.2015.06.067.

Monk, M, and A McLaren. 1981. “X-Chromosome Activity in Foetal Germ Cells of the Mouse.” *Journal of Embryology and Experimental Morphology* 63 (June): 75–84. http://www.ncbi.nlm.nih.gov/pubmed/7310296.

Monkhorst, Kim, Iris Jonkers, Eveline Rentmeester, Frank Grosveld, and

Joost Gribnau. 2008. “X Inactivation Counting and Choice Is a Stochastic Process: Evidence for Involvement of an X-Linked Activator.” *Cell* 132 (3): 410–21. https://doi.org/10.1016/j.cell.2007.12.036.

Murakami, K, T Ohhira, E Oshiro, D Qi, M Oshimura, and H Kugoh. 2009. “Identification of the Chromatin Regions Coated by Non-Coding Xist RNA.” *Cytogenetic and Genome Research* 125 (1): 19–25. https://doi.org/10.1159/000207514.

Nagano, Takashi, Yaniv Lubling, Tim J Stevens, Stefan Schoenfelder, Eitan Yaffe, Wendy Dean, Ernest D Laue, Amos Tanay, and Peter Fraser. 2013. “Single-Cell Hi-C Reveals Cell-to-Cell Variability in Chromosome Structure.” *Nature* 502 (7469): 59–64. https://doi.org/10.1038/nature12593.

Napoles, Mariana de, Jacqueline E Mermoud, Rika Wakao, Y Amy Tang, Mitusuhiro Endoh, Ruth Appanah, Tatyana B Nesterova, et al. 2004. “Polycomb Group Proteins Ring1A/B Link Ubiquitylation of Histone H2A to Heritable Gene Silencing and X Inactivation.” *Developmental Cell* 7 (5): 663–76. https://doi.org/10.1016/j.devcel.2004.10.005.

Naughton, Catherine, Duncan Sproul, Charlotte Hamilton, and Nick Gilbert. 2010a. “Analysis of Active and Inactive X Chromosome Architecture Reveals the Independent Organization of 30 Nm and Large-Scale Chromatin Structures.” *Molecular Cell* 40 (3): 397–409. https://doi.org/10.1016/j.molcel.2010.10.013.

———. 2010b. “Analysis of Active and Inactive X Chromosome Architecture Reveals the Independent Organization of 30 Nm and Large-Scale Chromatin Structures.” *Molecular Cell* 40 (3): 397–409. https://doi.org/10.1016/j.molcel.2010.10.013.

Navarro, P., I. Chambers, V. Karwacki-Neisius, C. Chureau, C. Morey, C. Rougeulle, and P. Avner. 2008. “Molecular Coupling of Xist

Regulation and Pluripotency." *Science* 321 (5896): 1693–95. https://doi.org/10.1126/science.1160952.

Navarro, Pablo, Michael Moffat, Nicholas P Mullin, and Ian Chambers. 2011. "The X-Inactivation Trans-Activator Rnf12 Is Negatively Regulated by Pluripotency Factors in Embryonic Stem Cells." *Human Genetics* 130 (2): 255–64. https://doi.org/10.1007/s00439-011-0998-5.

Navarro, Pablo, Andrew Oldfield, Julie Legoupi, Nicola Festuccia, Agnès Dubois, Mikael Attia, Jon Schoorlemmer, Claire Rougeulle, Ian Chambers, and Philip Avner. 2010. "Molecular Coupling of Tsix Regulation and Pluripotency." *Nature* 468 (7322): 457–60. https://doi.org/10.1038/nature09496.

Navarro, Pablo, Sylvain Pichard, Constance Ciaudo, Philip Avner, and Claire Rougeulle. 2005. "Tsix Transcription across the Xist Gene Alters Chromatin Conformation without Affecting Xist Transcription: Implications for X-Chromosome Inactivation." *Genes & Development* 19 (12): 1474–84. https://doi.org/10.1101/gad.341105.

Nesterova, Tatyana B, Claire E Senner, Janina Schneider, Tilly Alcayna-Stevens, Anna Tattermusch, Myriam Hemberger, and Neil Brockdorff. 2011. "Pluripotency Factor Binding and Tsix Expression Act Synergistically to Repress Xist in Undifferentiated Embryonic Stem Cells." *Epigenetics & Chromatin* 4 (1): 17. https://doi.org/10.1186/1756-8935-4-17.

Nora, Elphège P, Anton Goloborodko, Anne-Laure Valton, Johan H Gibcus, Alec Uebersohn, Nezar Abdennur, Job Dekker, Leonid A Mirny, and Benoit G Bruneau. 2017. "Targeted Degradation of CTCF Decouples Local Insulation of Chromosome Domains from Genomic Compartmentalization." *Cell* 169 (5): 930–944.e22. https://doi.org/10.1016/j.cell.2017.05.004.

Nora, Elphège P, Bryan R Lajoie, Edda G Schulz, Luca Giorgetti, Ikuhiro Okamoto, Nicolas Servant, Tristan Piolot, et al. 2012a. “Spatial Partitioning of the Regulatory Landscape of the X-Inactivation Centre.” *Nature* 485 (7398): 381–85. https://doi.org/10.1038/nature11049.

———. 2012b. “Spatial Partitioning of the Regulatory Landscape of the X-Inactivation Centre.” *Nature* 485 (7398): 381–85. https://doi.org/10.1038/nature11049.

Norris, D P, D Patel, G F Kay, G D Penny, N Brockdorff, S A Sheardown, and S Rastan. 1994. “Evidence That Random and Imprinted Xist Expression Is Controlled by Preemptive Methylation.” *Cell* 77 (1): 41–51. http://www.ncbi.nlm.nih.gov/pubmed/8156596.

Nozawa, Ryu-Suke, Koji Nagao, Ken-Taro Igami, Sachiko Shibata, Natsuko Shirai, Naohito Nozaki, Takashi Sado, Hiroshi Kimura, and Chikashi Obuse. 2013. “Human Inactive X Chromosome Is Compacted through a PRC2-Independent SMCHD1-HBiX1 Pathway.” *Nature Structural & Molecular Biology* 20 (5): 566–73. https://doi.org/10.1038/nsmb.2532.

Oda, Hisanobu, Ikuhiro Okamoto, Niall Murphy, Jianhua Chu, Sandy M Price, Michael M Shen, Maria Elena Torres-Padilla, Edith Heard, and Danny Reinberg. 2009a. “Monomethylation of Histone H4-Lysine 20 Is Involved in Chromosome Structure and Stability and Is Essential for Mouse Development.” *Molecular and Cellular Biology* 29 (8): 2278–95. https://doi.org/10.1128/MCB.01768-08.

———. 2009b. “Monomethylation of Histone H4-Lysine 20 Is Involved in Chromosome Structure and Stability and Is Essential for Mouse Development.” *Molecular and Cellular Biology* 29 (8): 2278–95. https://doi.org/10.1128/MCB.01768-08.

Ogawa, Yuya, and Jeannie T Lee. 2003. “Xite, X-Inactivation Intergenic Transcription Elements That Regulate the Probability of Choice.”

Molecular Cell 11 (3): 731–43. http://www.ncbi.nlm.nih.gov/pubmed/12667455.

Ohhata, Tatsuya, Claire E Senner, Myriam Hemberger, and Anton Wutz. 2011. "Lineage-Specific Function of the Noncoding Tsix RNA for Xist Repression and Xi Reactivation in Mice." *Genes & Development* 25 (16): 1702–15. https://doi.org/10.1101/gad.16997911.

OHNO, S, and T S HAUSCHKA. 1960. "Allocycly of the X-Chromosome in Tumors and Normal Tissues." *Cancer Research* 20 (May): 541–45. http://www.ncbi.nlm.nih.gov/pubmed/14428472.

Ohno, Susumu. 1967. *Sex Chromosomes and Sex-Linked Genes*. Vol. 1. Monographs on Endocrinology. Berlin, Heidelberg: Springer Berlin Heidelberg. https://doi.org/10.1007/978-3-642-88178-7.

Ohta, Hiroshi, Kazuki Kurimoto, Ikuhiro Okamoto, Tomonori Nakamura, Yukihiro Yabuta, Hidetaka Miyauchi, Takuya Yamamoto, et al. 2017. "*In Vitro* Expansion of Mouse Primordial Germ Cell-like Cells Recapitulates an Epigenetic Blank Slate." *The EMBO Journal* 36 (13): 1888–1907. https://doi.org/10.15252/embj.201695862.

Okamoto, I., Arie P Otte, C David Allis, Danny Reinberg, and Edith Heard. 2004. "Epigenetic Dynamics of Imprinted X Inactivation During Early Mouse Development." *Science* 303 (5658): 644–49. https://doi.org/10.1126/science.1092727.

Okamoto, Ikuhiro, Catherine Patrat, Dominique Thépot, Nathalie Peynot, Patricia Fauque, Nathalie Daniel, Patricia Diabangouaya, et al. 2011. "Eutherian Mammals Use Diverse Strategies to Initiate X-Chromosome Inactivation during Development." *Nature* 472 (7343): 370–74. https://doi.org/10.1038/nature09872.

Okita, Keisuke, Tomoko Ichisaka, and Shinya Yamanaka. 2007. "Generation of Germline-Competent Induced Pluripotent Stem Cells." *Nature* 448 (7151): 313–17.

https://doi.org/10.1038/nature05934.

Orishchenko, Konstantin E., Sophia V. Pavlova, Eugeny A. Elisaphenko, Vladimir V. Sherstyuk, Alexander V. Prinz, Alexander I. Shevchenko, Elena V. Dementyeva, and Suren M. Zakian. 2012. "A Regulatory Potential of the Xist Gene Promoter in Vole M. Rossiaemeridionalis." Edited by Laura Carrel. *PLoS ONE* 7 (5): e33994. https://doi.org/10.1371/journal.pone.0033994.

Panizza, S, T Tanaka, A Hochwagen, F Eisenhaber, and K Nasmyth. n.d. "Pds5 Cooperates with Cohesin in Maintaining Sister Chromatid Cohesion." *Current Biology : CB* 10 (24): 1557–64. Accessed October 22, 2018. http://www.ncbi.nlm.nih.gov/pubmed/11137006.

Pannetier, Maëlle, Eric Julien, Gunnar Schotta, Mathieu Tardat, Claude Sardet, Thomas Jenuwein, and Robert Feil. 2008. "PR-SET7 and SUV4-20H Regulate H4 Lysine-20 Methylation at Imprinting Control Regions in the Mouse." *EMBO Reports* 9 (10): 998–1005. https://doi.org/10.1038/embor.2008.147.

Panning, B, and R Jaenisch. 1996. "DNA Hypomethylation Can Activate Xist Expression and Silence X-Linked Genes." *Genes & Development* 10 (16): 1991–2002. http://www.ncbi.nlm.nih.gov/pubmed/8769643.

Parelho, Vania, Suzana Hadjur, Mikhail Spivakov, Marion Leleu, Stephan Sauer, Heather C Gregson, Adam Jarmuz, et al. 2008. "Cohesins Functionally Associate with CTCF on Mammalian Chromosome Arms." *Cell* 132 (3): 422–33. https://doi.org/10.1016/j.cell.2008.01.011.

Park, Kyung-Soon, Young Cha, Chun-Hyung Kim, Hee-Jin Ahn, Dohoon Kim, Sanghyeok Ko, Kyeoung-Hwa Kim, et al. 2013. "Transcription Elongation Factor Tcea3 Regulates the Pluripotent Differentiation Potential of Mouse Embryonic Stem Cells via the Lefty1-Nodal-Smad2 Pathway." *Stem Cells (Dayton, Ohio)* 31 (2): 282–92.

https://doi.org/10.1002/stem.1284.

Pasque, Vincent, Astrid Gillich, Nigel Garrett, and John B Gurdon. 2011. "Histone Variant MacroH2A Confers Resistance to Nuclear Reprogramming." *The EMBO Journal* 30 (12): 2373–87. https://doi.org/10.1038/emboj.2011.144.

Pasque, Vincent, Aliaksandra Radzisheuskaya, Astrid Gillich, Richard P Halley-Stott, Maryna Panamarova, Magdalena Zernicka-Goetz, M Azim Surani, and José C R Silva. 2012. "Histone Variant MacroH2A Marks Embryonic Differentiation in Vivo and Acts as an Epigenetic Barrier to Induced Pluripotency." *Journal of Cell Science* 125 (Pt 24): 6094–6104. https://doi.org/10.1242/jcs.113019.

Pasque, Vincent, Jason Tchieu, Rahul Karnik, Molly Uyeda, Anupama Sadhu Dimashkie, Dana Case, Bernadett Papp, et al. 2014. "X Chromosome Reactivation Dynamics Reveal Stages of Reprogramming to Pluripotency." *Cell* 159 (7): 1681–97. https://doi.org/10.1016/j.cell.2014.11.040.

Payer, Bernhard, Michael Rosenberg, Masashi Yamaji, Yukihiro Yabuta, Michiyo Koyanagi-Aoi, Katsuhiko Hayashi, Shinya Yamanaka, Mitinori Saitou, and Jeannie T. Lee. 2013. "Tsix RNA and the Germline Factor, PRDM14, Link X Reactivation and Stem Cell Reprogramming." *Molecular Cell*. https://doi.org/10.1016/j.molcel.2013.10.023.

Penny, G D, G F Kay, S A Sheardown, S Rastan, and N Brockdorff. 1996. "Requirement for Xist in X Chromosome Inactivation." *Nature* 379 (6561): 131–37. https://doi.org/10.1038/379131a0.

Pintacuda, Greta, Guifeng Wei, Chloë Roustan, Burcu Anil Kirmizitas, Nicolae Solcan, Andrea Cerase, Alfredo Castello, et al. 2017. "HnRNPK Recruits PCGF3/5-PRC1 to the Xist RNA B-Repeat to Establish Polycomb-Mediated Chromosomal Silencing." *Molecular Cell* 68 (5): 955–969.e10.

https://doi.org/10.1016/j.molcel.2017.11.013.

Plath, Kathrin, Dale Talbot, Karien M Hamer, Arie P Otte, Thomas P Yang, Rudolf Jaenisch, and Barbara Panning. 2004. "Developmentally Regulated Alterations in Polycomb Repressive Complex 1 Proteins on the Inactive X Chromosome." *The Journal of Cell Biology* 167 (6): 1025–35. https://doi.org/10.1083/jcb.200409026.

Polo, Jose M., Endre Anderssen, Ryan M. Walsh, Benjamin A. Schwarz, Christian M. Nefzger, Sue Mei Lim, Marti Borkent, et al. 2012. "A Molecular Roadmap of Reprogramming Somatic Cells into IPS Cells." *Cell* 151 (7): 1617–32. https://doi.org/10.1016/j.cell.2012.11.039.

Pullirsch, Dieter, Renate Härtel, Hiroyuki Kishimoto, Martin Leeb, Günter Steiner, and Anton Wutz. 2010. "The Trithorax Group Protein Ash2l and Saf-A Are Recruited to the Inactive X Chromosome at the Onset of Stable X Inactivation." *Development (Cambridge, England)* 137 (6): 935–43. https://doi.org/10.1242/dev.035956.

Rais, Yoach, Asaf Zviran, Shay Geula, Ohad Gafni, Elad Chomsky, Sergey Viukov, Abed AlFatah Mansour, et al. 2013. "Deterministic Direct Reprogramming of Somatic Cells to Pluripotency." *Nature* 502 (7469): 65–70. https://doi.org/10.1038/nature12587.

Rao, Suhas S.P., Miriam H. Huntley, Neva C. Durand, Elena K. Stamenova, Ivan D. Bochkov, James T. Robinson, Adrian L. Sanborn, et al. 2014. "A 3D Map of the Human Genome at Kilobase Resolution Reveals Principles of Chromatin Looping." *Cell* 159 (7): 1665–80. https://doi.org/10.1016/j.cell.2014.11.021.

Rao, Suhas S P, Su-Chen Huang, Brian Glenn St Hilaire, Jesse M Engreitz, Elizabeth M Perez, Kyong-Rim Kieffer-Kwon, Adrian L Sanborn, et al. 2017. "Cohesin Loss Eliminates All Loop Domains."

Cell 171 (2): 305–320.e24. https://doi.org/10.1016/j.cell.2017.09.026.

Ricci, Maria Aurelia, Carlo Manzo, María Filomena García-Parajo, Melike Lakadamyali, and Maria Pia Cosma. 2015. "Chromatin Fibers Are Formed by Heterogeneous Groups of Nucleosomes In Vivo." *Cell* 160 (6): 1145–58. https://doi.org/10.1016/j.cell.2015.01.054.

Ridings-Figueroa, Rebeca, Emma R Stewart, Tatyana B Nesterova, Heather Coker, Greta Pintacuda, Jonathan Godwin, Rose Wilson, et al. 2017. "The Nuclear Matrix Protein CIZ1 Facilitates Localization of Xist RNA to the Inactive X-Chromosome Territory." *Genes & Development* 31 (9): 876–88. https://doi.org/10.1101/gad.295907.117.

Rocha, Simão Teixeira da, Valentina Boeva, Martin Escamilla-Del-Arenal, Katia Ancelin, Camille Granier, Neuza Reis Matias, Serena Sanulli, et al. 2014. "Jarid2 Is Implicated in the Initial Xist-Induced Targeting of PRC2 to the Inactive X Chromosome." *Molecular Cell* 53 (2): 301–16. https://doi.org/10.1016/j.molcel.2014.01.002.

Rougeulle, Claire, Julie Chaumeil, Kavitha Sarma, C David Allis, Danny Reinberg, Philip Avner, and Edith Heard. 2004. "Differential Histone H3 Lys-9 and Lys-27 Methylation Profiles on the X Chromosome." *Molecular and Cellular Biology* 24 (12): 5475–84. https://doi.org/10.1128/MCB.24.12.5475-5484.2004.

Rousso, David L, Caroline Alayne Pearson, Zachary B Gaber, Amaya Miquelajauregui, Shanru Li, Carlos Portera-Cailliau, Edward E Morrisey, and Bennett G Novitch. 2012. "Foxp-Mediated Suppression of N-Cadherin Regulates Neuroepithelial Character and Progenitor Maintenance in the CNS." *Neuron* 74 (2): 314–30. https://doi.org/10.1016/j.neuron.2012.02.024.

Rowley, M Jordan, Michael H Nichols, Xiaowen Lyu, Masami Ando-Kuri, I Sarahi M Rivera, Karen Hermetz, Ping Wang, Yijun Ruan,

and Victor G Corces. 2017. “Evolutionarily Conserved Principles Predict 3D Chromatin Organization.” *Molecular Cell* 67 (5): 837–852.e7. https://doi.org/10.1016/j.molcel.2017.07.022.

Rubio, E. D., D. J. Reiss, P. L. Welcsh, C. M. Disteche, G. N. Filippova, N. S. Baliga, R. Aebersold, J. A. Ranish, and A. Krumm. 2008. “CTCF Physically Links Cohesin to Chromatin.” *Proceedings of the National Academy of Sciences* 105 (24): 8309–14. https://doi.org/10.1073/pnas.0801273105.

Rust, Michael J, Mark Bates, and Xiaowei Zhuang. 2006. “Sub-Diffraction-Limit Imaging by Stochastic Optical Reconstruction Microscopy (STORM).” *Nature Methods* 3 (10): 793–96. https://doi.org/10.1038/nmeth929.

Sado, T, M H Fenner, S S Tan, P Tam, T Shioda, and E Li. 2000. “X Inactivation in the Mouse Embryo Deficient for Dnmt1: Distinct Effect of Hypomethylation on Imprinted and Random X Inactivation.” *Developmental Biology* 225 (2): 294–303. https://doi.org/10.1006/dbio.2000.9823.

Sado, T, Z Wang, H Sasaki, and E Li. 2001. “Regulation of Imprinted X-Chromosome Inactivation in Mice by Tsix.” *Development (Cambridge, England)* 128 (8): 1275–86. http://www.ncbi.nlm.nih.gov/pubmed/11262229.

Sado, Takashi, Yuko Hoki, and Hiroyuki Sasaki. 2005. “Tsix Silences Xist through Modification of Chromatin Structure.” *Developmental Cell* 9 (1): 159–65. https://doi.org/10.1016/j.devcel.2005.05.015.

Sado, Takashi, Masaki Okano, En Li, and Hiroyuki Sasaki. 2004. “De Novo DNA Methylation Is Dispensable for the Initiation and Propagation of X Chromosome Inactivation.” *Development (Cambridge, England)* 131 (5): 975–82. https://doi.org/10.1242/dev.00995.

Sakakibara, Yuki, Koji Nagao, Marnie Blewitt, Hiroyuki Sasaki, Chikashi

Obuse, and Takashi Sado. 2018. “Role of SmcHD1 in Establishment of Epigenetic States Required for the Maintenance of the X-Inactivated State in Mice.” *Development* 145 (18): dev166462. https://doi.org/10.1242/dev.166462.

Santander, N. G., S. Contreras-Duarte, M. F. Awad, C. Lizama, I. Passalacqua, A. Rigotti, and D. Busso. 2013. “Developmental Abnormalities in Mouse Embryos Lacking the HDL Receptor SR-BI.” *Human Molecular Genetics* 22 (6): 1086–96. https://doi.org/10.1093/hmg/dds510.

Sardina, Jose Luis, Samuel Collombet, Tian V. Tian, Antonio Gómez, Bruno Di Stefano, Clara Berenguer, Justin Brumbaugh, et al. 2018. “Transcription Factors Drive Tet2-Mediated Enhancer Demethylation to Reprogram Cell Fate.” *Cell Stem Cell* 23 (5): 727–741.e9. https://doi.org/10.1016/j.stem.2018.08.016.

Sarma, Kavitha, Pierre Levasseur, Alexander Aristarkhov, and Jeannie T Lee. 2010. “Locked Nucleic Acids (LNAs) Reveal Sequence Requirements and Kinetics of Xist RNA Localization to the X Chromosome.” *Proceedings of the National Academy of Sciences of the United States of America* 107 (51): 22196–201. https://doi.org/10.1073/pnas.1009785107.

Sauvageau, Etienne, Moulay D. Rochdi, Morad Oueslati, Fadi F. Hamdan, Yann Percherancier, Jeremy C. Simpson, Rainer Pepperkok, and Michel Bouvier. 2014. “CNIH4 Interacts with Newly Synthesized GPCR and Controls Their Export from the Endoplasmic Reticulum.” *Traffic* 15 (4): 383–400. https://doi.org/10.1111/tra.12148.

Schoeftner, Stefan, Aditya K Sengupta, Stefan Kubicek, Karl Mechtler, Laura Spahn, Haruhiko Koseki, Thomas Jenuwein, and Anton Wutz. 2006. “Recruitment of PRC1 Function at the Initiation of X Inactivation Independent of PRC2 and Silencing.” *The EMBO Journal* 25 (13): 3110–22. https://doi.org/10.1038/sj.emboj.7601187.

Schotta, G. 2004. “A Silencing Pathway to Induce H3-K9 and H4-K20 Trimethylation at Constitutive Heterochromatin.” *Genes & Development* 18 (11): 1251–62. https://doi.org/10.1101/gad.300704.

Schulz, Edda G., Johannes Meisig, Tomonori Nakamura, Ikuhiro Okamoto, Anja Sieber, Christel Picard, Maud Borensztein, Mitinori Saitou, Nils Blüthgen, and Edith Heard. 2014. “The Two Active X Chromosomes in Female ESCs Block Exit from the Pluripotent State by Modulating the ESC Signaling Network.” *Cell Stem Cell* 14 (2): 203–16. https://doi.org/10.1016/j.stem.2013.11.022.

Schwarzer, Wibke, Nezar Abdennur, Anton Goloborodko, Aleksandra Pekowska, Geoffrey Fudenberg, Yann Loe-Mie, Nuno A Fonseca, et al. 2017. “Two Independent Modes of Chromatin Organization Revealed by Cohesin Removal.” *Nature* 551 (7678): 51–56. https://doi.org/10.1038/nature24281.

Seitan, Vlad C, Andre J Faure, Ye Zhan, Rachel Patton McCord, Bryan R Lajoie, Elizabeth Ing-Simmons, Boris Lenhard, et al. 2013. “Cohesin-Based Chromatin Interactions Enable Regulated Gene Expression within Preexisting Architectural Compartments.” *Genome Research* 23 (12): 2066–77. https://doi.org/10.1101/gr.161620.113.

Shah, Sandeep N., Candace Kerr, Leslie Cope, Elias Zambidis, Cyndi Liu, Joelle Hillion, Amy Belton, David L. Huso, and Linda M. S. Resar. 2012. “HMGA1 Reprograms Somatic Cells into Pluripotent Stem Cells by Inducing Stem Cell Transcriptional Networks.” Edited by Katriina Aalto-Setala. *PLoS ONE* 7 (11): e48533. https://doi.org/10.1371/journal.pone.0048533.

Sharman, G B. 1971. “Late DNA Replication in the Paternally Derived X Chromosome of Female Kangaroos.” *Nature* 230 (5291): 231–32. http://www.ncbi.nlm.nih.gov/pubmed/4926712.

Silva, José, Ian Chambers, Steven Pollard, and Austin Smith. 2006.

"Nanog Promotes Transfer of Pluripotency after Cell Fusion." *Nature* 441 (7096): 997–1001. https://doi.org/10.1038/nature04914.

Silva, Jose, Winifred Mak, Ilona Zvetkova, Ruth Appanah, Tatyana B Nesterova, Zoe Webster, Antoine H F M Peters, Thomas Jenuwein, Arie P Otte, and Neil Brockdorff. 2003. "Establishment of Histone H3 Methylation on the Inactive X Chromosome Requires Transient Recruitment of Eed-Enx1 Polycomb Group Complexes." *Developmental Cell* 4 (4): 481–95. http://www.ncbi.nlm.nih.gov/pubmed/12689588.

Silva, Jose, Jennifer Nichols, Thorold W Theunissen, Ge Guo, Anouk L van Oosten, Ornella Barrandon, Jason Wray, Shinya Yamanaka, Ian Chambers, and Austin Smith. 2009. "Nanog Is the Gateway to the Pluripotent Ground State." *Cell* 138 (4): 722–37. https://doi.org/10.1016/j.cell.2009.07.039.

Simon, Matthew D, Stefan F Pinter, Rui Fang, Kavitha Sarma, Michael Rutenberg-Schoenberg, Sarah K Bowman, Barry A Kesner, Verena K Maier, Robert E Kingston, and Jeannie T Lee. 2013. "High-Resolution Xist Binding Maps Reveal Two-Step Spreading during X-Chromosome Inactivation." *Nature* 504 (7480): 465–69. https://doi.org/10.1038/nature12719.

Singhal, Nishant, Johannes Graumann, Guangming Wu, Marcos J Araúzo-Bravo, Dong Wook Han, Boris Greber, Luca Gentile, Matthias Mann, and Hans R Schöler. 2010. "Chromatin-Remodeling Components of the BAF Complex Facilitate Reprogramming." *Cell* 141 (6): 943–55. https://doi.org/10.1016/j.cell.2010.04.037.

Smith, S, and B Stillman. 1989. "Purification and Characterization of CAF-I, a Human Cell Factor Required for Chromatin Assembly during DNA Replication in Vitro." *Cell* 58 (1): 15–25. http://www.ncbi.nlm.nih.gov/pubmed/2546672.

Sofueva, Sevil, Eitan Yaffe, Wen-Ching Chan, Dimitra Georgopoulou,

Matteo Vietri Rudan, Hegias Mira-Bontenbal, Steven M Pollard, Gary P Schroth, Amos Tanay, and Suzana Hadjur. 2013. “Cohesin-Mediated Interactions Organize Chromosomal Domain Architecture.” *The EMBO Journal* 32 (24): 3119–29. https://doi.org/10.1038/emboj.2013.237.

Song, Juan, Adrian Janiszewski, Natalie De Geest, Lotte Vanheer, Irene Talon, Taeho Oh, and Vincent Pasque. 2018. “Two Active X-Chromosomes Modulate the Growth, Pluripotency Exit and DNA Methylation Landscape of Mouse Naive Pluripotent Stem Cells through Different Pathways.” *BioRxiv*, March, 291450. https://doi.org/10.1101/291450.

Soufi, Abdenour, Greg Donahue, and Kenneth S Zaret. 2012. “Facilitators and Impediments of the Pluripotency Reprogramming Factors’ Initial Engagement with the Genome.” *Cell* 151 (5): 994–1004. https://doi.org/10.1016/j.cell.2012.09.045.

Spencer, Rebecca J, Brian C del Rosario, Stefan F Pinter, Derek Lessing, Ruslan I Sadreyev, and Jeannie T Lee. 2011. “A Boundary Element between Tsix and Xist Binds the Chromatin Insulator Ctcf and Contributes to Initiation of X-Chromosome Inactivation.” *Genetics* 189 (2): 441–54. https://doi.org/10.1534/genetics.111.132662.

Splinter, Erik, Helen Heath, Jurgen Kooren, Robert-Jan Palstra, Petra Klous, Frank Grosveld, Niels Galjart, and Wouter de Laat. 2006. “CTCF Mediates Long-Range Chromatin Looping and Local Histone Modification in the Beta-Globin Locus.” *Genes & Development* 20 (17): 2349–54. https://doi.org/10.1101/gad.399506.

Splinter, Erik, Elzo de Wit, Elphège P Nora, Petra Klous, Harmen J G van de Werken, Yun Zhu, Lucas J T Kaaij, et al. 2011. “The Inactive X Chromosome Adopts a Unique Three-Dimensional Conformation That Is Dependent on Xist RNA.” *Genes & Development* 25 (13): 1371–83. https://doi.org/10.1101/gad.633311.

Sridharan, Rupa, Michelle Gonzales-Cope, Constantinos Chronis, Giancarlo Bonora, Robin McKee, Chengyang Huang, Sanjeet Patel, et al. 2013. “Proteomic and Genomic Approaches Reveal Critical Functions of H3K9 Methylation and Heterochromatin Protein-1γ in Reprogramming to Pluripotency.” *Nature Cell Biology* 15 (7): 872–82. https://doi.org/10.1038/ncb2768.

Stadtfeld, Matthias, Nimet Maherali, Marti Borkent, and Konrad Hochedlinger. 2010. “A Reprogrammable Mouse Strain from Gene-Targeted Embryonic Stem Cells.” *Nature Methods* 7 (1): 53–55. https://doi.org/10.1038/nmeth.1409.

Stadtfeld, Matthias, Nimet Maherali, David T Breault, and Konrad Hochedlinger. 2008. “Defining Molecular Cornerstones during Fibroblast to IPS Cell Reprogramming in Mouse.” *Cell Stem Cell* 2 (3): 230–40. https://doi.org/10.1016/j.stem.2008.02.001.

Stefano, Bruno Di, Jose Luis Sardina, Chris van Oevelen, Samuel Collombet, Eric M. Kallin, Guillermo P. Vicent, Jun Lu, Denis Thieffry, Miguel Beato, and Thomas Graf. 2014. “C/EBPα Poises B Cells for Rapid Reprogramming into Induced Pluripotent Stem Cells.” *Nature* 506 (7487): 235–39. https://doi.org/10.1038/nature12885.

Stoop, Petra van der, Erwin A Boutsma, Danielle Hulsman, Sonja Noback, Mike Heimerikx, Ron M Kerkhoven, J Willem Voncken, Lodewyk F A Wessels, and Maarten van Lohuizen. 2008. “Ubiquitin E3 Ligase Ring1b/Rnf2 of Polycomb Repressive Complex 1 Contributes to Stable Maintenance of Mouse Embryonic Stem Cells.” Edited by Simon Williams. *PloS One* 3 (5): e2235. https://doi.org/10.1371/journal.pone.0002235.

Sugimoto, Michihiko, and Kuniya Abe. 2007. “X Chromosome Reactivation Initiates in Nascent Primordial Germ Cells in Mice.” *PLoS Genetics* 3 (7): e116.

https://doi.org/10.1371/journal.pgen.0030116.

Sultan, Faraz A, Jing Wang, Jennifer Tront, Dan A Liebermann, and J David Sweatt. 2012. "Genetic Deletion of Gadd45b, a Regulator of Active DNA Demethylation, Enhances Long-Term Memory and Synaptic Plasticity." *The Journal of Neuroscience : The Official Journal of the Society for Neuroscience* 32 (48): 17059–66. https://doi.org/10.1523/JNEUROSCI.1747-12.2012.

Sun, Sha, Brian C Del Rosario, Attila Szanto, Yuya Ogawa, Yesu Jeon, and Jeannie T Lee. 2013. "Jpx RNA Activates Xist by Evicting CTCF." *Cell* 153 (7): 1537–51. https://doi.org/10.1016/j.cell.2013.05.028.

Sunwoo, Hongjae, David Colognori, John E Froberg, Yesu Jeon, and Jeannie T Lee. 2017. "Repeat E Anchors Xist RNA to the Inactive X Chromosomal Compartment through CDKN1A-Interacting Protein (CIZ1)." *Proceedings of the National Academy of Sciences of the United States of America* 114 (40): 10654–59. https://doi.org/10.1073/pnas.1711206114.

Syed, Khaja Mohieddin, Sunu Joseph, Ananda Mukherjee, Aditi Majumder, Jose M. Teixeira, Debasree Dutta, and Madhavan Radhakrishna Pillai. 2016. "Histone Chaperone APLF Regulates Induction of Pluripotency in Murine Fibroblasts." *Journal of Cell Science* 129 (24): 4576–91. https://doi.org/10.1242/jcs.194035.

Tada, M., T Tada, L Lefebvre, S C Barton, and M A Surani. 1997. "Embryonic Germ Cells Induce Epigenetic Reprogramming of Somatic Nucleus in Hybrid Cells." *The EMBO Journal* 16 (21): 6510–20. https://doi.org/10.1093/emboj/16.21.6510.

Tada, M, Y Takahama, K Abe, N Nakatsuji, and T Tada. 2001a. "Nuclear Reprogramming of Somatic Cells by in Vitro Hybridization with ES Cells." *Current Biology : CB* 11 (19): 1553–58. http://www.ncbi.nlm.nih.gov/pubmed/11591326.

———. 2001b. “Nuclear Reprogramming of Somatic Cells by in Vitro Hybridization with ES Cells.” *Current Biology : CB* 11 (19): 1553–58. http://www.ncbi.nlm.nih.gov/pubmed/11591326.

Tada, T, Y Obata, M Tada, Y Goto, N Nakatsuji, S Tan, T Kono, and N Takagi. 2000. “Imprint Switching for Non-Random X-Chromosome Inactivation during Mouse Oocyte Growth.” *Development (Cambridge, England)* 127 (14): 3101–5. http://www.ncbi.nlm.nih.gov/pubmed/10862747.

Tahiliani, Mamta, Kian Peng Koh, Yinghua Shen, William A Pastor, Hozefa Bandukwala, Yevgeny Brudno, Suneet Agarwal, et al. 2009. “Conversion of 5-Methylcytosine to 5-Hydroxymethylcytosine in Mammalian DNA by MLL Partner TET1.” *Science (New York, N.Y.)* 324 (5929): 930–35. https://doi.org/10.1126/science.1170116.

Takagi, N, M A Yoshida, O Sugawara, and M Sasaki. 1983. “Reversal of X-Inactivation in Female Mouse Somatic Cells Hybridized with Murine Teratocarcinoma Stem Cells in Vitro.” *Cell* 34 (3): 1053–62. http://www.ncbi.nlm.nih.gov/pubmed/6627391.

Takagi, Nobuo, and Motomichi Sasaki. 1975. “Preferential Inactivation of the Paternally Derived X Chromosome in the Extraembryonic Membranes of the Mouse.” *Nature*. https://doi.org/10.1038/256640a0.

Takahashi, Kazutoshi, Kaoru Mitsui, and Shinya Yamanaka. 2003. “Role of ERas in Promoting Tumour-like Properties in Mouse Embryonic Stem Cells.” *Nature* 423 (6939): 541–45. https://doi.org/10.1038/nature01646.

Takahashi, Kazutoshi, Koji Tanabe, Mari Ohnuki, Megumi Narita, Tomoko Ichisaka, Kiichiro Tomoda, and Shinya Yamanaka. 2007. “Induction of Pluripotent Stem Cells from Adult Human Fibroblasts by Defined Factors.” *Cell* 131 (5): 861–72. https://doi.org/10.1016/j.cell.2007.11.019.

Takahashi, Kazutoshi, and Shinya Yamanaka. 2006a. “Induction of Pluripotent Stem Cells from Mouse Embryonic and Adult Fibroblast Cultures by Defined Factors.” *Cell* 126 (4): 663–76. https://doi.org/10.1016/j.cell.2006.07.024.

———. 2006b. “Induction of Pluripotent Stem Cells from Mouse Embryonic and Adult Fibroblast Cultures by Defined Factors.” *Cell* 126 (4): 663–76. https://doi.org/10.1016/j.cell.2006.07.024.

Tanaka, Satomi S., Yasuka L. Yamaguchi, Bonny Tsoi, Heiko Lickert, and Patrick P.L. Tam. 2005. “IFITM/Mil/Fragilis Family Proteins IFITM1 and IFITM3 Play Distinct Roles in Mouse Primordial Germ Cell Homing and Repulsion.” *Developmental Cell* 9 (6): 745–56. https://doi.org/10.1016/j.devcel.2005.10.010.

Tang, Y Amy, Derek Huntley, Giovanni Montana, Andrea Cerase, Tatyana B Nesterova, and Neil Brockdorff. 2010. “Efficiency of Xist-Mediated Silencing on Autosomes Is Linked to Chromosomal Domain Organisation.” *Epigenetics & Chromatin* 3 (1): 10. https://doi.org/10.1186/1756-8935-3-10.

Teller, Kathrin, Doris Illner, Stefanie Thamm, Corella S Casas-Delucchi, Rogier Versteeg, Mireille Indemans, Thomas Cremer, and Marion Cremer. 2011a. “A Top-down Analysis of Xa- and Xi-Territories Reveals Differences of Higher Order Structure at ≥ 20 Mb Genomic Length Scales.” *Nucleus (Austin, Tex.)* 2 (5): 465–77. https://doi.org/10.4161/nucl.2.5.17862.

———. 2011b. “A Top-down Analysis of Xa- and Xi-Territories Reveals Differences of Higher Order Structure at ≥ 20 Mb Genomic Length Scales.” *Nucleus (Austin, Tex.)* 2 (5): 465–77. https://doi.org/10.4161/nucl.2.5.17862.

———. 2011c. “A Top-down Analysis of Xa- and Xi-Territories Reveals Differences of Higher Order Structure at ≥ 20 Mb Genomic Length Scales.” *Nucleus (Austin, Tex.)* 2 (5): 465–77.

https://doi.org/10.4161/nucl.2.5.17862.

Teufel, Andreas, Eric A Wong, Mahua Mukhopadhyay, Nasir Malik, and Heiner Westphal. 2003. "FoxP4, a Novel Forkhead Transcription Factor." *Biochimica et Biophysica Acta* 1627 (2–3): 147–52. http://www.ncbi.nlm.nih.gov/pubmed/12818433.

Tian, Di, Sha Sun, and Jeannie T Lee. 2010. "The Long Noncoding RNA, Jpx, Is a Molecular Switch for X Chromosome Inactivation." *Cell* 143 (3): 390–403. https://doi.org/10.1016/j.cell.2010.09.049.

Tsai, Chia-Lun, Rebecca K Rowntree, Dena E Cohen, and Jeannie T Lee. 2008. "Higher Order Chromatin Structure at the X-Inactivation Center via Looping DNA." *Developmental Biology* 319 (2): 416–25. https://doi.org/10.1016/j.ydbio.2008.04.010.

Tsang, Leanna W K, Ninghe Hu, and D Alan Underhill. 2010. "Comparative Analyses of SUV420H1 Isoforms and SUV420H2 Reveal Differences in Their Cellular Localization and Effects on Myogenic Differentiation." Edited by Fatah Kashanchi. *PloS One* 5 (12): e14447. https://doi.org/10.1371/journal.pone.0014447.

Tsuchiya, Karen D, John M Greally, Yajun Yi, Kevin P Noel, Jean-Pierre Truong, and Christine M Disteche. 2004. "Comparative Sequence and X-Inactivation Analyses of a Domain of Escape in Human Xp11.2 and the Conserved Segment in Mouse." *Genome Research* 14 (7): 1275–84. https://doi.org/10.1101/gr.2575904.

Vidal, Simon E., Bhishma Amlani, Taotao Chen, Aristotelis Tsirigos, and Matthias Stadtfeld. 2014. "Combinatorial Modulation of Signaling Pathways Reveals Cell-Type-Specific Requirements for Highly Efficient and Synchronous IPSC Reprogramming." *Stem Cell Reports* 3 (4): 574–84. https://doi.org/10.1016/j.stemcr.2014.08.003.

Vielle, Anne, Jackie Lang, Yan Dong, Sevinc Ercan, Chitra Kotwaliwale, Andreas Rechtsteiner, Alex Appert, et al. 2012. "H4K20me1 Contributes to Downregulation of X-Linked Genes for C. Elegans

Dosage Compensation." Edited by William G. Kelly. *PLoS Genetics* 8 (9): e1002933. https://doi.org/10.1371/journal.pgen.1002933.

Vietri Rudan, Matteo, Christopher Barrington, Stephen Henderson, Christina Ernst, Duncan T Odom, Amos Tanay, and Suzana Hadjur. 2015. "Comparative Hi-C Reveals That CTCF Underlies Evolution of Chromosomal Domain Architecture." *Cell Reports* 10 (8): 1297–1309. https://doi.org/10.1016/j.celrep.2015.02.004.

Wallingford, Mary C., Hilary S. Gammill, and Cecilia M. Giachelli. 2016. "Slc20a2 Deficiency Results in Fetal Growth Restriction and Placental Calcification Associated with Thickened Basement Membranes and Novel CD13 and Lamininα1 Expressing Cells." *Reproductive Biology* 16 (1): 13–26. https://doi.org/10.1016/j.repbio.2015.12.004.

Wang, Chen-Yu, Teddy Jégu, Hsueh-Ping Chu, Hyun Jung Oh, and Jeannie T. Lee. 2018. "SMCHD1 Merges Chromosome Compartments and Assists Formation of Super-Structures on the Inactive X." *Cell* 174 (2): 406–421.e25. https://doi.org/10.1016/j.cell.2018.05.007.

Wang, Jianbo, Jesse Mager, Yijing Chen, Elizabeth Schneider, James C. Cross, Andras Nagy, and Terry Magnuson. 2001. "Imprinted X Inactivation Maintained by a Mouse Polycomb Group Gene." *Nature Genetics* 28 (4): 371–75. https://doi.org/10.1038/ng574.

Wang, Wei, Jian Yang, Hui Liu, Dong Lu, Xiongfeng Chen, Zenon Zenonos, Lia S Campos, et al. n.d. "Rapid and Efficient Reprogramming of Somatic Cells to Induced Pluripotent Stem Cells by Retinoic Acid Receptor Gamma and Liver Receptor Homolog 1." Accessed November 12, 2018. https://doi.org/10.1073/pnas.1100893108.

Welham, Melanie J., Emmajayne Kingham, Yolanda Sanchez-Ripoll, Benjamin Kumpfmueller, Michael Storm, and Heather Bone. 2011.

"Controlling Embryonic Stem Cell Proliferation and Pluripotency: The Role of PI3K- and GSK-3-Dependent Signalling." *Biochemical Society Transactions* 39 (2): 674–78. https://doi.org/10.1042/BST0390674.

Wells, Michael B, Martha J Snyder, Laura M Custer, and Gyorgyi Csankovszki. 2012. "Caenorhabditis Elegans Dosage Compensation Regulates Histone H4 Chromatin State on X Chromosomes." *Molecular and Cellular Biology* 32 (9): 1710–19. https://doi.org/10.1128/MCB.06546-11.

Wendt, Kerstin S, Keisuke Yoshida, Takehiko Itoh, Masashige Bando, Birgit Koch, Erika Schirghuber, Shuichi Tsutsumi, et al. 2008. "Cohesin Mediates Transcriptional Insulation by CCCTC-Binding Factor." *Nature* 451 (7180): 796–801. https://doi.org/10.1038/nature06634.

Williams, Lucy H, Sundeep Kalantry, Joshua Starmer, and Terry Magnuson. 2011. "Transcription Precedes Loss of Xist Coating and Depletion of H3K27me3 during X-Chromosome Reprogramming in the Mouse Inner Cell Mass." *Development (Cambridge, England)* 138 (10): 2049–57. https://doi.org/10.1242/dev.061176.

Wu, Hao, Junjie Luo, Huimin Yu, Amir Rattner, Alisa Mo, Yanshu Wang, Philip M. Smallwood, Bracha Erlanger, Sarah J. Wheelan, and Jeremy Nathans. 2014. "Cellular Resolution Maps of X Chromosome Inactivation: Implications for Neural Development, Function, and Disease." *Neuron* 81 (1): 103–19. https://doi.org/10.1016/J.NEURON.2013.10.051.

Wu, Qiang, Alexander W Bruce, Agnieszka Jedrusik, Peter D Ellis, Robert M Andrews, Cordelia F Langford, David M Glover, and Magdalena Zernicka-Goetz. 2009. "CARM1 Is Required in Embryonic Stem Cells to Maintain Pluripotency and Resist Differentiation." *Stem Cells (Dayton, Ohio)* 27 (11): 2637–45.

https://doi.org/10.1002/stem.131.

Wutz, Anton, Theodore P Rasmussen, and Rudolf Jaenisch. 2002a. "Chromosomal Silencing and Localization Are Mediated by Different Domains of Xist RNA." *Nature Genetics* 30 (2): 167–74. https://doi.org/10.1038/ng820.

———. 2002b. "Chromosomal Silencing and Localization Are Mediated by Different Domains of Xist RNA." *Nature Genetics* 30 (2): 167–74. https://doi.org/10.1038/ng820.

Xu, Huiling, Kuhendra Balakrishnan, Jordane Malaterre, Matthew Beasley, Yuqian Yan, Jeroen Essers, Esther Appeldoorn, et al. 2010. "Correction: Rad21-Cohesin Haploinsufficiency Impedes DNA Repair and Enhances Gastrointestinal Radiosensitivity in Mice." Edited by Kerstin Borgmann. *PLoS ONE* 5 (9). https://doi.org/10.1371/annotation/12224797-353c-4e9c-92f3-a0de9b527415.

Xu, Na, Mary E Donohoe, Susana S Silva, and Jeannie T Lee. 2007. "Evidence That Homologous X-Chromosome Pairing Requires Transcription and Ctcf Protein." *Nature Genetics* 39 (11): 1390–96. https://doi.org/10.1038/ng.2007.5.

Yamada, Norishige, Yuko Hasegawa, Minghui Yue, Tomofumi Hamada, Shinichi Nakagawa, and Yuya Ogawa. 2015. "Xist Exon 7 Contributes to the Stable Localization of Xist RNA on the Inactive X-Chromosome." Edited by Jeannie T. Lee. *PLoS Genetics* 11 (8): e1005430. https://doi.org/10.1371/journal.pgen.1005430.

Yamaji, Masashi, Yoshiyuki Seki, Kazuki Kurimoto, Yukihiro Yabuta, Mihoko Yuasa, Mayo Shigeta, Kaori Yamanaka, Yasuhide Ohinata, and Mitinori Saitou. 2008. "Critical Function of Prdm14 for the Establishment of the Germ Cell Lineage in Mice." *Nature Genetics* 40 (8): 1016–22. https://doi.org/10.1038/ng.186.

Yang, F., T. Babak, J. Shendure, and C. M. Disteche. 2010. "Global

Survey of Escape from X Inactivation by RNA-Sequencing in Mouse." *Genome Research* 20 (5): 614–22. https://doi.org/10.1101/gr.103200.109.

Yang, Fan, Xinxian Deng, Wenxiu Ma, Joel B Berletch, Natalia Rabaia, Gengze Wei, James M Moore, et al. 2015. "The LncRNA Firre Anchors the Inactive X Chromosome to the Nucleolus by Binding CTCF and Maintains H3K27me3 Methylation." *Genome Biology* 16 (1): 52. https://doi.org/10.1186/s13059-015-0618-0.

Yu, Yong, Dan Liang, Qing Tian, Xiaona Chen, Bo Jiang, Bin-Kuan Chou, Ping Hu, et al. 2014. "Stimulation of Somatic Cell Reprogramming by ERas-Akt-FoxO1 Signaling Axis." *Stem Cells (Dayton, Ohio)* 32 (2): 349–63. https://doi.org/10.1002/stem.1447.

Zhang, Li-Feng, Khanh D Huynh, and Jeannie T Lee. 2007. "Perinucleolar Targeting of the Inactive X during S Phase: Evidence for a Role in the Maintenance of Silencing." *Cell* 129 (4): 693–706. https://doi.org/10.1016/j.cell.2007.03.036.

Zuin, Jessica, Jesse R Dixon, Michael I J A van der Reijden, Zhen Ye, Petros Kolovos, Rutger W W Brouwer, Mariëtte P C van de Corput, et al. 2014. "Cohesin and CTCF Differentially Affect Chromatin Architecture and Gene Expression in Human Cells." *Proceedings of the National Academy of Sciences of the United States of America* 111 (3): 996–1001. https://doi.org/10.1073/pnas.1317788111.

Zvetkova, Ilona, Anwyn Apedaile, Bernard Ramsahoye, Jacqueline E Mermoud, Lucy A Crompton, Rosalind John, Robert Feil, and Neil Brockdorff. 2005. "Global Hypomethylation of the Genome in XX Embryonic Stem Cells." *Nature Genetics* 37 (11): 1274–79. https://doi.org/10.1038/ng1663.

Research articles resulting from the PhD

- Thesis work

A dual in vivo and in vitro screening approach identifies critical factors for pluripotency and X-chromosome reactivation.

Generoso SF., Sadrejev R., Karchenko P., Stadtfeld M., Kurimoto K., Hochedlinger K., Park P., Saitou M., Lee JT and Payer B.

Manuscript in preparation.

- Collaboration project

Expression changes as a function of growth rate: are fibroblasts yeast?

Badia M*., **Generoso SF***., Payer B., Carey L.

*Equal contribution

Manuscript in preparation.